2-15-2017

Synthesis of novel, highly bio-based monomeric materials derived from lignocellulosic biomass and their respective epoxy resins, polycarbonates, and polyesters

Joseph Randall Mauck
Rowan University

SYNTHESIS OF NOVEL, HIGHLY BIO-BASED MONOMERIC MATERIALS DERIVED FROM LIGNOCELLULOSIC BIOMASS AND THEIR RESPECTIVE EPOXY RESINS, POLYCARBONATES, AND POLYESTERS

by

Joseph Randall Mauck

A Thesis

Submitted to the
Department of Chemical Engineering
Henry M. Rowan College of Engineering
In partial fulfillment of the requirements
For the degree of
Master of Science in Chemical Engineering
at
Rowan University
December 16, 2016

Thesis Chair: Joseph F. Stanzione, III, Ph.D.

Dedications

For Mom, Dad, and Meagan

Acknowledgements

First and foremost I wish to express my deepest gratitude to Dr. Joseph F. Stanzione, III; my graduate advisor, teacher, mentor, teammate, hunting partner, and thesis chair. For the past 16 months, Dr. Stanzione has encouraged me through difficult academic times, guided me in research decision-making, and most importantly, given me the opportunity to study and perform this work and become a contributing part of the greater biomaterials research community. Dr. Stanzione's thoughtful guidance gave me countless opportunities to investigate new ideas and experience their corresponding successes and failures by my own hand. In addition to the wealth of academic resources Dr. Stanzione made available to me, he was equally interested in developing well-rounded students through participation in athletics and outdoor activities, things I also believe to be important to an individual's learning and growth.

Just as important as the guidance of my advisor was the environment of shared ideas that was fostered between my fellow graduate students and me. For this, I must thank my office colleagues: Alexander Bassett, Elyse Baroncini, Laura Osorno, Stephen Dipasquale, and Liana Wuchte. Without their accepting of me into their network of shared knowledge, completing this work would not have been possible.

I would like to thank our collaborators at the Army Research Lab, Drs. Joshua Sadler and John La Scala, for their thoughtful analysis of my questions and ideas and for serving on my thesis committee. Drs. Santosh Yadav and Giuseppe Palmese at Drexel University are also acknowledged for their collaborative insights on research manuscripts and for their generously allowing the use of their instrumentation. I am gratefully indebted to the Army Research Laboratory and their funding through Cooperative Agreements W911NF-14-1-

0086 and W911NF-15-2-0017 as well as funding through SERDP Project number WP03-015.

Finally, I must thank my loving family who supported my graduate school endeavors every step of the way. This includes my mom and dad, Linda and Rick Mauck, my brother and sister, Richie and Lindsay Mauck, and my ever-supportive girlfriend Meagan Kinneer. Without all of you being there at every step of this journey, this truly would have been an impossible undertaking. Thank you, and I love all of you more than you could know.

Abstract

Joseph R. Mauck
SYNTHESIS OF NOVEL, HIGHLY BIO-BASED MONOMERIC MATERIALS DERIVED FROM LIGNOCELLULOSIC BIOMASS AND THEIR RESPECTIVE EPOXY RESINS, POLYCARBONATES, AND POLYESTERS
2016-2017
Joseph F. Stanzione, III, Ph.D.
Master of Science in Chemical Engineering

The development of high performance polymers from renewable feedstocks is a crucial step toward a global economy that is less dependent on fossil resources and has been a field of increasing study. The development of novel and interesting bio-based monomers, resins, and functional building blocks is critical to the improvement of polymers produced across the field, as well as to increasing the resource base from which chemical and materials engineers can draw to meet specific polymer property requirements. To this end, interesting tri-functional (trisguaiacol) and 4-vinyl guaiacol based hetero-difunctional monomers were developed and screened for preliminary polymer properties. The applications of these and other similar building blocks for various polymer applications are numerous and varied and, therefore, are worthy of investigation and inclusion in the body of this work.

Currently, most plastics, synthetic fibers, and composite materials that are ubiquitous throughout every aspect of modern life utilize petrochemical feedstocks, an unsustainable model for the future. Lignin, cellulose, and hemicellulose are the most abundant renewable biopolymers in the world and offer a sustainable alternative for fine chemicals and platform molecules in the future. Depolymerized, these biomass sources afford many different building block chemicals that can be functionalized and utilized in polymer and materials

applications. In this work, epoxy resins, polycarbonates, and polyesters derived from lignin were synthesized and characterized by ^{1}H-NMR, ^{13}C-NMR, FTIR, GPC, DMA, TGA, and DSC. In the case of epoxy resins, a cellulose-derived diamine curing agent, *5,5'*-methylenedifurfurylamine (DFDA), was used alongside lignin-derived glycidyl ethers to prepare highly bio-based thermosetting resins. Lignin-derived aromatic polycarbonates and polyesters were also synthesized to investigate the utility of bio-based monomers in important thermoplastics. The resulting polymers displayed high thermal stability and high moduli as well as moderate glass transition temperatures due to high aromatic content and other unique structural effects.

Table of Contents

Table of Contents (Continued)

Table of Contents (Continued)

List of Figures

Figure Page

List of Tables

Chapter 1

Introduction

1.1 Overview

Recent global awareness of the unsustainability of fossil resource utilization and of the human and environmental health impacts of using plastics produced from fossil resources has sparked an explosion of research in the area of biomass conversion to fine chemicals, platform chemicals, and subsequent polymers. The potential for the production of building block chemicals and resultant polymers and materials from biomass feedstocks, such as lignin, cellulose, and hemicellulose, offers an alternative route to the materials that build, fuel, and shape the modern world. Yet, many gaps still exist in the development of lignin-based chemicals, monomers, and polymers.

1.2 Chemical Building Blocks from Biomass

As early as 1874 with the outcry of a Pennsylvanian geologist, warnings about the decline of fossil resource reserves have been ever-present.[1] While advances in computing technology have allowed for more accurate predictions of "peak oil," and while there is still much disagreement over the precise timing of the depletion of fossil resources, the general consensus, even among the oil and gas industry, is that such resources are in fact unsustainable.[2, 3] In the decades since the 1970's, nearly every major economic recession event has been precipitated from a spike in crude oil prices.[3] Even though more recent projections actually show the global supply of oil and gas resources to be increasing, the costs (both monetary and environmental) of obtaining them will be higher than ever before. It is with this eventuality in mind that researchers for the past several decades have become interested in the utilization of renewable feedstocks as sources of

chemicals traditionally produced from fossil resources, including oil and natural gas. Significant progress has been made in the bio-derivation of polymers used in many different applications such as epoxy resins, polycarbonates, vinyl ester resins, polystyrenes, polymer composites, and many more.[4-7] Equally important has been the development of techniques for the breakdown of raw biomass into useful chemicals as the building blocks of those polymer materials. Lignin, cellulose, and hemicellulose, the three biopolymers that combine to give structure to land plants, have been targeted as sources for these chemicals.

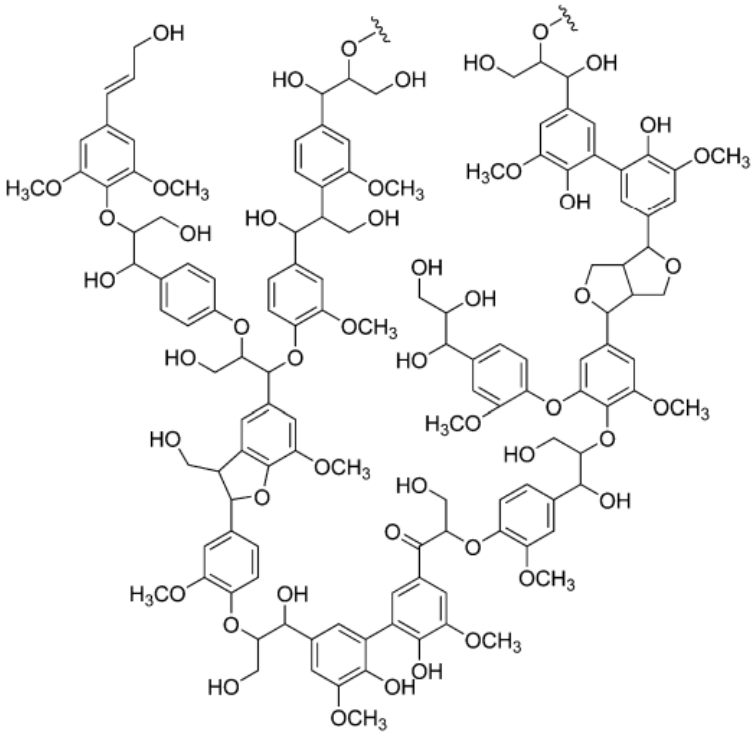

Figure 1. A proposed general structure of lignin.[8, 9]

Lignin (Figure 1), a ubiquitous byproduct of the pulp and paper making industry, is typically burned at the production facility for cheap energy recovery.[9-11] Yet, lignin has been proven to be depolymerizable into (methoxy)phenols such as phenols (**1**), guaiacols (**2**), syringols (**3**), and catechols (**4-6**) as well as hydroxyl- and methoxyl-substituted aromatic carbonyls such as syringaldehyde (**7**), vanillin (**8**), and vanillic acid (**9**) (Figure 2).[12, 13] The highly aromatic nature of lignin and its depolymerization products is the main allure of this resource due to the strength and rigidity it imparts. Other biomass-derived polymer precursors such as plant oils (which are substantially easier to obtain than lignin-based monomers) are often composed of fatty acids and similar structures containing long carbon chains. These long chains, while imparting flexibility and toughness to resultant polymers, often suppress glass transition temperatures and rigidity. While much research in this field is currently focused on the downstream applications of lignocellulosic chemicals, the proposed next generation of biomass refineries can be outlined in schematic form in Figure 3.[14]

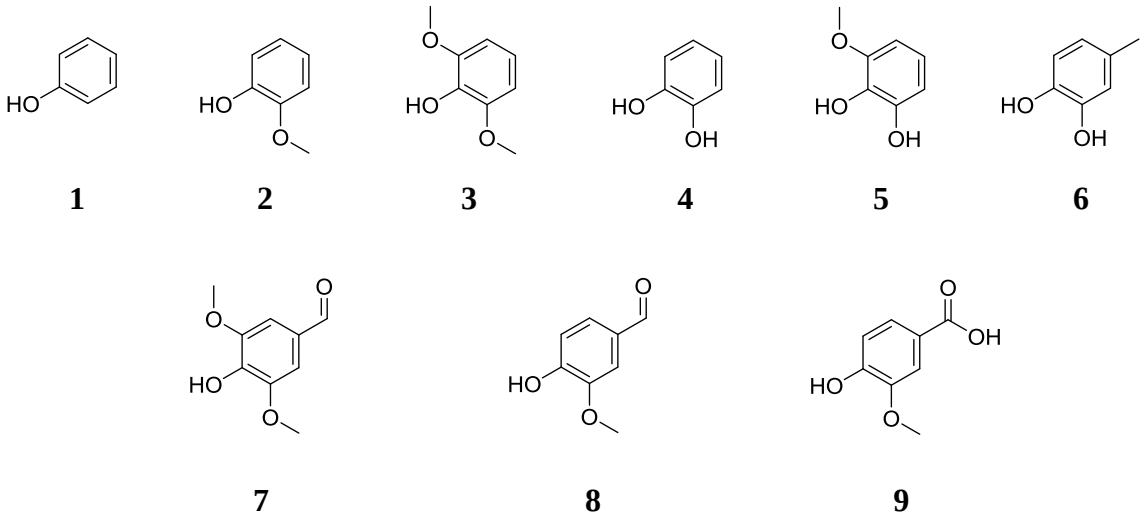

Figure 2. Common (methoxy)phenols and aromatic carbonyls derived from lignin.

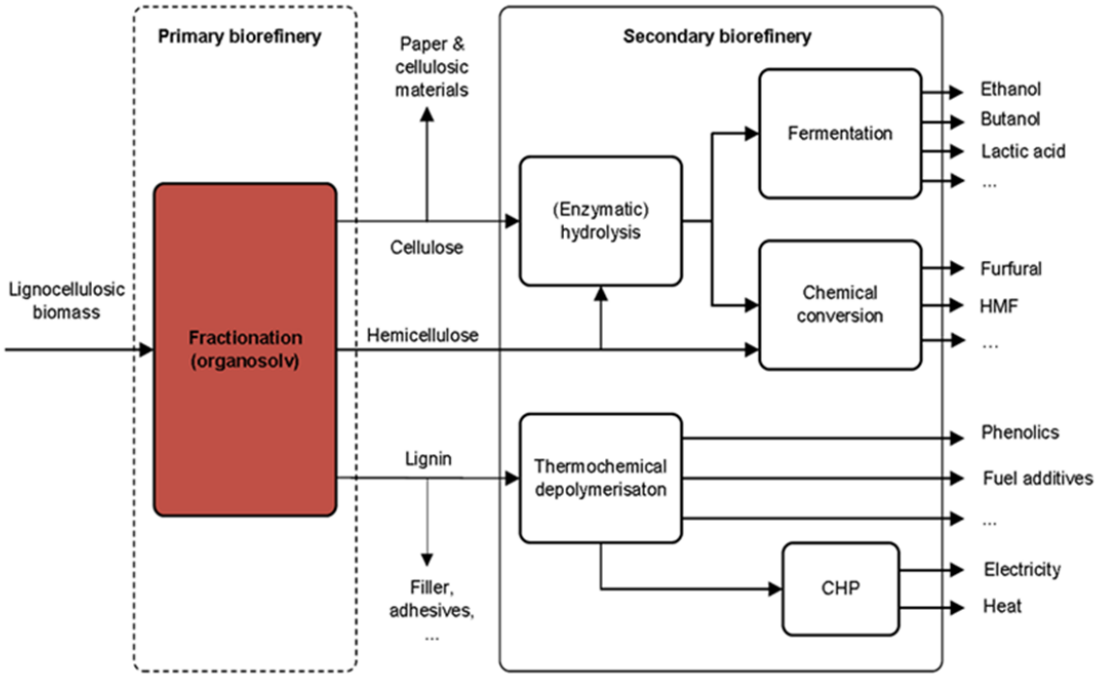

Figure 3. Next generation lignocellulosic biorefinery.[14]

Other potentially valuable species derived from lignin are phenyl propanoids like eugenol, resveratrol, coniferyl alcohol, and cinnamic acid (Figure 4).[15-21]

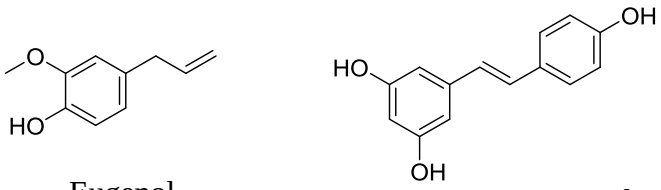

Eugenol

Resveratrol

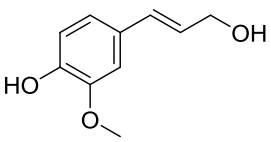

Coniferyl Alcohol

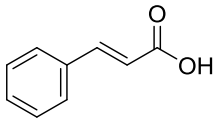

Cinnamic Acid

Figure 4. Phenyl propanoids derived from lignin.

In particular, vanillin (4-hydroxy-3-methoxybenzaldehyde) (**8**) has already been proven to be a valuable polymer building block due to the breadth of its possible sources and the many chemical transformations it can undergo to yield precursors to polymers with high performance properties (Figure 5).[22-24]

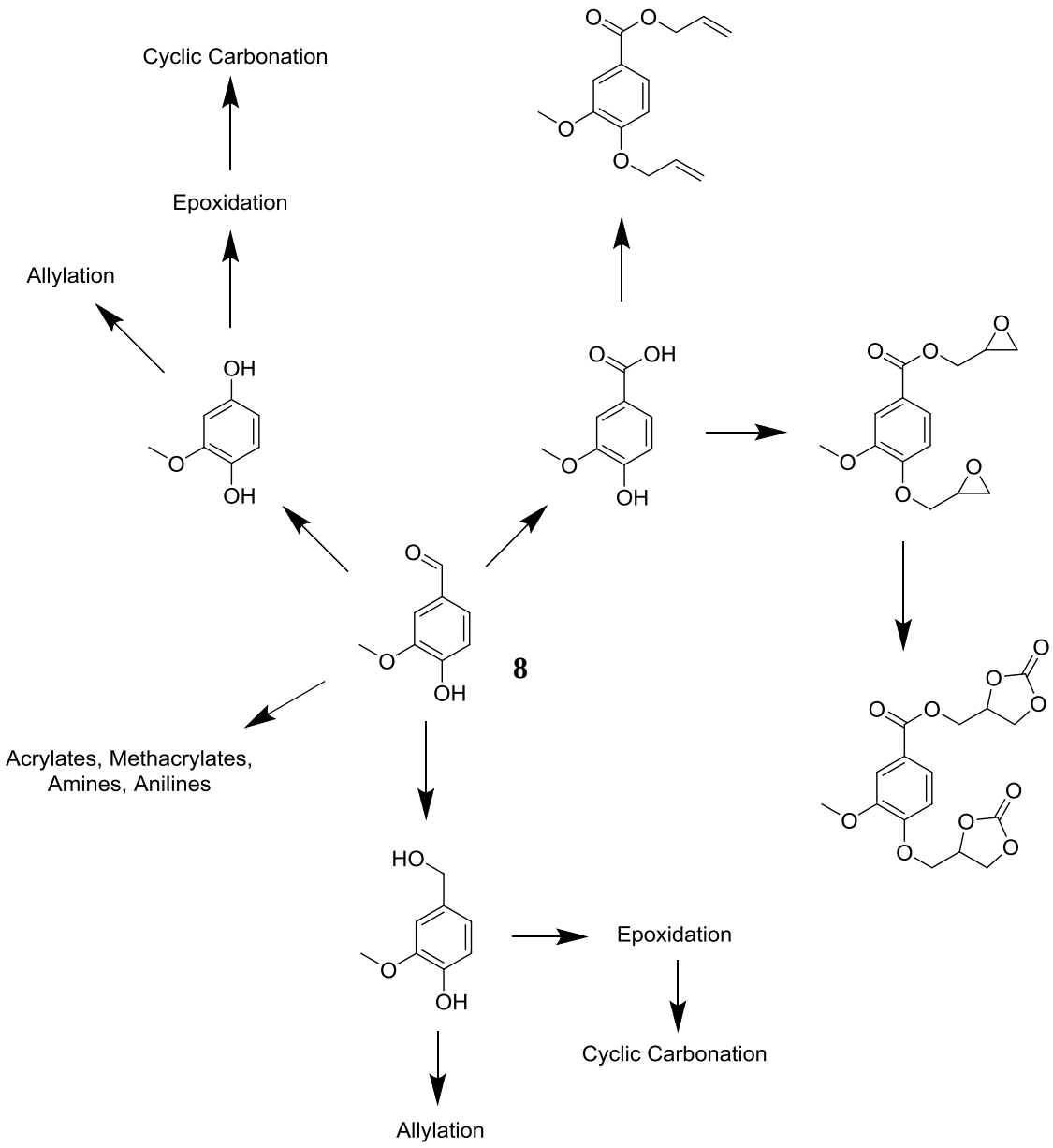

Figure 5. Vanillin as a platform chemical for various polymer applications.[22]

Currently, 15% of the world vanillin market is comprised of lignin-derived vanillin, with most of the remaining 85% being petrochemical derived (Figure 6).[25] Less than 1% of the global vanillin market is a product of the cultivation of vanilla beans.[12, 26] One of the main allures of lignin utilization is the fact that it is currently produced on a large scale (50 million tons produced annually), and is currently a waste product.[12] This means that any switch to chemicals from lignin do not require the diversion of land space from the growth of food crops. This has been one of the main drawbacks of bio-based fuel production; using the edible portions of crops to make fuel diminishes the supply of food for the world.[27]

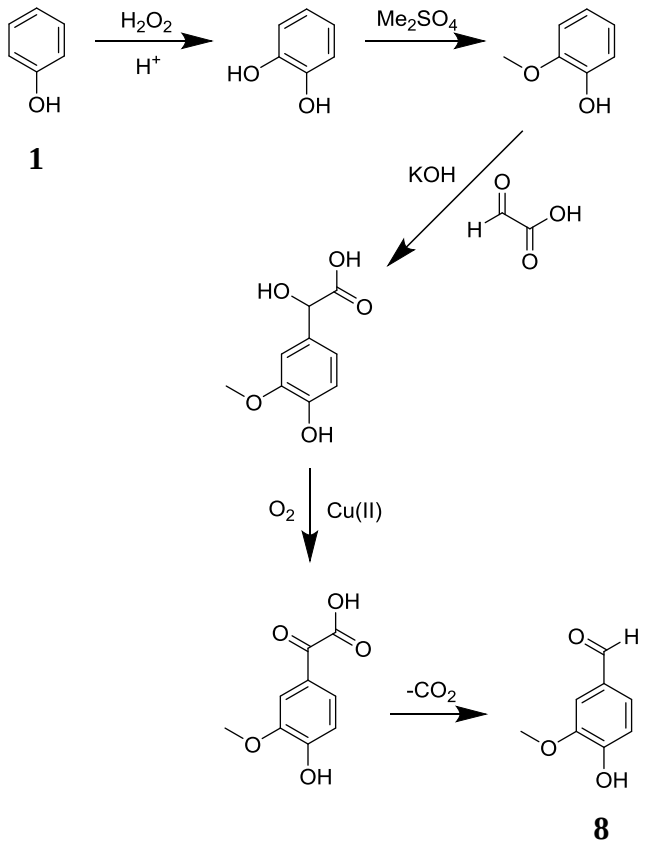

Figure 6. Example of petrochemical synthesis of vanillin from phenol.[12, 23, 26, 28]

Cellulose and hemicellulose are biopolymers made up of sugars and can be depolymerized into furanyls (Figure 7); proven to be equally valuable as chemical building blocks.

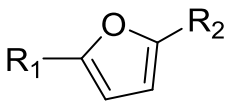

Figure 7. General furanyl species with two substituent groups (R_1 and R_2).

Cellulose (Figure 8) is comprised exclusively of linked glucose molecules[29], while hemicellulose (Figure 9) is composed of various monosaccharides of both the 5- and 6-membered ring variety (pentoses and hexoses).[30]

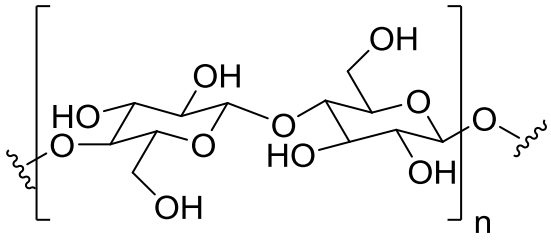

Figure 8. Structure and repeat unit (cellobiose) of cellulose.

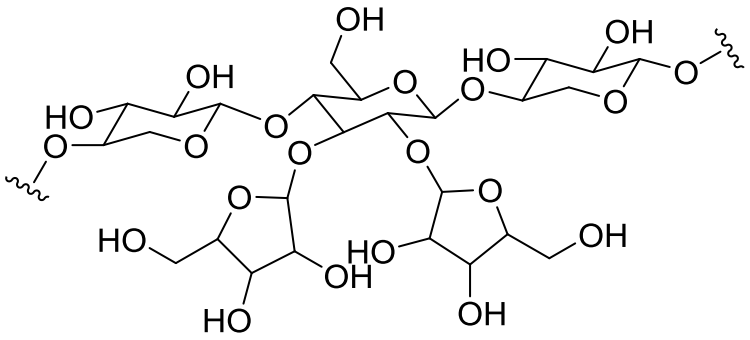

Figure 9. Structure of hemicellulose (shown with generic pentose side groups).

The body of work regarding the degradation of both cellulose and hemicellulose to their base sugars is extensive and growing.[29, 31, 32] Notably, furans and furan derivatives can be obtained from these base saccharides and, in turn, utilized in polymer applications.[29, 31-35] Hydroxymethylfurfural (HMF) (**10**) (Figure 10) has been proven to be a versatile platform chemical derived from cellulosics due to the numerous functionalizations it can undergo before subsequent polymerization.[29]

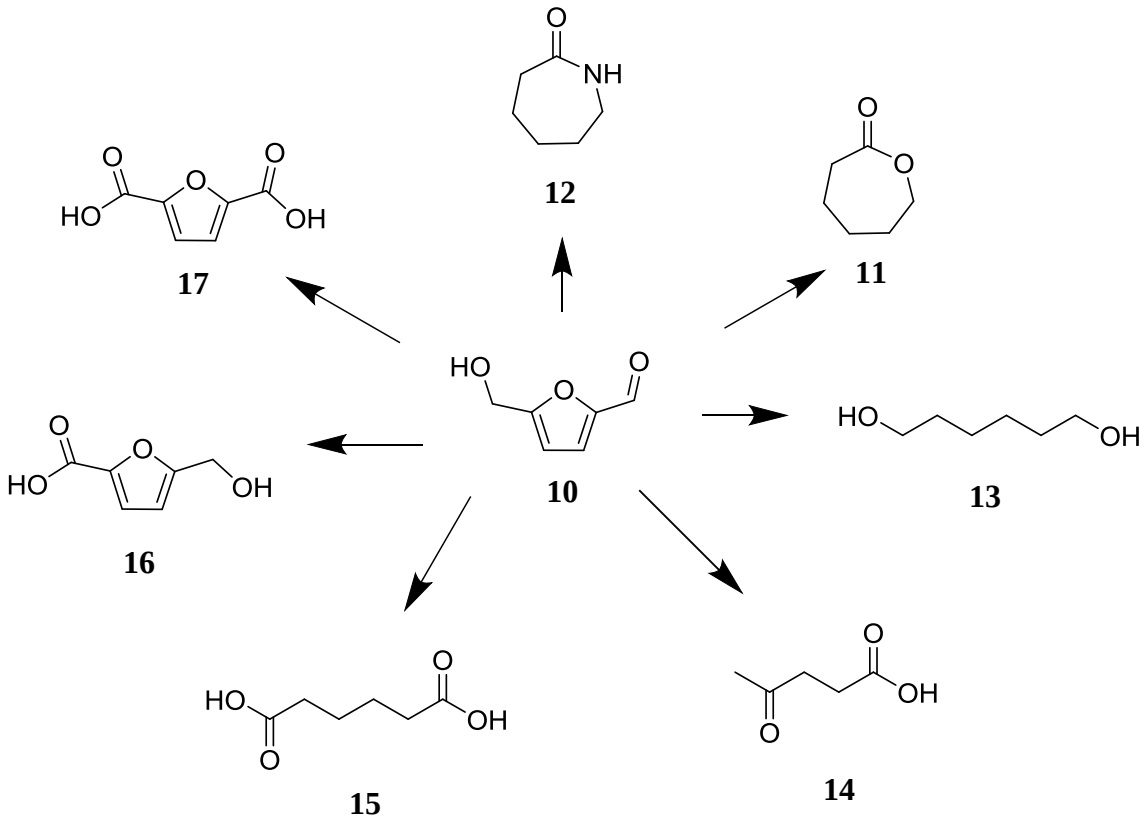

Figure 10. Structure of hydroxymethylfurfural and possible derivatives.[29]

Caprolactone (**11**) is commonly utilized as a precursor to caprolactam (**12**) and in ring opening polymerizations to form polyesters.[36] Caprolactam is the building block of Nylon 6, a high performance polymer used in high strength fibers including instrument strings as well as in high strength mechanical parts.[37] 1,6-hexanediol (**13**) is a key building block in many different polymers such as polyesters and polyurethanes where the long carbon chain imparts toughness and flexibility to the polymer, albeit at the expense of glass transition temperature (T_g).[37] Levulinic acid (**14**) is another platform chemical that can find applications in many areas such as polyesters and polyamides.[38] Succinic acid (**15**) is a dicarboxylic acid used extensively in industrial polyesters and polyamides.[39] 5-

hydroxymethylfuroic acid (**16**) is another example of an HMF-derived chemical with difunctional handles for use in polymers or as an intermediate to higher value chemicals.[29] Furandicarboxylic acid (**17**) is an emerging high-value platform chemical which is anticipated to be key to many kinds of polymers as a replacement for terephthalate in plastics.[29]

The utilization of current waste biomass as sources of chemical building blocks will be critical in the future as fossil resource reserves become harder and more expensive to locate and extract. Additionally, bio-based polymers offer the potential to present lower toxicity[40] or better performance properties than current petrochemical-derived polymers. Direct use of partially broken-down biomass such as bio-oils have already been investigated, but tend to yield lower-performing polymers suitable only for certain low-value applications.[41] Through the past several years of global research, it has become clear that biomass feedstocks offer an abundance of various core structures from aromatics to furans as well as numerous functionalities with the ability to generate additional functionality synthetically downstream. Therefore, there is great potential for lignocellulosic biomass to provide polymer building blocks to produce high performance polymers with unique properties and decreased toxicities not possible via current petrochemical routes.

1.3 Bisphenols

No review of high performance polymers would be complete without an overview of bisphenols. Earning perhaps the most recognition by name, bisphenol A (BPA) (*4,4'*-isopropylidenebisphenol) (**18**) was first synthesized and reported by Russian chemist Aleksandr Dianin in 1891.[42] Produced by the coupling of phenol with acetone (**19**)

(Figure 11) in the presence of an acid catalyst, the synthesis of BPA has not markedly changed since its discovery.

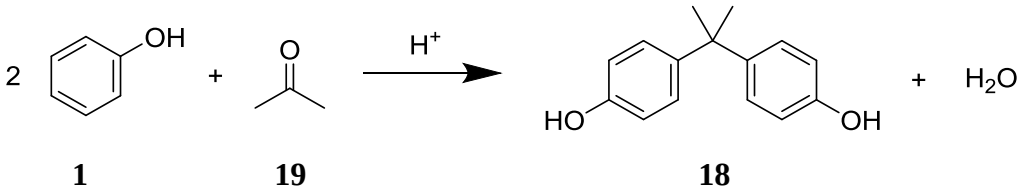

Figure 11. Reaction scheme for the synthesis of BPA.

Although initially researched in the early 20th century as a synthetic estrogen, the high isomeric purity, the ease of production, and the rigid aromatic structure of BPA made it a viable candidate for incorporation into polymeric materials.[42] The production of BPA globally was estimated at around 12 billion pounds in 2011, and growing at 5% annually.[43] While polycarbonate (74% of BPA use) and epoxy resin (20% of BPA use) applications comprised the vast majority of BPA utilization throughout the next several decades,[43] BPA is also commonly used in applications such as thermal paper coatings, flame retardants, powder paints, and dye developers.[44] Despite the myriad applications for BPA, just as scientists in the 1930's had suggested, the toxic endocrine disrupting effects of BPA exposure jumped to the forefront of the discussion over the effects of exposure to chemicals that make up everyday polymers and plastics.[42] It would become known that even at very high degrees of polymerization, unreacted monomer could leach out of the bulk polymer into contacting fluids or biological material.[45-47] The proliferation of microwaves in the latter half of the 20th century also served to exacerbate

the problems surrounding BPA-containing plastics. Microwaving polycarbonate food and beverage containers has been shown to degrade the polymer structure and facilitate the release of BPA monomer into the consumable contents of the container.[48] Current estimates indicate that more than 90% of people in developed countries contain BPA and its metabolites in their urine.[47] BPA mimics estradiol (Figure 12), a hormone associated with the development of reproductive tissue in several organisms, including humans.[49, 50]

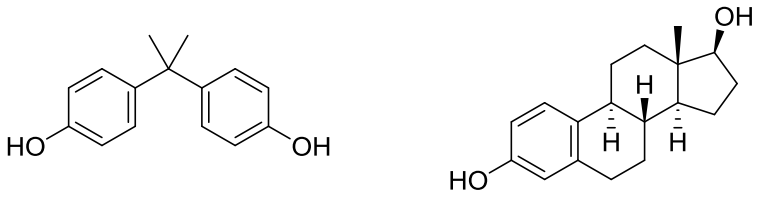

Figure 12. BPA (left) and the hormone it mimics, estradiol (right).

Various effects at all stages of human development from fetal and neonatal growth to adult maturation have been linked to BPA exposure including neurochemical changes associated with behavioral abnormalities such as hyperactivity, learning deficiencies, aggression, tendencies toward drug dependency, sperm and oocyte production abnormalities in adults, disruption of hormone production and fertility, immune disorders, increased growth rates, and early sexual maturation in children.[49]

Since the realization of the hazardous effects of BPA exposure, chemists have sought to replace it with similarly high-performing, yet safer alternatives.[51] However, this endeavor has proven difficult. Subtle alterations to the chemical structure of BPA often proves to significantly decrease the properties imparted to the end polymer, or fail to reduce

its toxicity enough to be socially relevant.[51] Analogues such as bisphenol F (BPF) (**20**), sulfur-bridged bisphenol (SBBP), oxygen-bridged bisphenol (OBBP), bisphenol S (BPS), bisphenol B (BPB), bisphenol E (BPE), and 4-cumylphenol (HHP) have been proven to be just as hazardous as BPA.[52, 53] The structures of these BPA analogues are shown in Figure 13 below.

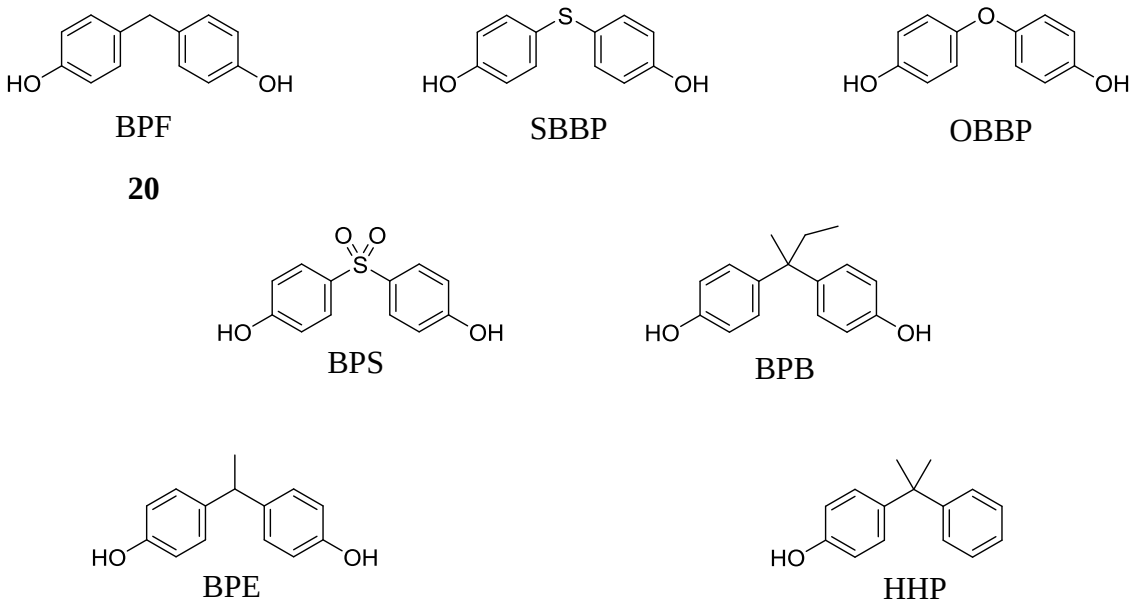

Figure 13. Structures of BPA alternative chemicals.

A quick glance at the above alternatives to BPA reveals that most efforts to date have been focused on alteration of the bisphenolic structure at the bridging site. However, none of these species have been proven to be less toxic than BPA, and in most cases yield polymers exhibiting decreased performance properties compared to identical polymers made using BPA. With this in mind, BPA replacements that target the ring substituents

for alternation are the next generation of this research. To this end, Hernandez et al. recently reported the synthesis of bisguaiacol (BG) (**21**) from vanillyl alcohol (**22**) and guaiacol (**2**) (Figure 14); a fully lignin-derived bisphenolic compound as a potential replacement for BPA.

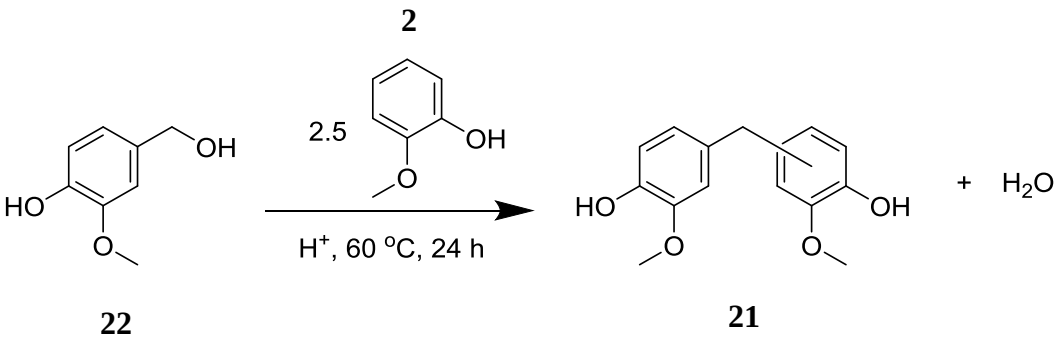

Figure 14. Synthesis of bisguaiacol (BG).[54]

While the BG monomer has been shown to be less toxic than BPA,[40] the properties of epoxy resins produced using it were significantly lower than those of BPA containing epoxy resins.[54] The synthesis of BG also results in a distribution of isomers that serve to decrease end polymer properties. The synthesis of BPA, however, is a highly selective reaction yielding greater than 95% of the *p,p'* isomer (regarding the positions of the hydroxyl groups relative to the bridge site), which is shown above in Figures 10 and 11, because phenolic hydroxyl groups are primarily para-directing for substitutions onto the aromatic ring.[55] In the case of some of the BPA alternatives shown in Figures 13 and 14, such as BPF and BG, the coupling reactions yield wide isomer distributions (82% *p,p'*, 15% *p,m'*, 3% *p,o'* for BG; 29% *p,p'*, 17% *o,o'*, 47% *o,p'*, and novalacs for BPF)[54, 56], interfering with the ability of the bisphenolic moieties in a polymer to orient and stack to

afford better properties. The isomer distributions associated with some of the alternatives to BPA effectively result in a less homogeneous and lower-performing end polymer. The synthesis of BPA, however affords a uniform product that can be produced cheaply in high quantities without the need for expensive purification methods. The uniform conformation of BPA means that its incorporation into growing polymer chains imparts regularity to the polymer in terms of chain linearity. The combination of linearized polymer chains, rigid aromatic rings in the backbone, and the possibility of stabilizing π-π stacking effects between polymer segments makes BPA indispensable in polymers. These properties are critical to polymers such as polycarbonates where high strength and toughness but with certain degrees of flexibility are required.

The second greatest consumption of BPA globally is in epoxy resins. The isomeric uniformity and the aromatic backbone of BPA imparts strength to the polymer network that forms upon reaction of glycidyl ether groups and amines. Epoxy resins are used extensively for their electrical resistance as socket and lighting components as well as in coatings and adhesives.[57, 58] Their highly crosslinked nature lends them high thermal stability and the ability to resist water and many organic solvents.

1.4 Glycidyl Ethers

The epoxide (also known as oxirane) (Figure 15) is the fundamental component of a glycidyl ether and is one of the reactive groups in the crosslinking reaction that forms epoxy-amine resins.[37] Discovered in the United States and Switzerland just prior to World War II, epoxy resins were initially sought after for dental applications. However, their high strength, good adhesive properties, and chemical resistance made them well-suited for many different applications.[59, 60]

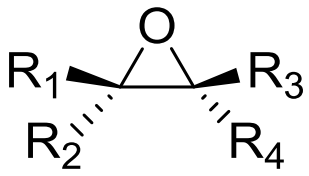

Figure 15. General structure of an epoxide functional group.

The epoxide is a very reactive functional group, susceptible to nucleophilic attack on the strained and electron-poor carbon atoms that make up two corners of its triangular shape. The reaction of amines with epoxides will be discussed in greater depth in Section 1.5. Epoxides can be formed via two major pathways: glycidation via epichlorohydrin (**23**) or other halohydrin, or via halohydroxylation of an alkene followed by base-initiated ring closure via an intramolecular S_N2 reaction (Figure 16).[37]

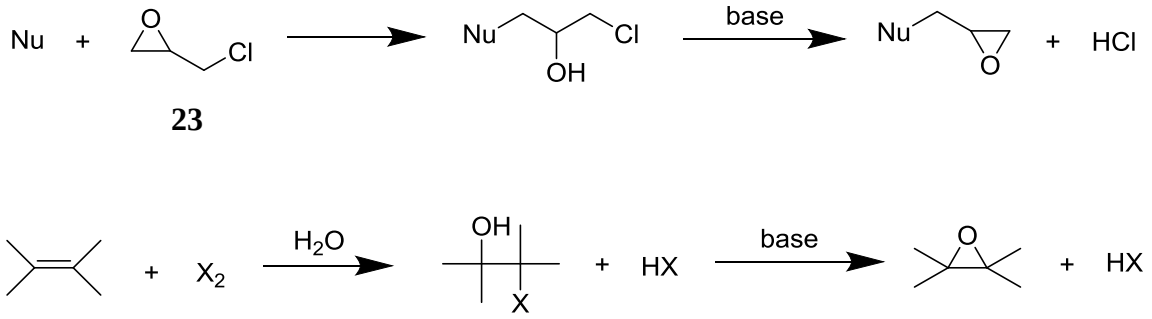

23

Figure 16. Mechanisms of two commercial epoxide synthetic pathways.

Epoxy resins find use in applications requiring good chemical and electrical resistance such as anti-corrosive protective coatings and paints, electrical wire insulation, and high strength applications such as those often found in the aerospace industry.

Epichlorohydrin has been a critical species in the development and proliferation of epoxy resins throughout global markets and industries. Historically, epichlorohydrin has been produced by the treatment of allyl chloride, a chlorinated derivative of petro-derived propylene, with hypochlorous acid resulting in a dichlorinated glycerol-type structure that is ring-closed with base as shown above.[61] This process is reliant on fossil resources and uses hazardous chemicals. However, epoxy resins are too versatile to easily eliminate. Recently, a process has been developed to produce epichlorohydrin from glycerol, a cheap byproduct of biodiesel production. The process, currently pursued by both Dow Chemical and Solvay, dichlorinates glycerol using hydrochloric acid and a carboxylic acid catalyst followed by the now familiar ring closure via base treatment. This method is considered a completely green alternative production scheme compared to its historical alternative.[62]

1.5 Epoxy-Amine Thermosets

Polymers can be loosely categorized into two main types; thermoplastics and thermosets. Thermoplastics are generally characterized by their ability to melt into a molten liquid state and be reformed into another shape.[37] Thermosets generally do not exhibit this ability due to high degrees of crosslinking between different polymer chains.[37] Often, thermosets are so highly crosslinked that individual chains nearly cannot be distinguished from one another, and the polymer is then considered to be networked. Figure 17 schematically shows the difference between a non-crosslinked thermoplastic, a lightly crosslinked polymer, and a highly crosslinked network thermoset.

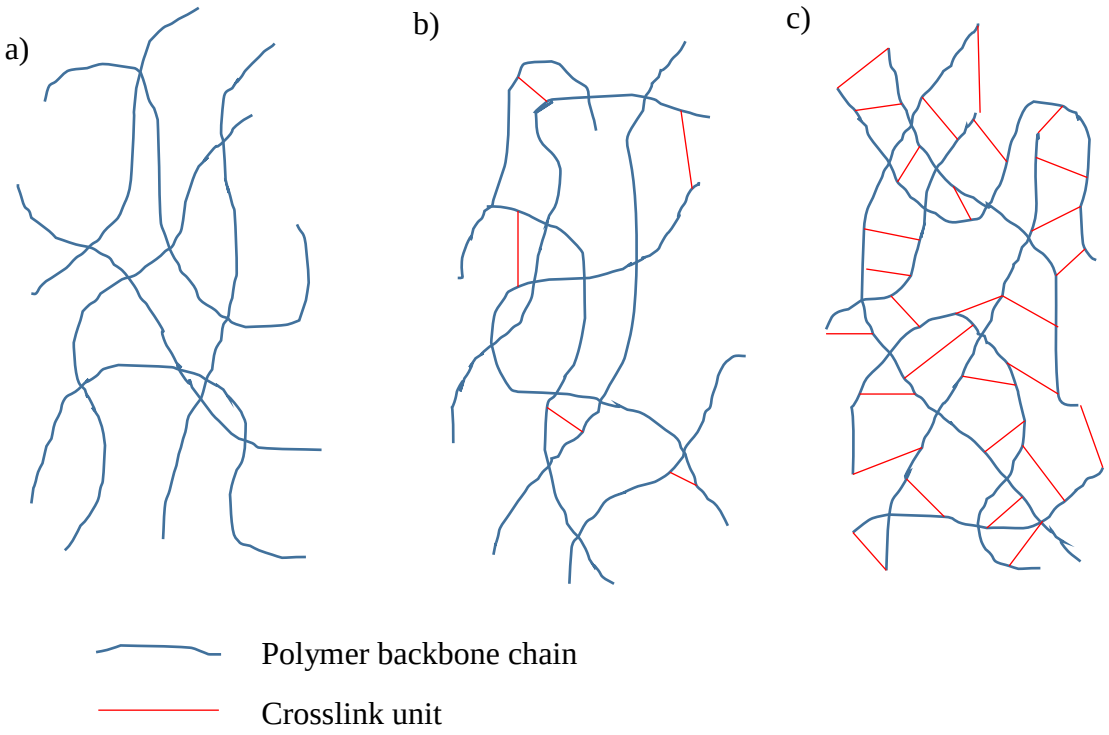

Figure 17. Schematic representations of a) uncrosslinked polymer chains, b) lightly crosslinked polymer, and c) highly crosslinked network polymer.

Epoxy-amine polymers are always highly crosslinked network polymers due to the two-fold reactivity of the amine functional group as shown in Figure 18.

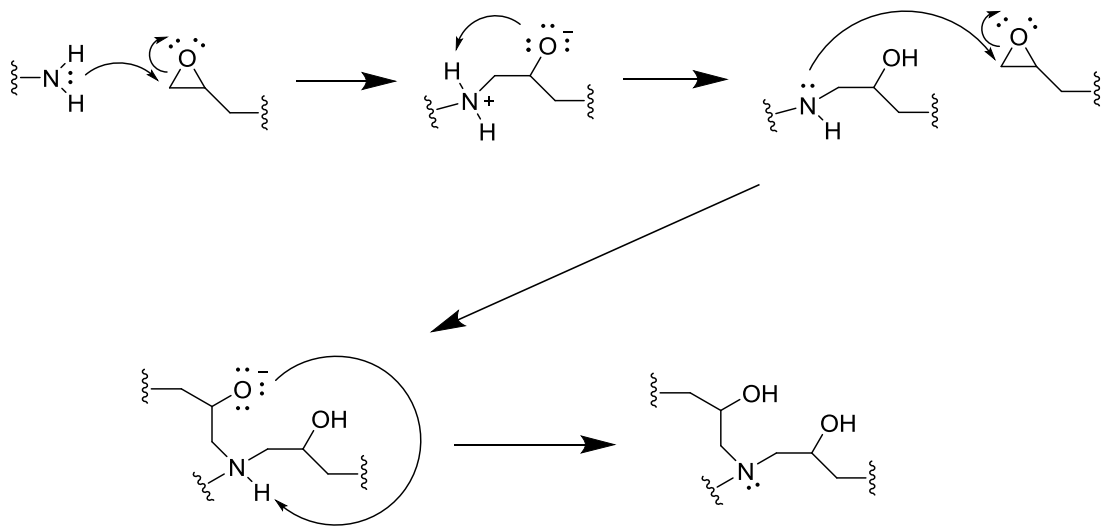

Figure 18. Mechanism of epoxy-amine reaction.

As illustrated above, amines react to form two linkages each. By utilizing diamines, each amine molecule can then form four linkages within the polymer network. In the case of difunctional bisphenol-based epoxy resins (Figure 19), the polymer network can propagate and become highly crosslinked as more reactions occur.

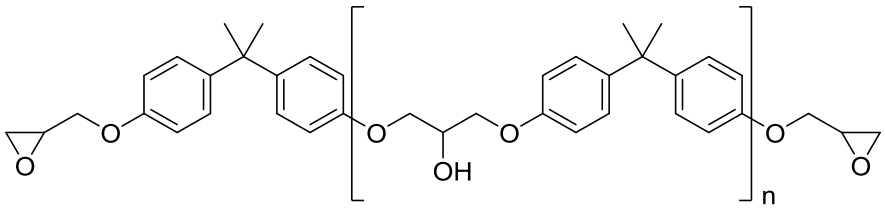

Figure 19. Structure of a bisphenolic diepoxy of BPA (diglycidyl ether of BPA (DGEBA)).

In general, a more highly crosslinked epoxy-amine system will exhibit a higher T_g than a like system with lesser crosslinking.[63] This property benefit comes at the expense of

strength, as a more rigid network tends to be more brittle than a more fluid network. With this in mind, a trifunctional analogue of BG, trisguaiacol (TrisG) (**24**) was hypothesized (Figure 20) and will be discussed in more detail in Chapter 4. The presence of three epoxy moieties would increase the amount of crosslinking between polymer chains in the network, and presumably increase the T_g of the epoxy-amine system relative to a like system made using BG.

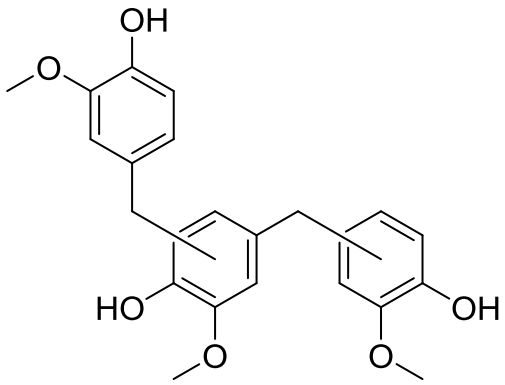

24

Figure 20. Structure of proposed triepoxy trisguaiacol (TrisG).

1.6 Polycarbonates and Polyesters

Polycarbonate has historically been produced by the reaction of bisphenol with phosgene (**25**), a toxic gas used as a weapon in World War I.[64, 65] A general reaction scheme of polycarbonate synthesis is given in Figure 21.

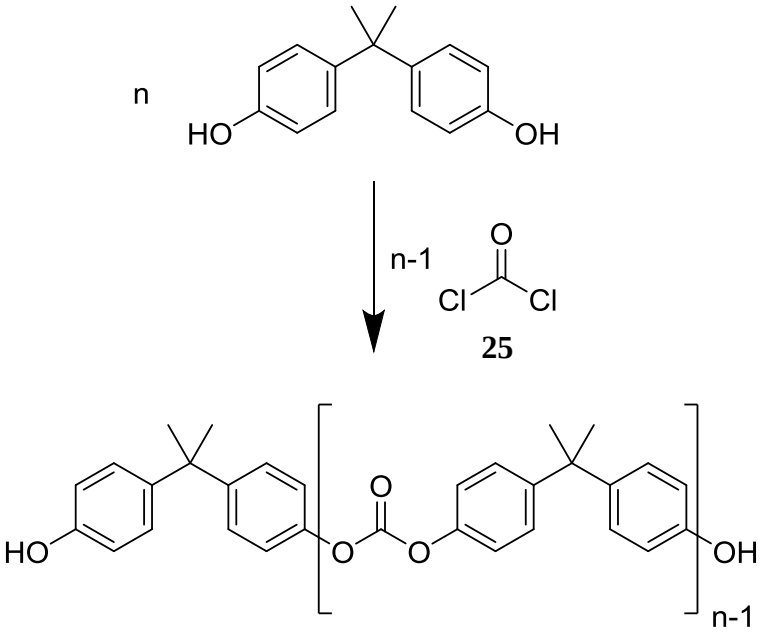

Figure 21. Scheme for the synthesis of polycarbonate from BPA and phosgene.

Polycarbonates are utilized in applications where optical clarity, and high strength energy absorption is required, such as in sports equipment, safety glass like eyewear and bullet-resistant sheeting, and automotive headlight lenses.[51, 64] The high aromaticity of the backbone chain lends a high-strength material.[51] Until recently, polycarbonate was used in the manufacture of bottles. Baby bottles made of BPA-polycarbonate were notorious for leaching residual BPA monomer into baby formula and milk, exposing infants to excessive concentrations of the hazardous chemical.[45, 46]

To avoid the use of phosgene, a synthetic method adapted from Martin et al. was used in this work which utilized p-nitrophenyl chloroformate as the carbonate source.[66] Other methods which bypass phosgene include condensation using dimethyl and diphenyl carbonates and even carbon dioxide as the carbonate source.[64, 67, 68] Many monomers

can be applied to polycarbonate synthesis, such as terpenes and quinones, which can also be bio-derived and expand the body of knowledge surrounding the use of xylochemicals in polymer applications.[69, 70]

Polyesters are another common class of polymers used in fibers for their strength and flexibility such as in clothing, ropes, conveyor and safety belts, and in plastic reinforcement for their high energy absorptive properties.[71, 72] They are typically synthesized via the condensation of a dicarboxylic acid (such as terephthalic acid (**26**))with an aliphatic diol; as in the production of polyethylene terephthalate (PET) (Figure 22).[73]

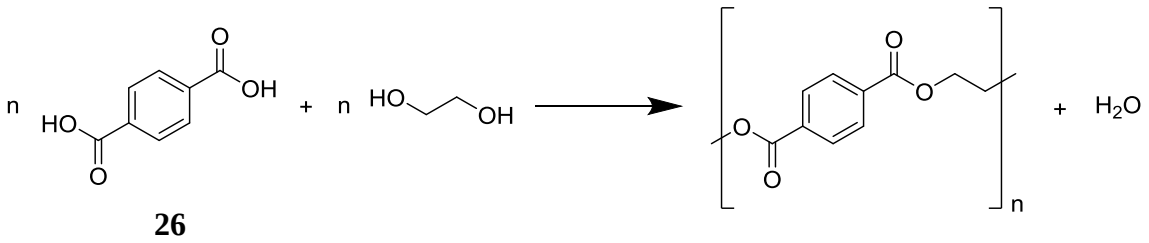

26

Figure 22. Condensation polymerization of PET.

The combination of aromatic rings and alkyl carbon chains in the polymer backbone lends a combination of strength and flexibility to the polymer.[74, 75] Increasing the aromatic content of the polymer backbone serves to boost the rigidity and thermal stability of the resultant material. A class of polyesters called polyarylates fit into this niche. Polyarylates are produced from the condensation of the acid chloride derivative of a dicarboxylic acid (**27**) with an aromatic diol (Figure 23).

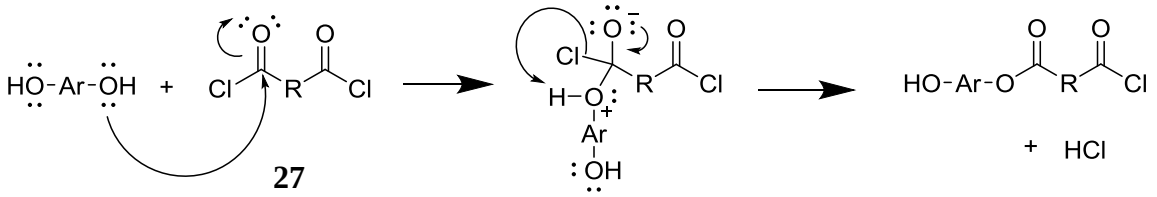

Figure 23. Mechanism of polyarylate condensation reaction.

The most common commercial polyarylates are polybisphenol-A terephthalate the product of condensation reaction between BPA and terephthalic acid chloride) and poly-4-hydroxybenzoate (Figure 24).[71]

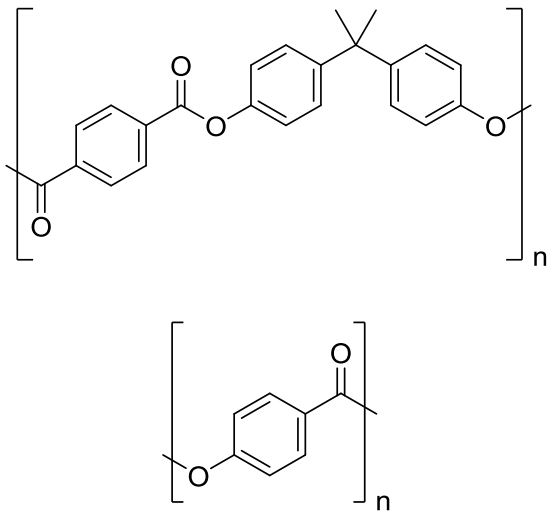

Figure 24. Polybisphenol-A terephthalate (top) and poly-4-hydroxybenzoate (bottom).

These polyarylates can exhibit some of the greatest heat resistances among clear polymer resins as well as excellent resistance to UV radiation.[71] These properties make polyarylates suitable for applications where weathering resistance is required such as in

coatings for solar panels or in high strength fiber applications such as advanced ropes and cables.[71, 76]

In this work, a preliminary investigation of the use of BG in the production of polyarylate was begun. Succinic acid is a four-carbon dicarboxylic acid which can be derived from biomass via the fermentation of glucose in biomass.[77, 78] In fact, this process is estimated to also require 60% less energy compared to the traditional petrochemical succinic acid production route.[77] Subsequently, through a reaction with thionyl chloride, carboxylic acids can be converted to acid chlorides, making succinyl chloride, and diacid chlorides of various carbon chain lengths, potentially biobased monomers for use in polyarylates.[79] If the condensation polymerization were to utilize BG, a highly-biobased polyarylate system could be produced to replace the high performance polyarylates of today which are petrochemical based (Figure 25).

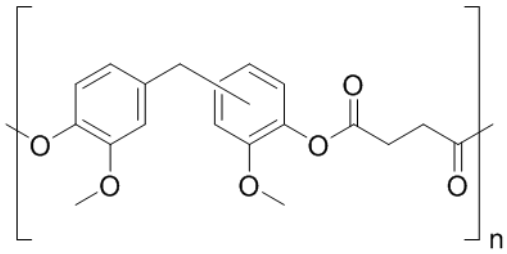

Figure 25. Highly bio-based polyarylate of BG and succinyl chloride.

1.7 Novel and Hetero-Difunctional Monomers and Polymers

Historically, polymers have often been designed from monomers that, while maybe being multifunctional, contained the same functional groups at every functional site.[37]

Examples of this include epoxy-amine polymers which are built from diepoxies and diamines, species that are individually multihomofunctional. Other polymers that utilize multihomofunctional monomers include polycarbonates, polyesters, polyethylene terephthalate and most other condensation polymers. Polymers such as polystyrene (**28**) which polymerize free-radically, often contain only one reactive functional group through which the polymerization progresses (Figure 26), but can also contain multihomofunctional species such as divinylbenzenes and dimethacrylates as well.[37]

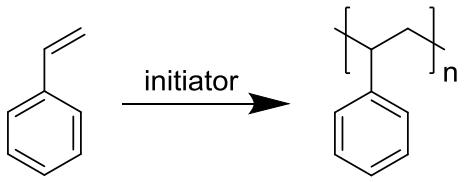

29 **28**

Figure 26. Styrene, a monofunctional monomer used to make polystyrene plastics.

Styrene (**29**) is a volatile human carcinogen used in the manufacture of many kinds of consumer goods from electrical and thermal insulation products, packaging materials, food-use items, automobile parts, and carpet manufacturing just to name a few.[80] Polystyrene packaging materials have been notorious for environmental persistence in landfills, and alternatives to this specific application which are composed of wheat and starches and are water soluble have recently been developed. However, the elimination of this hazardous chemical is an issue of increasing importance, as environmental and human health concerns become more prominent. Acrylates and methacrylates of lignin-derived

phenolics can be readily-accessible potential styrene replacements, owing to their reactive vinyl-type functionality.

Another potential styrene-like monomer available from lignocellulose is 4-vinyl guaiacol (4VG) (**30**). The enzymatic decomposition of lignocellulose-component ferulic acid (**31**) affords 4VG, a buckwheat flavor found in certain beers as a product of yeast activity and decarboxylation (Figure 27).[81]

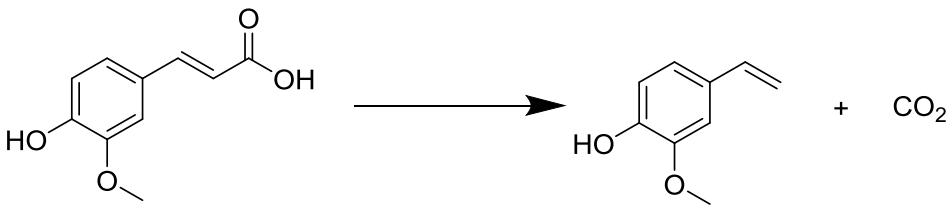

31 **30**

Figure 27. Enzymatic conversion of ferulic acid to 4VG.[81]

Functionalization of the hydroxyl site in 4VG should yield potential styrene replacement monomers. In particular, acetylation and allylation should afford novel monofunctional and hetero-difunctional styrene replacements.

In Chapter 1 of this thesis lignin and cellulosic biomass were presented as sources of valuable chemical building blocks as potential replacements for analogous petrochemicals in high performance polymer applications; in particular in epoxy-amine thermoset resins and in polycarbonates and polyesters. Chapter 2 will describe the general instrumental methods used to characterize the species synthesized in this work. Chapter 3 will detail the materials and experimental methods used in this work. A comprehensive discussion of

results including the properties of the synthesized polymers and novel monomers will be made in Chapter 4. Finally, Chapter 5 will offer conclusions and recommendations for future work beyond the scope of this thesis.

Chapter 2

Characterization Methods

2.1 Introduction

In this chapter, the various instrumental methods that were employed in this work to characterize both purchased and synthesized molecular species will be described. This chapter will serve as an overview of the fundamental underlying principles behind each characterization technique, with more detailed analysis of specific species in later section of this work. Of greatest importance to this work were nuclear magnetic resonance spectroscopy (NMR), gel permeation chromatography (GPC), Fourier transform infrared spectroscopy (FTIR), dynamic mechanical analysis (DMA), thermogravimetric analysis (TGA), differential scanning calorimetry (DSC), high resolution mass spectrometry (HRMS), melting point analysis (MP), and density determination.

2.2 Nuclear Magnetic Resonance Spectroscopy (NMR)

The first report of the use of NMR in bulk materials was in 1946 and was of such significance to merit the awarding of a Nobel Prize in physics.[82] Since then, NMR spectroscopy has become one of the most utilized methods for molecular characterization. An NMR experiment can take less than a minute to produce results that can definitively confirm or discount the presence and structure of a species in a sample. NMR spectroscopy is useful for determining the number of distinct atoms of the type being examined. Proton (^{1}H-NMR) and carbon (^{13}C-NMR) are two of the most common nuclei to study by NMR.[55, 83] Atoms with either an odd mass or atomic number or both possess any number of quantum spin states. These nuclei behave as if they were spinning. When placed in the path of an applied magnetic field, the nucleus begins to precess about its own spin

axis. The frequency of precession is proportional to the strength of the magnetic field. This precession of a charged nucleus generates an oscillating electric field with the same frequency as the precession. If the supplied radio waves from the magnetic field are of the same frequency as the generated electric field, the energies are coupled and absorbed by the nucleus, causing a spin change called resonance (Figure 28).[83] This change of spin state, and the associated change in energy of the nucleus via the release of radio waves is what is detected by the instrument.

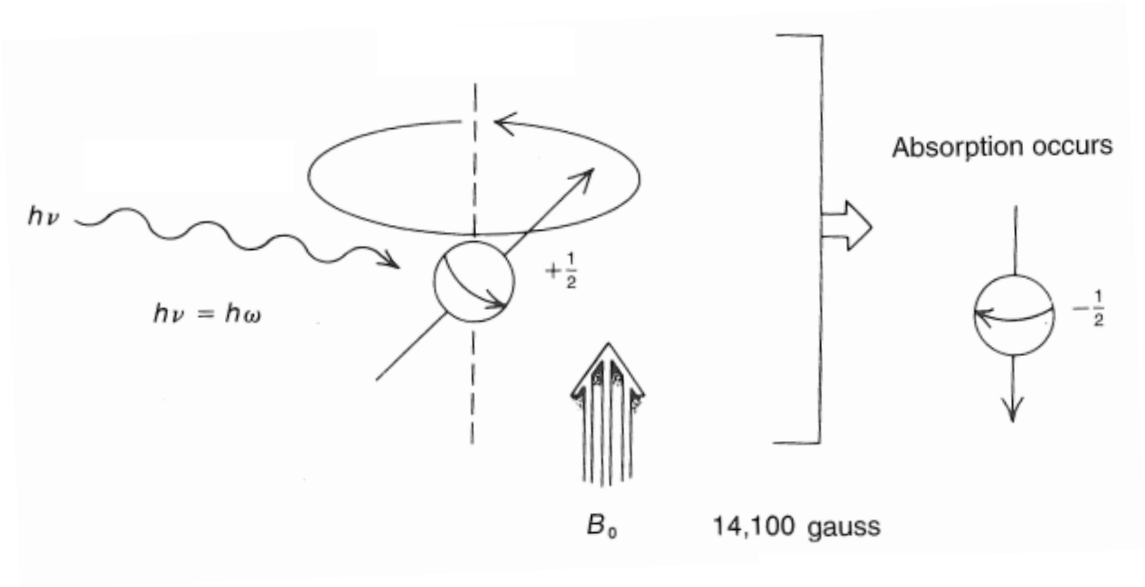

Figure 28. Schematic of precession, absorption, and resonance spin flip of an NMR active nucleus.[83]

According to basic effects of electronegative inductive electron shifting, as well as regular organic structural electron resonance effects, different atoms in a species are typically surrounded by unique amounts of electron density. In an applied magnetic field such as that found during an NMR experiment, this electron cloud which surrounds a

nucleus is forced to circulate. This circulation generates a counter magnetic field opposing the applied magnetic field. This opposing field effectively "shields" that nucleus from some of the applied magnetic field. As a result of different levels of electronic shielding of atoms in a species, the nuclei precess at different rates and thus absorb radio waves of different frequencies with different strengths.[83] By pulsing the electric field repeatedly for very short amounts of time, all of the nuclei can be excited at once. These nuclei then relax back to their lower energy state, and in doing so all emit varying frequencies of radiation dependent on the amount of electronic shielding they experience. The intensity of the energy decay versus time is acquired by the instrument. It is in this way that Fourier Transform (FT) NMR data is processed. The chemical shift (a field-independent measure of a nucleus's NMR signal location) can then be determined by applying a mathematical model called Fourier transform to convert the time domain data into frequency domain data, and ultimately be compared with data acquired from any spectrometer.

2.3 Fourier Transform Infrared Spectroscopy (FTIR)

Infrared spectroscopy (IR) generally refers to the visualization of functional groups that are present in a sample by measuring the different wavelengths of infrared radiation that are absorbed by the various types of bonds that could be present. Infrared radiation is of the required wavelengths and frequencies to cause vibration of the bonds in molecules. Bonds must exhibit a time-dependent dipole in order to absorb infrared radiation. This means that completely symmetric bonds (such as those in H_2 or Cl_2) do not absorb infrared radiation and therefore will not be visible via an IR experiment.

While electromagnetic radiation is typically measured in wavelength (the distance between two wave fronts in a single wave), the domain of IR experiments is measured in

wavenumber (the reciprocal of the wavelength measured in centimeters). This allows for a direct relationship between wavenumber and wave energy; whereas an inverse relationship exists between wavelength and wave energy.

The most common use of IR experiments is for the determination of structural features or functional groups in a molecule. Different groups can exhibit any or all of several types of bond vibrations. Stretching vibrations can be symmetric or asymmetric, while bending vibrations can consist of in-plane scissoring or rocking, or out of plane wagging or twisting.[83] For example, a methyl group ($-CH_3$) could exhibit both symmetric stretching (all three C-H bonds elongating or contracting in sync) and asymmetric stretching (two of the C-H bonds elongating at the same time as the other one is contracting). These two different modes of vibration absorb infrared radiation nearly 100 cm^{-1} apart (~2872 cm^{-1} for symmetric stretching, ~2962 cm^{-1} for asymmetric stretching). While this example is one of absorption in the mid-IR wavelengths, the FTIR experiments in this thesis primarily used near-IR wavelengths to characterize polymer resins.

2.4 Gel Permeation Chromatography (GPC)

Gel permeation chromatography is an analytical technique that is often included under the larger classification of size exclusion chromatography (SEC) techniques.[84] Trumping other traditional polymer characterization techniques, such as ultracentrifugation, SEC and GPC in particular have become highly automated and quite precise methods for polymer size and dispersity determination.[85] In a GPC experiment, a mixture containing various-sized compounds is applied to a solvent stream (often THF, DMF, or similar) and pumped through any number of columns packed with porous material and ultimately through a detector. In the case of GPC, the columns are packed with

crosslinked polystyrene gel polymer, which is macro- and micro-porous. Molecules are fractionated inside the columns based on their size.[84] Larger molecules cannot penetrate the smaller pores in the gel material and so are flushed through the system and arrive at the detector faster. Smaller molecules can explore the smaller pores and thus take longer to elute from the columns. Figure 29 details a schematic representation of a GPC system.

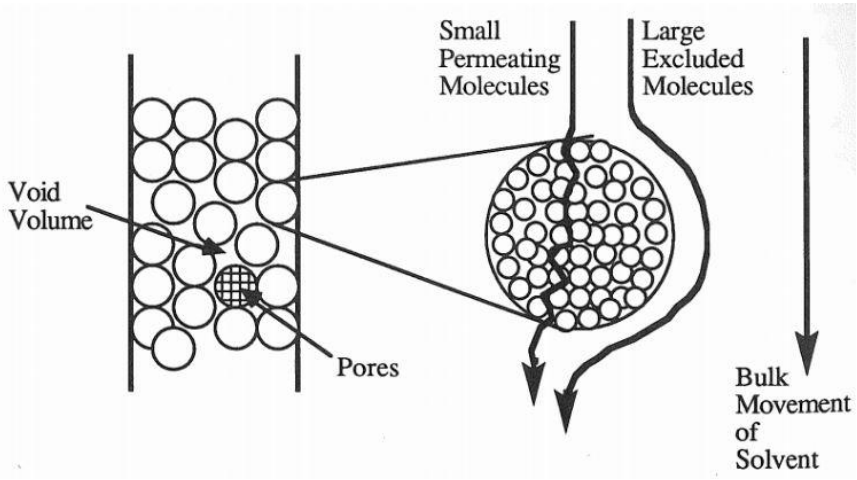

Figure 29. Schematic representation of GPC column and porous gel packing.[84]

Using standard samples of known and precise molecular weight, a GPC instrument can be calibrated to provide data on samples that are run through it. The exact mathematical methods used to calibrate the instrument used in this work and to subsequently lend meaning to the data output by the instrument with regard to samples prepared in this work will be discussed in the appropriate sections.

2.5 Dynamic Mechanical Analysis (DMA)

The purpose of performing a DMA experiment on a polymer is to determine the sample's viscoelastic properties such as moduli and transition temperatures.[86] During

dynamic mechanical testing, a constant sinusoidal strain is applied to a thin bar or film of a polymer sample. The stress response to the applied strain is recorded as function of time or temperature. The applied strain, unlike in fatigue testing, is not large enough to cause permanent deformation of the sample. The sample is simultaneously heated through a temperature gradient while being subjected to the sinusoidal strain. The strain function (ε) can be given by eq. 1, where ε^0 is the amplitude of the applied sinusoidal strain, ω is the frequency of oscillation, and t is time.

$$\varepsilon = \varepsilon^0 \sin(\omega t) \tag{1}$$

The resulting stress function (σ) is also oscillatory and is given as eq. 2, where σ^0 is the amplitude of the resultant stress function and δ is the phase angle between the stress and strain functions and is a measure of the viscous response of the material to strain.

$$\sigma = \sigma^0 \sin(\omega t + \delta) \tag{2}$$

Many polymers are classified as viscoelastic materials; they exhibit neither completely elastic behavior ($\delta = 0$) nor completely viscous behavior ($\delta = \pi/2$) and their behavior can be better described using a complex modulus (E^*, eq 3) which contains both real and imaginary components.

$$E^* = E' + iE'' \tag{3}$$

E' is the storage modulus, a measure of the energy stored in a polymer resulting from elasticity is given by eq 4.

$$E' = \left(\frac{\sigma^0}{\varepsilon^0}\right) cos\delta \tag{4}$$

The loss modulus, E'', is a measure of the energy lost due to motion within the polymer sample and is given by eq 5.

$$E'' = \left(\frac{\sigma^0}{\varepsilon^0}\right) sin\delta \tag{5}$$

Finally, the ratio of the loss and storage moduli called tanδ is another often-used parameter for the characterization of thermomechanical properties (eq 6).

$$tan\delta = \frac{sin\delta}{cos\delta} = \frac{E''}{E'} \quad (6)$$

Polymers at low temperature are typically stiff and glassy. As they are heated to and past their glass transition temperature, long-range molecular motions within the polymer become possible, characterized by a sharp decrease in E' and corresponding increase and peak in E''. Both the peaks of E'' and tan δ are used to quantify the glass transition temperature of a sample, however in this work the peak of E'' was primarily used because it offers a more conservative estimate of the polymer's glass transition temperature. The DMA testing performed in this work was done using single-cantilever clamp geometry (Figure 30).

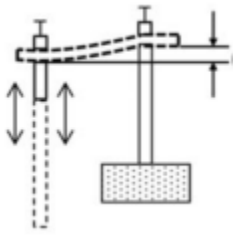

Figure 30. Schematic of single cantilever clamp geometry in DMA.

2.6 Thermogravimetric Analysis (TGA)

Thermogravimetric analysis experiments are performed on polymer samples to determine their thermal stability. TGA experiments in general measure the thermal and thermooxidative stability (TTOS) of a sample,[86] however in this work all TGA

experiments were performed in inert atmosphere and so thermooxidative stability was not investigated. During a TGA experiment, a small sample of a polymer is placed on a highly stable pan (in this work, platinum pans were used) and is subjected to a temperature gradient in a furnace. The pan mass is constant throughout the heating cycle, and so the instrument is able to measure the mass that is lost due to thermal degradation of the polymer. While some may use the retention of certain physical properties at high temperatures as the key criterion for thermal stability,[86] in this work the retention of mass and the temperature at which degradation begins were used as the criterion for thermal stability classification. While mass retention alone is not enough to determine a polymer's thermal stability, these experiments are much faster, cheaper, and easier to perform compared to high temperature property retention studies.[86]

The exact modes of thermal degradation are widely varied and can be very complex. For any chemical bonds that are broken by thermal energy new chemical bonds can form, resulting in substantially different physical material of comparable mass. However, two main types of degradation can occur; depolymerization and random chain scission.[86] Depolymerization can be imagined as the reverse of radical polymerization. Once a bond breaks into two radical species, those radicals proliferate and go on to break more bonds in the polymer in chain reaction style. In random chain scission, any bonds along the polymer backbone can break in any order until the final degraded state is reached.

2.7 Differential Scanning Calorimetry (DSC)

DSC experiments are useful for determining the various transitions that a polymer may exhibit such as glass transition temperature, melting temperature, and crystallization

temperatures. In this work, DSC was used to estimate the T_g of polymers which were not formed into uniform bars for standard DMA testing such as polycarbonate powders.

A DSC instrument consists of two identical cells; one containing a sample, and the other containing nothing as a reference (Figure 31).

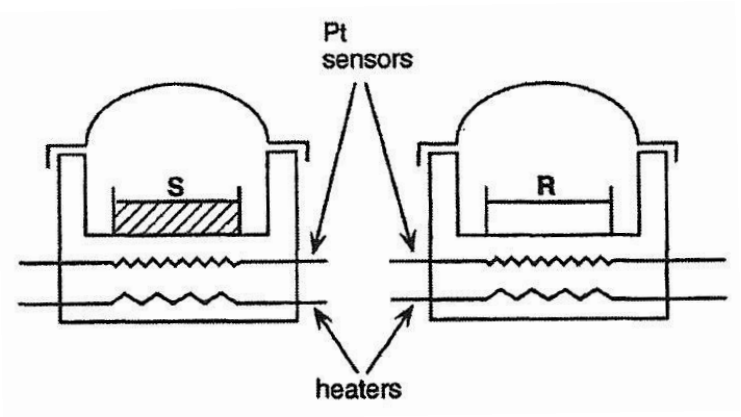

Figure 31. Schematic of a differential scanning calorimeter.[37]

A temperature gradient is applied to both pans simultaneously, and energy required to get each pan to the required temperature at any given time is detected by a sensor. When the sample inside the sample pan undergoes a transition (such as glass transition), the sensor detects a release of energy as the chains begin to move within the polymer (by requiring less supplied energy to maintain the sample's temperature). This internal energy release from the polymer contributes to the temperature of the pan and thus the instrument need apply less energy to that pan. This change in energy output is what is measured by a DSC instrument.

2.8 High Resolution Mass Spectrometry (HRMS)

Mass spectrometry predates all of the other instrumental methods described to this point. As early as the late 1890's research toward the mass-to-charge ratio of the electron and the deflection of anode would uncover the fundamental principles behind mass spectrometry and lead to two Nobel prizes (1906 – J. J. Thomson, 1911 – Wilhelm Wein).[83] The earliest mass spectrometer that would be recognizable today was built in 1918 by A. J. Dempster, however the use of mass spectrometry would not become commonplace in analytical research until the 1950's when instrumentation became less costly and more reliable.[83] Modern mass spectrometers generally consist of five components. First, a sample inlet where the compounds to be analyzed are brought from the ambient laboratory atmosphere and pressure to the high vacuum environment of the spectrometer leads to an ionization chamber where the molecules are transformed into gas phase ions by any of a number of methods to be discussed shortly. Next, these ions are accelerated by magnetic fields to a mass analyzer unit which separates the ions based on their mass-to-charge ratio. The separated ions are then counted by a detector and the information is recorded by a computer system.

Various ionization methods have been developed, each with their own strengths and drawbacks. The simplest and most common method of ionization is electron ionization (EI) (Figure 32).[83] In EI-MS, a metal filament is heated to several thousand degrees Celsius, emitting a stream of high energy electrons. These electrons are drawn across the path of the sample molecules from the sample inlet, and impact with them. The generated cationic molecule fragments from the molecule-electron impacts are draw forward into the

system by accelerating plates toward the mass analyzer. The majority of the sample molecules are left un-impacted and are drawn off via vacuum.

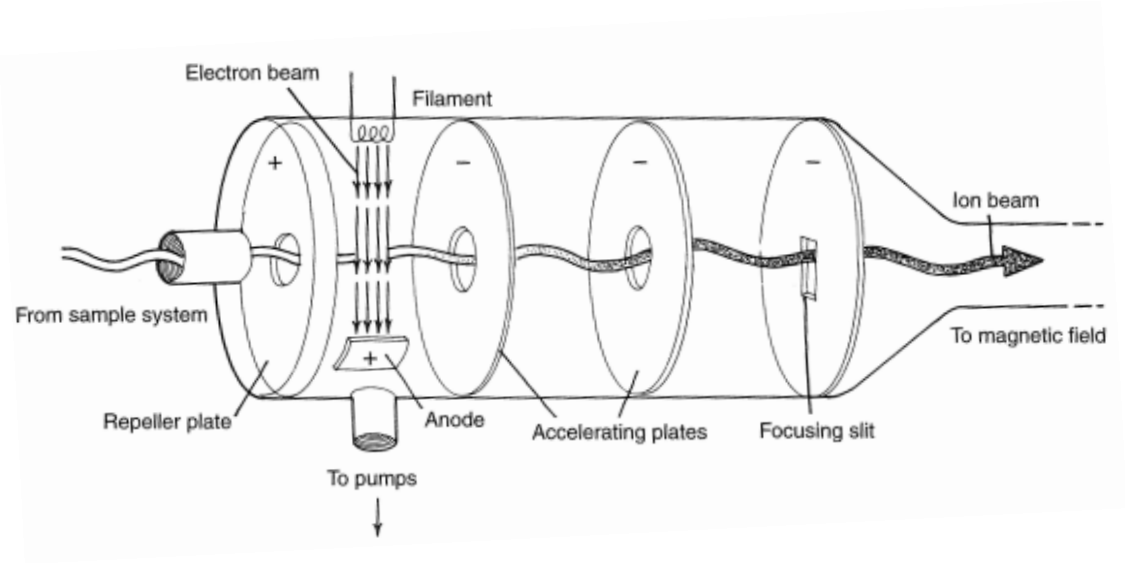

Figure 32. Schematic of an EI-MS ionization chamber.[83]

Another common ionization technique is chemical ionization (CI). In CI-MS an ionized reagent gas is introduced in high excess to the sample gas. Common compounds used as chemical ionization reagents include methane, ammonia, and methanol. If methane is used as the reagent gas, the typical ion formed between collisions of ionized reagent gas and sample molecules is protonated sample. The sample ions that form are thusly a combination of protonated sample molecule and protonated fragmented sample molecule. Varying the reagent gas results in the formation of different potential molecular adducts and fragmentation patterns.

Liquid injection field desorption ionization (LIFDI) MS is a type of desorption ionization technique. Desorption ionization involves the dispersion of the sample molecules in a matrix or solvent before a high energy beam of ions, atoms, or electrons is introduced.[83] The high energy beam produces clusters of the sample and matrix molecules which go on to ionize and proceed toward the mass analyzer as with the other techniques. The various other ionization techniques available for use in mass spectrometry are equally interesting, but discussion of them is beyond the scope of this work.

2.9 Density

Density measurements were taken of all cured polymers produced in this study. Using a density kit which attaches to a precision balance, density values could be obtained using Archimedes Principle according to eq 7.

$$\frac{solid\ density}{liquid\ density} = \frac{solid\ weight,dry}{solid\ weight,dry - solid\ weight,immersed} \quad (7)$$

The methodology involves weighing the sample on its own, then weighing the sample submerged in a known mass of liquid (usually water). While no universal correlations between polymer density and polymer properties have been developed to date, density measurements can be useful for comparing similar polymer systems and for predicting properties between similar polymers. In this work, density measurements were used to show that degradation did not occur during DMA analysis, indicated by no change in density of the sample pre and post DMA.

2.10 Melting Point (MP)

One of the simplest, and no doubt first chemical characterization techniques ever used is the melting point analysis. Most organic, non-crosslinked compounds possess a melting point at some temperature. The use of a melting point apparatus allows the precise

measurement of the melting point or melting point range of a sample. Any deviation from the exact melting point is an indication of the presence of impurities in the sample. MP analysis was used in this work to characterize all solid monomer species. MP analysis is not useful for characterizing epoxy-amine thermosets because those systems are highly crosslinked network polymers and therefore do not possess a melting point.

Chapter 3

Experimental Methods and Materials

3.1 Introduction

The materials and methods utilizing them will be discussed in this section. For the synthesis of polymers, methods and performance characteristics analysis will be discussed. The methods for the synthesis and characterization of novel monomeric materials will also be presented in the appropriate sections.

3.2 Materials

Vanillyl alcohol (4-hydroxy-3-methoxy benzyl alcohol, 99%), guaiacol (2-methoxyphenol, 99%), gastrodigenin (4-hydroxybenzyl alcohol, 99%), hydroquinone (benzene-1,4-diol, 99%), 4-dimethylaminopyridine (4-DMAP, 99%), BPA (97%), allyl bromide (99%, stabilized), potassium hydrogen phthalate (KHP, 99.99%), succinic acid (SA, 99%), succinyl chloride (SuccCl, 95%), potassium carbonate (K_2CO_3, anhydrous, > 99%), tetrabutylammonium bromide (TBAB, 99%), tetraethylammonium bromide (TEAB 99%), and deuterated chloroform (CDCl3, 99.8 atom % d) were purchased from Acros Organics. Epichlorohydrin (> 99%), Acetonitrile (99.8%, anhydrous), dimethylformamide (DMF, anhydrous, 99.8%), lithium bromide (LiBr, > 99%), triethylamine (Et_3N, > 99.5%), *p*-nitrophenyl chloroformate (96%), 4-vinyl guaiacol (2-methoxy-4-vinylphenol, 4-VG, > 98%), benzyltriethylammonium chloride (BTEAC, 99%), glacial acetic acid (> 99%), and Dowex® DR-2030 hydrogen form acid catalyst were purchased from Sigma Aldrich. Dichloromethane (DCM, 99.9%), tetrahydrofuran (Optima THF, 99.9%), hexanes (> 98.5%), ethyl acetate (EtOAc, > 99.5%), methanol (99.9%), ethanol (anhydrous), sodium borohydride ($NaBH_4$), sodium bicarbonate ($NaHCO_3$), sodium sulfate (Na_2SO_4)

(anhydrous), sodium hydroxide (pellets), toluene (99.9%), and perchloric acid (60%) were purchased from Fischer Scientific. Syringaldehyde (3,5-dimethoxy-4-hydroxybenzaldehyde, > 98%) and syringol (2,6-dimethoxyphenol, 99%) were purchased from Alfa Aesar. Acetic anhydride (> 99%) was purchased from Fluka Analytical. Crystal violet in glacial acetic acid indicator solution (1% w/v) was purchased from RICCA Chemical Company. Epon™ Resin 828 (diglycidyl ether of bisphenol A, DGEBA) was obtained from Momentive Specialty Chemicals Inc. BPF was obtained from TCI Chemicals. Compressed argon gas (Ar, 99.999%) and liquid nitrogen coolant were purchased from Praxair or Airgas. Polystyrene gel permeation chromatography (GPC) standards were obtained from Waters Corporation. DFDA (*5,5'*-methylenedifurfurylamine) was received from the Palmese research group at Drexel University, USA. BPA and BPF were purified by recrystallization in a 1:1 solution of glacial acetic acid and water before use. *p*-nitrophenyl chloroformate was purified by sublimation before use. All other materials were used as received.

3.3 Synthesis and Characterization of Lignin-Derived Diepoxy Monomers

BG, lignin-derived diepoxy monomers DGEGd, DGEVA, DGEBG, and DGEHQ, and furanyl diamine curing agent were synthesized as previously described in literature.[33, 35, 54] The diepoxy monomers were purified via silica gel flash chromatography on a Grace Reveleris X2 system using gradients of hexanes and ethyl acetate. The epoxy equivalent weights (EEWs) of epoxy monomers were determined according to ASTM D1652[87] in triplicate to obtain EEW values (Table 1), which were in agreement with those found in literature.[54] A solution of 0.1 *N* perchloric acid in glacial acetic acid was standardized against potassium hydrogen phthalate (KHP) using crystal violet indicator

(0.1% solution in glacial acetic acid). A co-reactant solution of 100 g TEAB dissolved in 400 mL of glacial acetic acid was made for use in the second titration step.

To a small flask equipped with a stir bar approximately 0.4 grams of epoxy monomer and 10 mL of DCM were added. The mixture was stirred to effect dissolution and 10 mL of TEAB solution and 6 drops of crystal violet indicator solution were added. The solution was titrated with the standardized 0.1 *N* perchloric acid solution to a blue-green endpoint stable for several minutes. The EEW of each epoxy sample was determined in replicate and an average value obtained for use in epoxy-amine resins. The formulas for determining EEW are given by eqs 8 and 9 where E is the weight percent epoxide, V is the volume of standardized perchloric acid solution used to titrate the sample, N is the actual normality of the perchloric acid solution, and W is the mass of sample used in each trial.

$$E = 4.3 \times V \times {}^{N}/_{W} \tag{8}$$

$$EEW = 43 \times {}^{100}/_{E} \tag{9}$$

Table 1

Epoxy equivalent weights of monomer species

Epoxy Resin	***EEW* [g/eq]**	***MW* [g/mol]**	***n*[a)]**
EPON828	190	340+284*n*	0.14
DGEGd	120	236+180*n*	0.02
DGEVA	133	266+210*n*	0.00
DGEBG	186	372+316*n*	0.00
DGEHQ	111	222+166*n*	0.00

[a)] n = average repeat unit based on EEW and MW

The very low n-values (average repeat unit) of the bio-derived epoxy species, along with NMR and melting point characterizations confirm the presence of high-purity monomeric species which allows for direct structure-property comparison between polymers composed of these compounds.

3.4 Synthesis and Characterization of Highly Bio-Derived Epoxy-Amine Thermosets

Thermoset resins consisting of DGEGd, DGEVA, DGEHQ, or DGEBG and diamine curing agent DFDA (Figure 33) were prepared in 1:1 stoichiometry relative to reactive amine hydrogens and epoxy functionality.

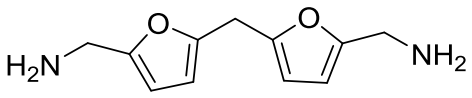

Figure 33. Diamine curing agent *4,4'*-methylenedifurfurylamine (DFDA).

DGEGd is a liquid at room temperature and DGEVA is a low-melting solid (mp ≈ 45 °C) and therefore both of these species could be used in 100% proportions along with the diamine curing agent. Due to DGEHQ and DGEBG being high-melting solids (mp = 114 °C and 110 °C, respectively), resin blends with DGEGd were developed to incorporate these species into thermosets, the EEWs of which were determined using eq 10, where W_{total} is the total weight of the resin, W_{E1} and W_{E2} are the weights of epoxies 1 and 2, respectively, and EEW_{E1} and EEW_{E2} are the epoxy equivalent weights of epoxies 1 and 2, respectively.

$$EEW_{\text{Blend}} = \frac{W_{\text{Total}}}{\frac{W_{\text{E1}}}{\text{EEW}_{\text{E1}}} + \frac{W_{\text{E2}}}{\text{EEW}_{\text{E2}}}} \quad (10)$$

In order to ensure stoichiometric addition of amine to the epoxy, the system's *phr* was used (eq 11), where *phr* is the parts of amine per hundred parts epoxy resin and *AHEW* is the amine hydrogen equivalent weight ($AHEW_{DFDA}$ = 51.57 g/eq).[35]

$$phr = \frac{\text{AHEW}\times 100}{EEW_{Blend}} \tag{11}$$

EEW stoichiometric data on the resin blends synthesized in this work are summarized in Table 2.

Table 2

Epoxy equivalent weights of epoxy resin blends

	DGEGd: DGEBG: DFDA		**DGEGd: DGEHQ: DFDA**	
W_{DGEGd}:W_E[a)]	***EEW* (g/eq)**	***phr***	***EEW* (g/eq)**	***phr***
1.00:0.00	120	43.04	120	43.04
0.75:0.25	131	39.24	117	44.00
0.50:0.50	145.55	35.43	115	44.96

[a)] W_E = weight fraction DGEBG or DGEHQ in blend before addition of DFDA.

In total, seven thermosets were produced for characterization in the structure-property relationship study of these highly bio-based epoxy-amine systems. Thermogravimetric analysis of each thermoset was performed on a TA Instruments Discovery thermogravimetric analyzer (≈ 2 mg samples, Pt sample pans, ramp to 600 °C at 20 °C min^{-1} in Ar atmosphere, 10 mL min^{-1} balance and sample gas flowrates). DMA was performed on uniform bars of each epoxy-amine thermoset using a TA Instrument Q800 dynamic mechanical analyzer (1.0 Hz frequency, Poisson's ration = 0.35, deflection amplitude of

oscillation = 7.5 μm, ramp from 0 °C to 200 °C at 2 °C min^{-1}). n-FTIR measurements were obtained in the range of 4000-8000 cm^{-1} at room temperature using a Thermo Scientific Nicolet iS50 FTIR spectrometer (64 scans, 8 cm^{-1} resolution, transmission mode) in dry air atmosphere.

3.5 Extent of Cure

The near-IR spectrum encompasses wavenumbers between 4000 and 10000 cm^{-1} and is especially useful to this work for distinguishing absorptions typical of oxiranes and amines. These peaks can be quantified to determine an extent of cure, or the amount of each group that has reacted to form polymer. A typical n-FTIR spectrum showing both pre- and post-cure spectra is shown in Figure 34.

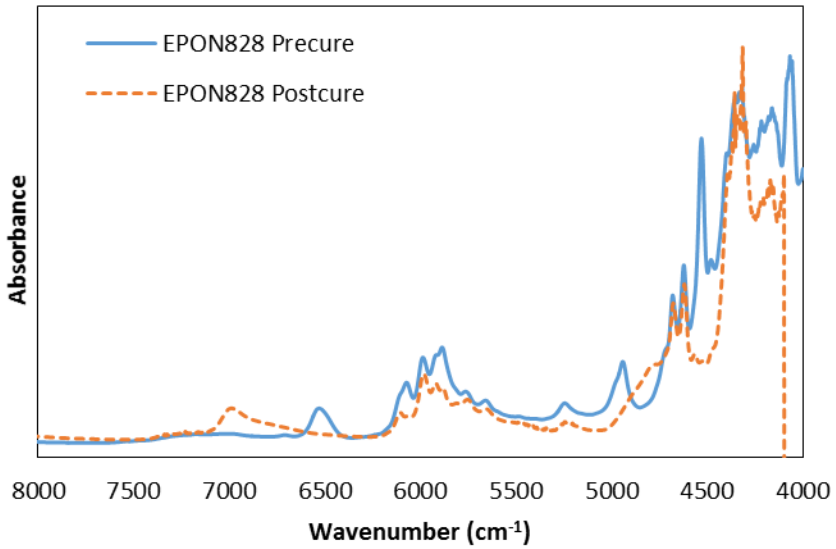

Figure 34. Typical n-FTIR spectrum used to determine extent of cure (EPON828 resin blended with DFDA).

Several peaks in the spectrum above are indicative of the functional groups that participate in the epoxy-amine curing reaction. In the pre-cure spectrum, oxirane functional groups of the epoxy molecules are visible around 4500 cm^{-1} with primary amine functionality around 5000 cm^{-1} and both primary and secondary amine functionalities are visible at approximately 6500 cm^{-1}. As described in Chapter 1, hydroxyl groups are formed as a result of the epoxy-amine reactions, and these can be seen as a broad peak around 7000 cm^{-1} in the post-cure spectrum. It is also important to point out the complete lack of oxirane and amine signals in the postcure spectrum, indicating complete reaction (≈ 100% extent of cure) within the limits of IR analysis as well as a blend consisting of nearly exact 1:1 stoichiometry between epoxy and amine functionalities. The equation used to quantify the extent of cure of resins produced in this work is given by eq 12, where the peaks around 5900 cm^{-1} are used as a reference.

$$Extent\ of\ Cure = \frac{\left(Abs_{4530}/Abs_{ref}\right)_{precure} - \left(Abs_{4530}/Abs_{ref}\right)_{postcure}}{\left(Abs_{4530}/Abs_{ref}\right)_{precure}} \quad (12)$$

3.6 Synthesis and Characterization of Lignin-Derived Bisphenolic Polycarbonate

The stoichiometric ratios of the reagents used in the three different polycarbonate syntheses were consistent (Figure 35).

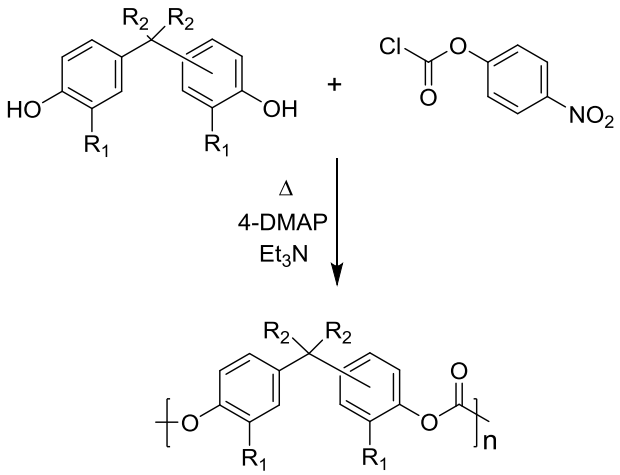

Figure 35. Reaction scheme for the synthesis of polycarbonate.

The synthesis of polycarbonate using BG (in Figure 35 R_1 is OCH_3 and R_2 is hydrogen) will be described here while analogous procedures were used using BPA (R_1 is hydrogen and R_2 is CH_3 in Figure 35) and BPF (R_1 and R_2 are hydrogen in Figure 35). BG (1 eqv) and 4-DMAP (0.03 eqv) were added to a three-necked round bottom flask. Acetonitrile was added to these reagents to form a 0.26 *M* solution and the flask was purged with Ar gas. Another round bottom flask was charged with *p*-nitrophenylchloroformate (1 eqv) and acetonitrile was added to form a 0.5 *M* solution and this flask was also purged with Ar gas. The solution containing *p*-nitrophenylchloroformate was cannulated into the flask containing the other solution of reagents and stirred. 2 equivalents of triethylamine was added dropwise to this final mixture over two minutes and an aliquot (to be referred to as t = 0) was immediately removed and quenched in methanol. The reaction mixture was heated to 70 °C and stirred for 48 hours. Aliquots were again removed after 1, 3, 24 and 48 hours of reaction and quenched in methanol. Aliquots were stirred in warm methanol to remove all traces of yellow color to yield fine white powder polycarbonates of BG, BPA, and BPF.

Polycarbonates were analyzed via GPC to determine the molecular weight of each aliquot to visualize the growth of the polymer chains. Due to solubility differences between the three polycarbonates, and even between aliquots of like polycarbonate, GPC was performed on either a Waters 717 module in DMF with 0.05 *M* LiBr (for BG-PC and BPF-PC) or on a Waters 2695 Separations module in THF (for BPA-PC). NMR spectra of the final aliquots of each polycarbonate were obtained in deuterated DCM (DCM-d_2). DSC analysis was performed on the final aliquot of each polycarbonate species to estimate the T_g of each polymer using a TA Instruments Q1000 differential scanning calorimeter (≈ 3 mg samples, ramp to 200 °C at 10 °C min^{-1} in N_2 atmosphere). Thermogravimetric analysis of each final aliquot was performed on a TA Instruments Discovery thermogravimetric analyzer (≈ 2 mg samples, Pt sample pans, ramp to 600 °C at 20 °C min^{-1} in N_2 atmosphere). ^{1}H NMR spectra are available in Appendix A.

3.7 Synthesis of Biomass-Derived Bisphenolic Polyarylate

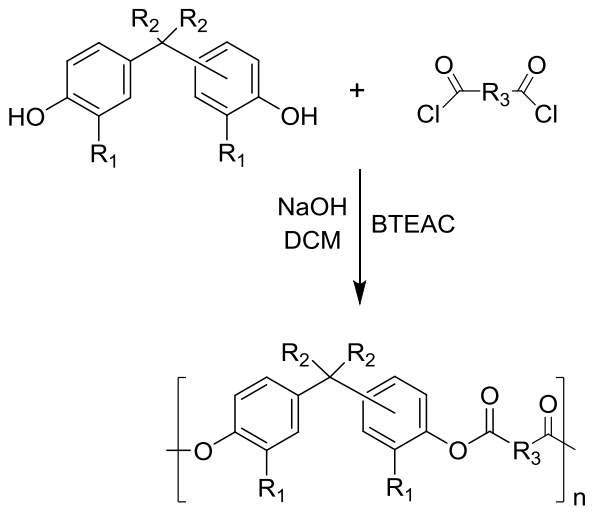

Figure 36. General reaction scheme for the synthesis of polyarylates.

The general reaction scheme for the preparation of bisphenolic polyarylates is given in Figure 36. In Figure 36, for BPA, R_1 is hydrogen and R_2 is CH_3. For BG, R_1 is OCH_3 and R_2 is hydrogen. R_3 is ethylene for succinyl chloride. To a 3-necked round bottom flask equipped with a mechanical stirrer was added BPA (2.00 g, 0.008761 mol), BTEAC (0.01996 g, 1 mol %), and 1 *M* aqueous NaOH solution (21.03 mL). This mixture was stirred to effect dissolution of phenolate into the aqueous media. To a constant pressure dropping funnel was added DCM (52.6 mL) and SuccCl (0.9658 mL, 0.008761 mol). This mixture of acid chloride was added dropwise over 20 minutes to the aqueous solution along with very vigorous mixing. Upon complete addition of the acid chloride, the biphasic reaction mixture was vigorously mixed for 3 hours at room temperature.

The biphasic mixture was allowed to settle and the contents were poured directly into an Erlenmeyer flask containing an equal volume of ethanol. A product resembling brown taffy precipitated. This brown material was collected and stirred in hot water overnight to wash away salts. The lighter colored tan polyarylate product was then dried and crushed into a fine powder in a mortar. DSC and GPC analysis were performed. ^{1}H-NMR of the produced polymer is available in Appendix A.

3.8 Novel and Hetero-Difunctional Monomers and Styrene Replacement

Two hetero-difunctional monomeric species were synthesized from 4-VG to be used in preliminary free-radical polymerization to assess potential polymer properties of these styrene replacements. Allylated 4-VG (Al4VG) and acetylated 4-VG (Ac4VG) were synthesized as follows.

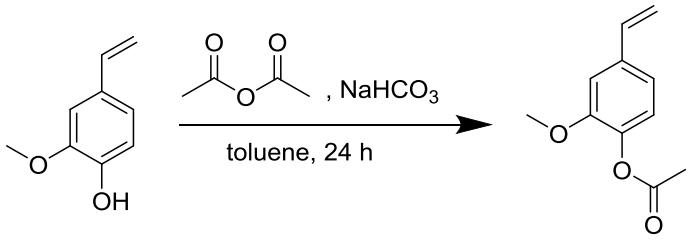

Figure 37. Reaction scheme for the synthesis of Ac4VG.

To synthesize Ac4VG (Figure 37), a round bottom flask equipped with a magnetic stir bar was charged with 4-VG (3.00 g, 0.01998 mol), toluene (120 mL), sodium bicarbonate (3.357 g, 0.03996 mol), and acetic anhydride (9.4433 mL, 0.0999 mol). The reaction mixture was allowed to stir at room temperature for 24 hours before the mixture was vacuum filtered and the organic filtrate was concentrated under reduced pressure. DCM was added to the resultant residue, and the organic phase was extracted with water three times before drying over sodium sulfate and concentrating again under reduced pressure. The resultant oil was purified via flash chromatography (hexanes/EtOAc eluent) to produce Ac4VG as a clear oil in 67% yield.

^{1}H NMR ($CDCl_3$, 400 MHz) δ ppm 2.31 (3 H, s), 3.85 (3 H, s), 5.24-5.26 (1 H, dd, J = 10.8, 0.6 Hz), 5.68-5.72 (1 H, d, J = 17.6 Hz), 6.65-6.72 (1 H, dd, J = 17.6, 10.8 Hz), 6.99-7.01 (3 H, m).

^{13}C NMR ($CDCl_3$, 101 MHz) δ ppm 20.65 (1 C, s), 55.81 (1 C, s), 109.88 (1 C, s), 114.08 (1 C, s), 118.91 (1 C, s), 122.75 (1 C, s), 136.27 (1 C, s), 139.42 (1 C, s), 151.07 (1 C, s), 169.02 (1 C, s).

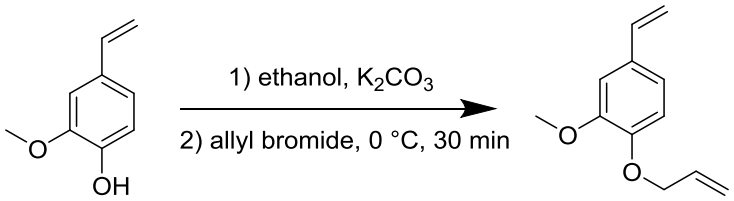

Figure 38. General reaction scheme for the synthesis of Al4VG.

To synthesize Al4VG (Figure 8), a round bottom flask equipped with a magnetic stir bar was charged with 4-VG (3.00 g, 0.01998 mol) and enough ethanol to form a 0.5 *M* solution (39.96 mL). This mixture was cooled in an ice bath and K_2CO_3 (5.5229 g, 0.03996 mol) was added and stirred for 10 minutes. Allyl bromide (3.4780 mL, 0.03996 mol) was added dropwise via syringe and the reaction was stirred for 30 minutes in the ice bath. The reaction vessel was then removed from the ice bath and allowed to stir for 6 days at room temperature. Water was then added, and the mixture was extracted 3 times with hexane. The combined organic phase was washed with brine and dried over Na_2SO_4 and concentrated under reduced pressure. The resultant pale yellow oil was purified via flash chromatography using hexanes/EtOAc as eluent solvent to yield a clear oil Al4VG product in 58% yield.

^{1}H NMR ($CDCl_3$, 400 MHz) δ ppm 3.90 (3 H, s), 4.60-4.63 (2 H, dt, J = 5.3, 1.6 Hz), 5.14-5.16 (1 H, dd, J = 11, 0.7 Hz), 5.27-5.30 (1 H, dq, J = 10.4, 1.4 Hz), 5.38-5.43 (1 H, dq, J = 17.3, 1.6), 5.59-5.64 (1 H, dd, J = 17.6, 0.9 Hz), 6.05-6.12 (1 H, m), 6.61-6.68 (1 H, dd, J = 17.6, 10.8), 6.82-6.84 (1 H, m), 6.90-6.92 (1 H, m), 6.97-6.98 (1 H, d, J = 2.1).

^{13}C NMR ($CDCl_3$, 101 MHz) δ ppm 55.87 (1 C, s), 69.85 (1 C, s), 109.00 (1 C, s), 111.89 (1 C, s), 113.22 (1 C, s), 117.98 (1 C, s), 119.28 (1 C, s), 131.04 (1 C, s), 133.25 (1 C, s), 136.46 (1 C, s), 147.93 (1 C, s), 149.45 (1 C, s).

3.9 Synthesis of Trisguaiacol

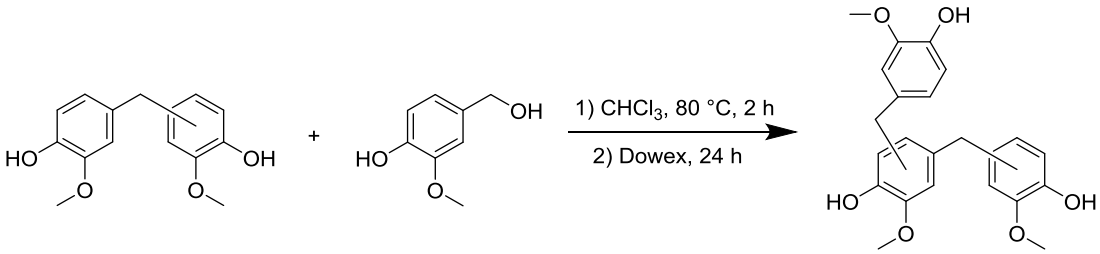

Figure 39. General reaction scheme for the synthesis of trisguaiacol.

To synthesize trisguaiacol (Figure 39), to a three necked round bottom flask equipped with a reflux condenser and magnetic stir bar was added vanillyl alcohol (1.00 g, 0.0065 mol), BG (8.441 g, 0.032 mol), and a minimum of chloroform to just dissolve all the solids. The reaction vessel was stirred and heated to relux (≈ 80 °C) for 2 hours before Dowex catalyst (1.05 g, 10 wt%) was added. The reaction mixture was allowed to stir at reflux overnight. The reaction mixture was allowed to cool down to room temperature and was vacuum filtered to remove the catalyst particles. The organic filtrate was extracted three times with water, dried over sodium sulfate, and concentrated under reduced pressure. The resultant solid mixture was purified via flash chromatography to yield a clear viscous liquid which foamed when placed under strong vacuum to remove trace solvents. Several weeks under vacuum were insufficient to remove all residual solvent, and ethyl acetate could be observed in ^{1}H-NMR (spectrum available in Appendix A). ^{13}C-NMR of the product trisguaiacol (**24**) produced inconclusive results, presumably due to the high number of isomers present in the sample.

3.10 Synthesis of Bissyringol

Bissyringol (BS) was synthesized from the coupling of syringyl alcohol with syringol via the same method used for the synthesis of BG. Syringyl alcohol (**32**)was first produced via a classic sodium borohydride reduction of syringaldehyde (**7**) (Figure 40).[88]

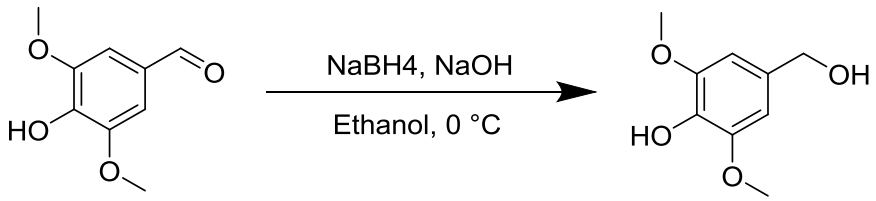

7 **32**

Figure 40. Reaction scheme for the reduction of syringaldehyde to syringyl alcohol.

Syringaldehyde (10 g, 0.055 mol) and ethanol (16.5 mL) were added to a round bottom flask and stirred magnetically. To an attached constant pressure dropping funnel a solution of $NaBH_4$ (2.077 g, 0.055 mol) in 1 *M* NaOH (16.05 mL) was added. The reaction flask was immersed in an ice bath and the $NaBH_4$ solution was slowly added dropwise to allow the release of generated hydrogen gas. Upon complete addition of the $NaBH_4$ solution, the reaction flask was removed from the ice bath and allowed to stir for 5 minutes at room temperature to complete reaction. The flask was returned to the ice bath and 6 *M* hydrochloric acid was added dropwise until the reaction mixture reached a pH of 3. This mixture was allowed to stir for 10 minutes in the ice bath. The reaction mixture was vacuum filtered and washed with ice cold water. The filter cake was collected and dried to yield a fluffy white powder syringyl alcohol (7.9719 g) (Figure 31) in 79% yield.

^{1}H NMR ($CDCl_3$, 400 MHz) δ ppm 1.66 (1 H, s broad), 3.89 (6 H, s), 4.61 (2 H, s), 5.52 (1 H, s broad), 6.61 (2 H, s).

^{13}C NMR ($CDCl_3$, 101 MHz) δ ppm 56.28 (2 C, s), 65.71 (1 C, s), 103.84 (2 C, s), 132.03 (1 C, s), 134.18 (1 C, s), 147.08 (2 C, s).

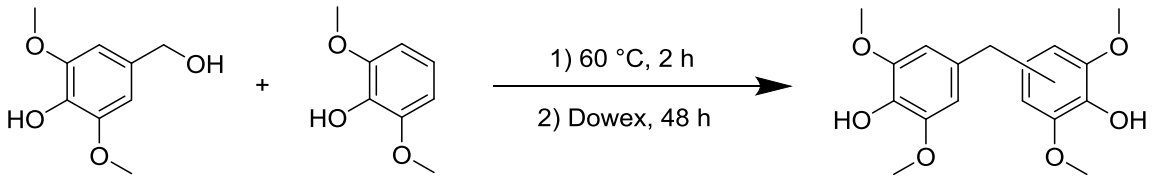

32 **3** **33**

Figure 41. General reaction scheme for the synthesis of bissyringol.

Bissyringol (**33**) was synthesized using the produced syringyl alcohol (Figure 41). Syringyl alcohol (2.00 g, 0.0109 mol) and syringol (4.18 g, 0.02715 mol) were added to a three necked round bottom flask. The mixture was magnetically stirred and warmed to 60 °C in an oil bath to melt the syringol and dissolve the syringyl alcohol. This mixture was stirred at 60 °C for 2 hours and Dowex catalyst (0.62 g, 10 wt%) was added. The reaction mixture was allowed to stir at temperature for 2 days before it was dissolved in DCM and vacuum filtered to remove the catalyst particles. The organic filtrate was extracted with an equal volume of water three times and the organic phase was then dried over sodium sulfate and concentrated under reduced pressure to yield a thick dark brown oil. This product contained a mixture of excess reagent syringol, product bissyringol, and residual unreacted syringyl alcohol. While syringol was removable, complete separation of syringyl alcohol from bissyringol was impossible via flash chromatography after several attempts.

Chapter 4

Results and Discussion

4.1 Introduction

The main objectives of this work were to produce and characterize a series of epoxy-amine thermoset resins derived nearly entirely from lignocellulosic biomass as well as to screen a recently developed and promising bisphenolic analogue of BPA (BG) in polycarbonate and polyester applications. Secondarily, novel monomeric species derived from lignin and other biomass were developed and preliminary testing was performed on their resultant polymers.

4.2 Highly Bio-Based Epoxy-Amine Thermosets

The bio-based contents of each epoxy-amine thermoset resin were calculated using the carbon contents of each sample as the basis. The lignin derived phenolics were considered to be fully bio-derived. Epichlorohydrin was also considered to contain only bio-derived carbon atoms based on the Solvay glycerol to epichlorohydrin process. Therefore every carbon atom in the lignin-derived diepoxies can be considered bio-based. The diamine curing agent, DFDA is synthesized by the bridging of two furfurylamines with formaldehyde, leaving only that formaldehyde carbon atom in DFDA as not bio-derived. Table 3 summarizes the bio-derived contents of each cured resin.

Table 3

Bio-derived carbon contents of epoxy-amine thermosets

Epoxy Resin Cured with DFDA	Bio-derived Carbon Content (%)
100% EPON828[a]	17.21
100% DGEGd	97.33
100% DGEVA	97.43
25:75 DGEBG:DGEGd	97.51
50:50 DGEBG:DGEGd	97.70
25:75 DGEHQ:DGEGd	96.84
50:50 DGEHQ:DGEGd	97.26

[a)]estimate assumes bio-based epichlorohydrin used

The cured resins synthesized in this work were all examined by n-FTIR to determine the extent of cure of the resins. High extents of cure are critical for obtaining the best possible performance properties in cured resins. Unreacted groups serve to plasticize the polymer network, decreasing crosslinking and lowering T_g and stiffness. Within the limits of FTIR spectroscopy all resins were greater than 99% cured with respect to consumption of the epoxy functionality. The equations and signals used in extent of cure determinations are discussed in detail in Chapter 3 of this work and n-FTIR spectra of all resins produced in this work are available in Appendix B.

The major property characterization methods used in this work were DMA and TGA. Major structure-property relationships were in agreement with those of similar systems found in literature.[54] The use of DFDA produced cured resins possessing high thermal

stability. TGA thermograms and experimental results are shown and summarized in Figure 42 and Table 4 respectively.

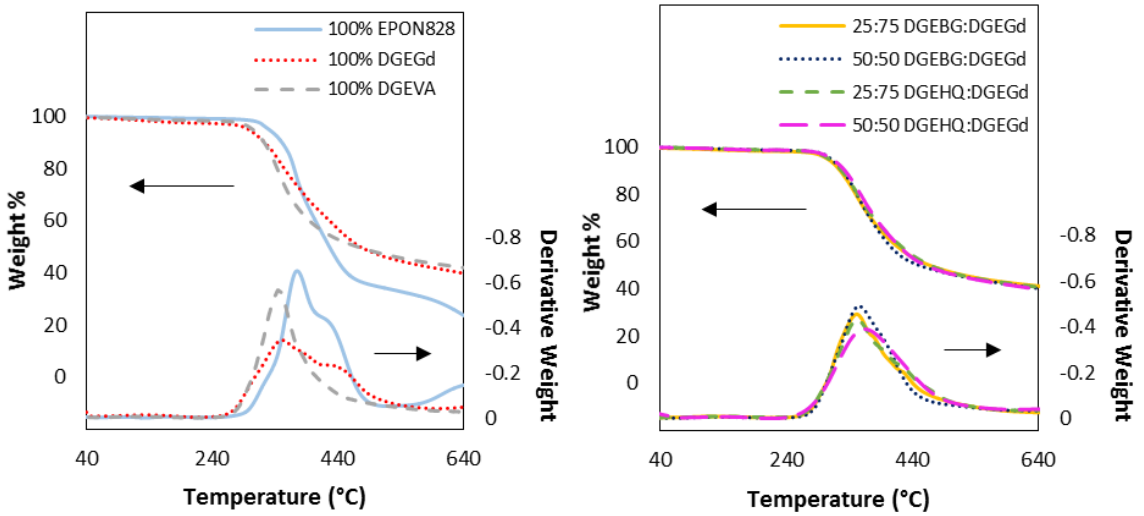

Figure 42. TGA thermograms of epoxy-amine thermoset resins.

Table 4

Thermogravimetric properties of highly bio-based epoxy-amine thermosets

Epoxy Resin Cured with DFDA	***IDT*** **(°C)**	$T_{50\%}$ **(°C)**	T_{max} **(°C)**	**Char Yield (wt%)**
100% EPON828	330	426	374	22.6
100% DGEGd	297	476	351	39.6
100% DGEVA	304	471	345	41.8
25:75 DGEBG:DGEGd	306	466	352	41.0
50:50 DGEBG:DGEGd	311	450	356	39.9
25:75 DGEHQ:DGEGd	308	467	354	40.2
50:50 DGEHQ:DGEGd	313	460	365	39.4

The initial degradation temperature (*IDT*) was taken to be the temperature at 5 wt% loss of sample and is the primary indicator of overall polymer stability. Two other parameters commonly used for thermal stability characterization are the temperature at 50 wt% sample loss ($T_{50\%}$) and the temperature at max degradation rate (T_{max}). Char yield refers the weight of sample residue left after completion of the heating gradient in a TGA experiment. Notably, the char yields of all of the bio-derived resins are high compared to the commercial BPA-based resin system (EPON828). These char yields support the hypothesis of Hu et al. that the furan rings in DFDA are capable of rearranging into more stable structures when thermal stress is applied to a cured epoxy-amine resin.[35] Due to the higher molecular weight of the oligomerized EPON828 epoxy resin, a stoichiometric mixture with DFDA required fewer moles (and therefore less mass) of the curing agent. This molecular weight difference leads to a decreased furan content in the EPON828 thermoset relative to all of the other bio-based epoxy samples.

The lignin-derived diepoxy resins possess a combination of heightened $T_{50\%}$ values and char yields with *IDT*s and T_{max} values similar to EPON828-containing resin, indicating overall superior thermal stability compared to the commercial epoxy resin. However, the slightly higher *IDT* and T_{max} displayed by the EPON828 thermoset may be attributed to the lack of cleavable substituents (such as methoxy groups). The data suggest this is the case, as the increased stabilizing furan content present in all of the bio-derived thermosets (due to lower epoxy molecular weights) would serve to slow the degradation rate after initial decomposition. This is observed in the data where non-EPON828 samples begin to degrade at lower temperature (due to cleavable substituents) but then degrade more gradually (due to higher furan content) relative to EPON828 thermoset. These TGA results

preliminarily confirm the viability of epoxies derived from lignin and cellulose-derived diamines in future high-temperature epoxy-amine thermoset applications.

Due to the importance of sample dimensions (span-to-thickness ratios) in DMA testing,[89] thick and thin samples were made in order to acquire accurate data in the different regimes of the polymer throughout the temperature gradient. At lower temperatures, the polymer behaves like a glassy solid. As the temperature is increased, the polymer passes through its T_g, and begins to behave as a rubbery solid. Samples with lower span-to-thickness ratios have been shown to display more accurate T_gs and rubbery regime data, while samples with higher span-to-thickness ratios (> 10) are more useful for the determination of accurate glassy regime data (i.e. storage modulus). For this reason, samples were prepared with uniform dimensions of 17.5 mm × 12 mm × 2.9 mm (thick samples) and 17.5 × mm 12 mm × 1.6 mm (thin samples) in order to obtain accurate data for each cured resin in all temperature regimes. While the body of materials science literature is not in complete agreement on where to measure the T_g (at the peak of the loss modulus curve or at the peak of the tan δ curve), in this work the T_g of samples by DMA was taken to be the temperature at the peak of the loss modulus. This is because the loss modulus peak usually coincides more closely with the inflection point of the storage modulus curve and is typically at a lower temperature than the tan δ peak and thus offers a more conservative estimate of T_g. The peak of the tan δ curve is taken to be T_g by some because this peak is clearly visible for nearly all polymers, whereas loss moduli can sometimes be broad or display no clear peak. DMA thermograms of thick and thin samples and a data summary of each system are given in Figures 43 and 44 and Table 5 respectively.

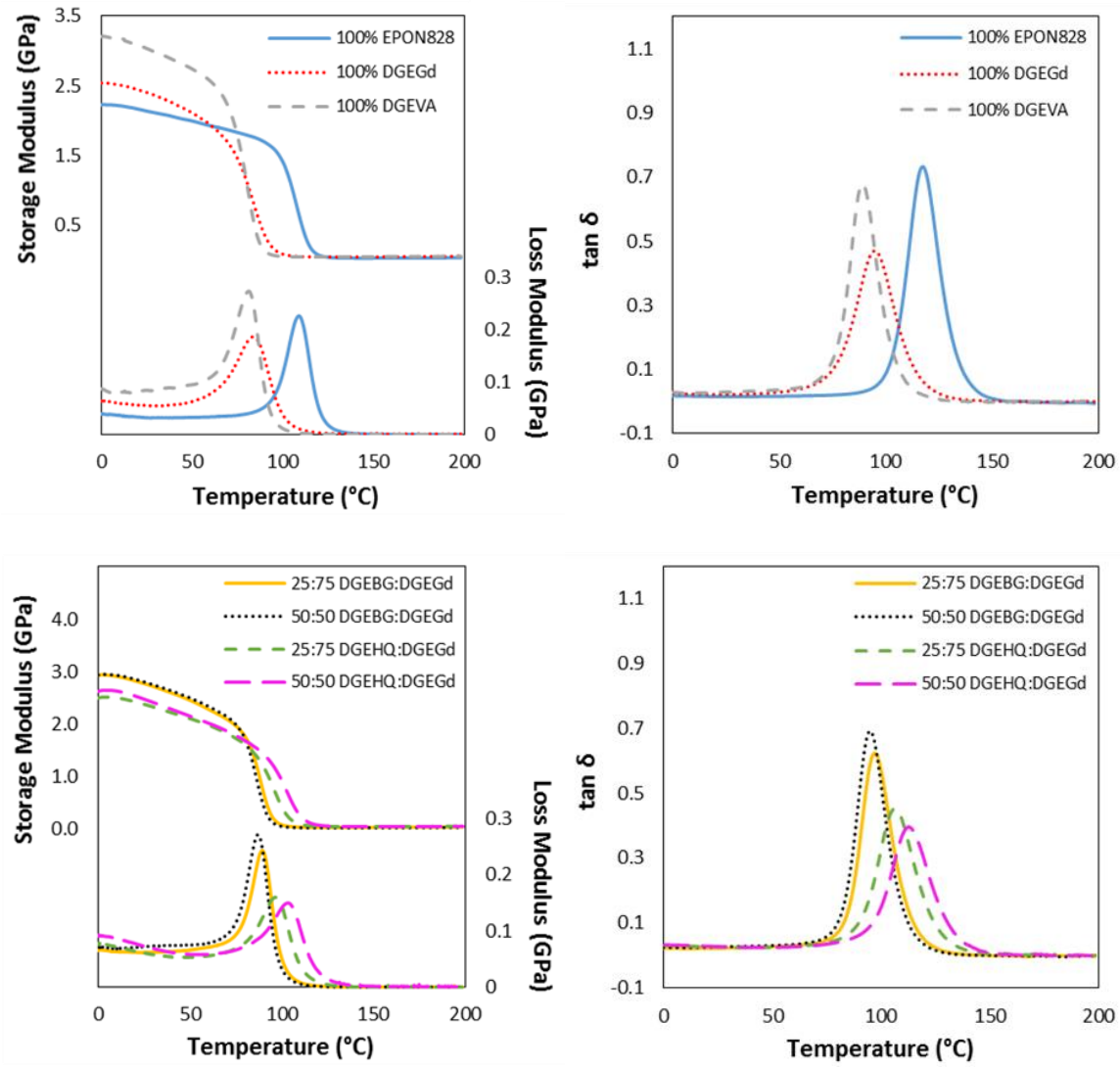

Figure 43. DMA thermograms of thick samples (17.5 mm × 12 mm × 2.9 mm).

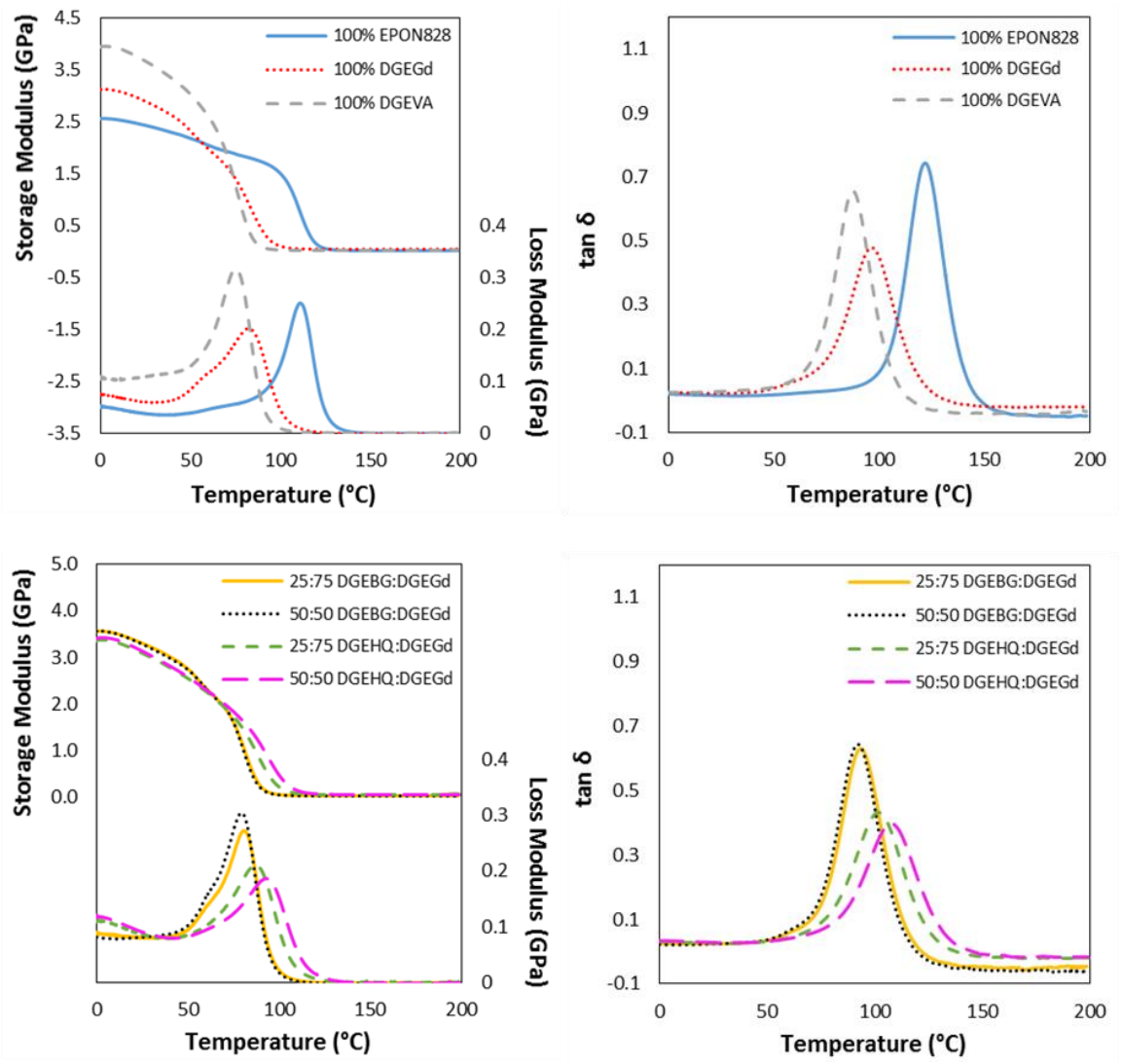

Figure 44. DMA thermograms of thin samples (17.5 mm × 12 mm × 1.6 mm, span-to-thickness ratio > 10).

Table 5

Summary of thermomechanical data of thick and thin cured resins

Epoxy Resin Cured with DFDA	T_g[a] (°C)	tan δ max[b]	E' at 25 °C[c] (GPa)	MW_c (g/mol)	ρ_c (mol/cm^3)
100% EPON828	109	0.732	2.44	460	0.00262
100% DGEGd	84	0.470	2.90	254	0.00497
100% DGEVA	81	0.679	3.68	333	0.00382
25:75 DGEBG:DGEGd	90	0.624	3.30	321	0.00392
50:50 DGEBG:DGEGd	87	0.692	3.29	354	0.00357
25:75 DGEHQ:DGEGd	97	0.452	3.10	264	0.00479
50:50 DGEHQ:DGEGd	103	0.397	3.12	213	0.00598

[a] T_g taken as peak of E''
[b] tan δ max of thick samples tabulated
[c] E' at 25 °C obtained from thin samples

A comprehensive structure-property relationship study previously performed by Hernandez et al.[54] determined that the methylene spacer between two aromatic rings (as in resins containing DGEBG) and between aromatic ring and epoxy functionality (as in resins containing DGEVA and DGEGd) decreases T_g and modulus while the presence of methoxy substituents was shown to decrease T_g but increase glassy modulus. The increased modulus observed in species containing methoxy groups is theorized to be caused by hydrogen bonding between the hydroxyls formed during the epoxy-amine reaction and the methoxy oxygen. The EPON828-DFDA thermoset is expected to have the highest T_g based on this information from previous results. The slight difference in the T_g of the DGEBA-DFDA sample compared with results from a previous study by Hu et al. may be due to instrumental differences and sample mounting variation on the DMA.[35]

Likewise, the combination of methylene spacer between the aromatic ring and epoxy moiety as well as the presence of the methoxy functionality in DGEVA results in cured resins with the lowest T_g. The DGEGd-containing resin differs from DGEVA-resin only by the lack of methoxy functionality, and produces a thermoset with a slightly higher T_g, but a lower modulus as a result. DGEHQ, while usually not considered a bio-derived monomer by those in the field, was used in this work for comparative purposes versus DGEGd to confirm effects of methylene spacers on resin properties. Comparisons between pure DGEGd- and DGEHQ-containing cured resins in this work also support data found in literature.[54] The reduced amount of methylene spacers in DGEHQ-containing cured resins affords higher T_gs and glassy moduli compared to the DGEGd thermosets. DGEBG-containing resins exhibit very high storage moduli at 25 °C (imparted by the methoxy moieties) but decreased T_g relative to EPON828 samples due to the methoxies and the methylene spacer between aromatic rings for DGEBG samples. Also, to be considered is the methylene spacer between the furan rings and the amine functionality in DFDA. It is hypothesized that the methylene spacers between furan rings and between furan and amine functionality in DFDA serve to decrease T_g in systems containing DFDA due to similar free-rotation and mobility effects as in the case of methylene-spaced epoxy monomers.

Molecular weight between crosslinks (MW_c) data were calculated using the minimum value of the storage modulus for the thick samples using the theory of rubber elasticity (eq 13) where ρ is the cured resin density, R is the gas constant, $T_{E'min}$ is the temperature at which the storage modulus is minimized, and E'_{min} is the minimum value of the storage modulus. Only thick samples are stiff enough to ensure reliable modulus data in the rubbery regime.

$$MW_c = \frac{3\rho RT_{E'_{min}}}{E'_{min}} \quad (13)$$

No legitimate trend was observable between cured resin density and glassy modulus, however if replicates of this work were done, a trend might emerge. Considering the high extent of cure for all cured resins, trends between crosslink density and MW_c can be observed. Comparing DGEGd and DGEVA cured resins illustrates that as the molecular weight of the epoxy monomer is increased, the MW_c increases and related decrease in crosslink density is observed accordingly. This trend can also be seen when comparing the two samples in each of the resin blend systems. Because the EPON828 epoxy resin is an oligomer with n-value equal to 0.14, that cured resin exhibits the highest MW_c and consequently the lowest crosslink density.

The maximum height of the tan δ peaks in DMA thermograms support the conclusion that higher degrees of crosslinking leads to lower chain mobility, even at the same degrees of polymerization.[54] Indeed, the resins in this work with the highest tan δ peaks exhibited the lowest crosslink densities.

Overall, the thermomechanical properties and thermal stability exhibited by the cured resins produced in this study were similar to comparable thermosets reported in literature, but contain much higher bio-derived content. This heightened bio-derivation alone makes these tunable-property thermosets of immediate and significant value as replacements for less-sustainably sourced and more hazardous incumbent resins.

4.3 Lignin-Derived Polycarbonate

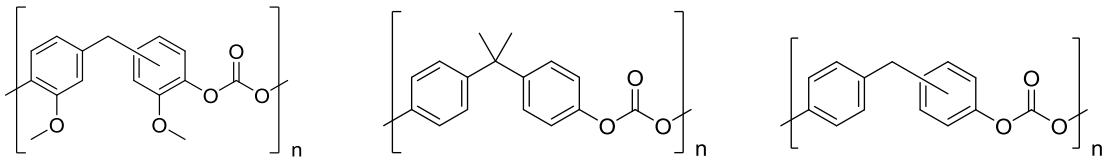

BG-PC BPA-PC BPF-PC

Figure 45. Structures of the repeat units of BG-PC (left), BPA-PC (middle), and BPF-PC (right).

The production of BG-PC, BPA-PC, and BPF-PC (Figure 45) produced interesting results. The three different polycarbonates were not universally soluble in a single solvent, and different aliquot times of the same polycarbonate species also did not possess similar solubility. For GPC analysis, BPA-PC was most soluble in THF while BPF-PC and BG-PC were most soluble in DMF with 0.05 *M* LiBr. A summary of the molecular weight distributions (number-averaged molecular weight ($\bar{M}_n$) and weight-averaged molecular weight ($\bar{M}_w$), and polydispersity index ($Đ$)) of the final polycarbonates is given in Table 6.

Table 6

Molecular weights of polycarbonates

Sample	Interval (h)	$\bar{M}_n$ (g/mol)	$\bar{M}_w$ (g/mol)	$Đ$
BG-PC	48	19100	39000	2.04
BPA-PC	24	26128	41439	1.59
BPF-PC	48[a]	18100	34028	1.88

[a] data extrapolated from initial data points.

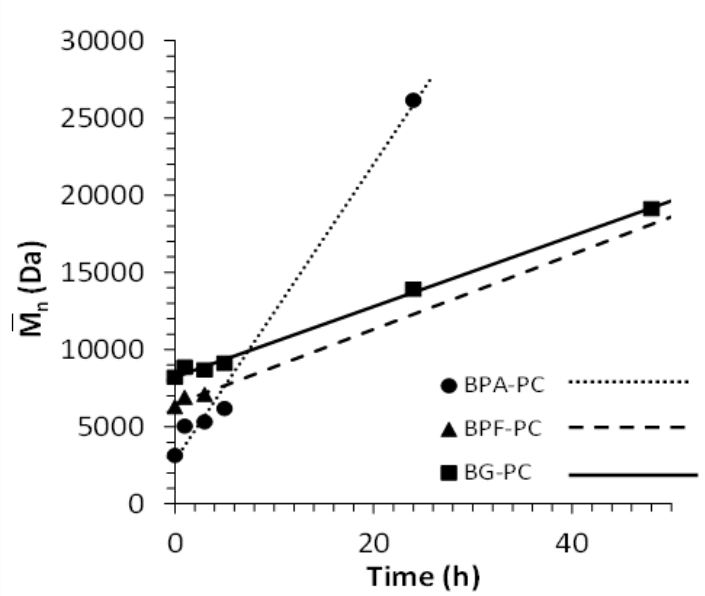

Figure 46. $\overline{M}_n$ (determined by GPC) as a function of aliquot time.

An interesting result was observed when the number-averaged molecular weight was plotted against aliquot time (Figure 46). Chain growth may be related to the linearity of the bisphenolic monomer material. The BPA used in this work was highly pure *p,p'* isomer. This would result in less steric hindrance for phenol oxygen attacks on the chloroformate carbonyl. The BPF and BG that were used to produce polycarbonates were a mixture of isomers. Presumably, molecular torsion in these species could lead to decreased reaction rates as reactive conformations were less likely to form between the bisphenol and the chloroformate group. BPF-PC was highly insoluble in available GPC solvents after 3 hours of reaction and therefore GPC data is unavailable for BPF-PC after that time. However, a linear fit of the available BPF-PC GPC data mirrors that of BG-PC, supporting the hypothesis that monomer configuration contributes significantly to polymerization rate. Also supporting this hypothesis is the bridging species in the three

monomers. BPA is bridged with an isopropylene group, whereas BG and BPF are bridged with methylene groups. The isopropylene group has been shown to cause barrier to rotation of the bisphenol of 10 kcal•mol^{-1}, while BG and BPF would be freer to rotate and twist into conformations unfavorable to polymerization.

The results of TGA and DSC experiments (done in singlet due to instrument access limitations) are summarized in Table 7 with the TGA thermograms shown overlaid in Figure 47 and the DSC trace of BG-PC showing the T_g of the polymer in Figure 48.

Table 7

TGA and DSC results summary of polycarbonates

Sample	***IDT*** **(°C)**	$T_{50\%}$ **(°C)**	T_{max} **(°C)**	**Char Content (%)**	T_g **(°C)**
BG-PC	375	455	450	24.2	99.7
BPA-PC	440	543	545	23.2	150
BPF-PC	369	546	501	40.5	118.6

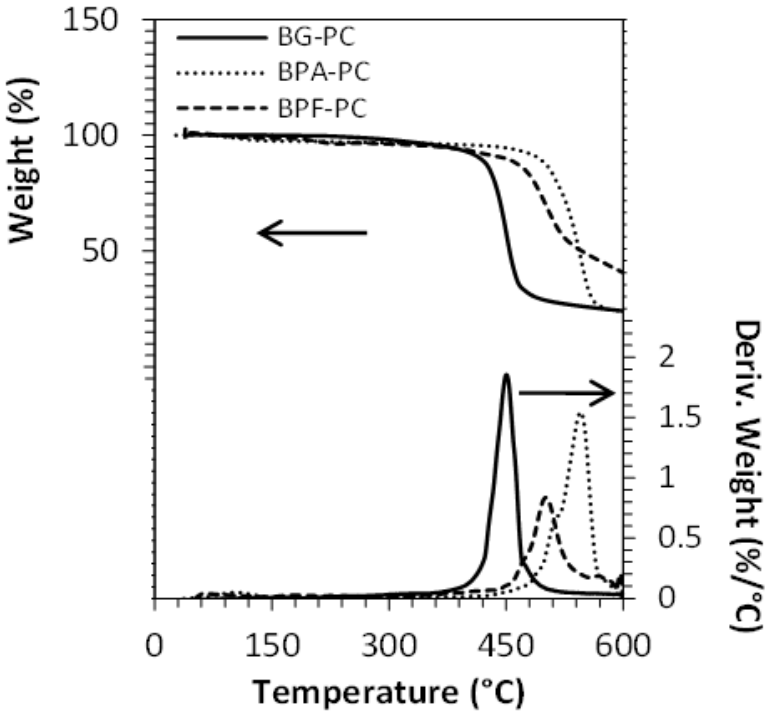

Figure 47. Overlaid TGA thermograms of BG-PC, BPA-PC, and BPF-PC.

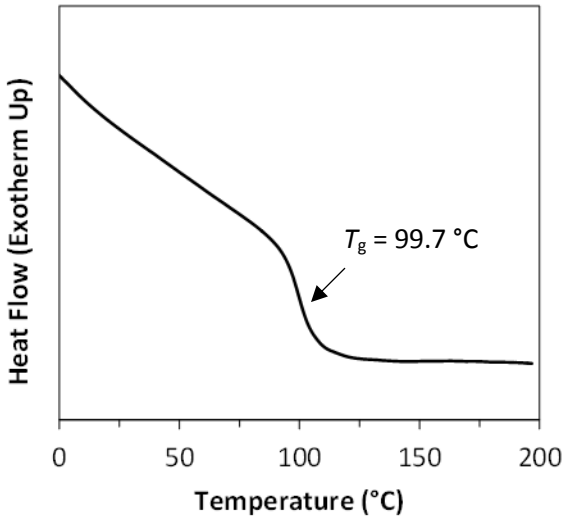

Figure 48. DSC thermogram of BG-PC showing T_g.

BPA-PC exhibited the highest T_g most likely due to the aforementioned linearity attributing to tighter chain packing relative to the twisted and contorted chains of BPF-PC and BG-PC. BG-PC demonstrated the lowest T_g of the three polymers. The methoxy groups have been shown in previous work to lower the T_g of epoxy-amine thermosets and so similar effects could be occurring here. Overall molecular weight is not anticipated to have a significant effect on T_g in this case because the critical entanglement molecular weight (M_c) of BPA-PC is 4,800 Da and it can be inferred that the M_c of BPF-PC and BG-PC will not be very different from this value. If this is the case, the weight of each generated polycarbonate is upwards of 20,000 Da and therefore well-removed from their probable M_c.

Previous studies have shown that methoxy substituents can donate electrons to the aromatic rings, decreasing thermal stability. Indeed, BG-PC exhibited the lowest combined thermal stability with *IDT* similar to that of BPF-PC and much lower than that of BPA-PC and significantly lower $T_{50\%}$ and T_{max} values compared to both BPF-PC and BPA-PC. High char contents are expected from polycarbonate species, and this trend was observed of the polycarbonates in this work. The higher char content of BPF-PC may be attributed to a small content of novalac present in the starting material. Presumably, even a very small novalac content can be amplified in the bulk polymer sample. Novalacs could act as crosslinkers for the polymer chains and cause an observable drop in solubility (as was observed with BPF-PC) as well as heightened thermal stability.

4.4 Biomass-Derived Polyesters

The application of BG to other types of polymers is critical for building the base of information about that species' applications in various polymer applications. BG has

already proven valuable in epoxy-amine systems and has been preliminarily shown to have potential toward polycarbonate applications. The development of a BG-based polyester proved more difficult than the production of similar polycarbonate. Attempts to polymerize BG with succinic acid under relatively mild conditions yielded discolored, glassy, low molecular weight product. Harsher conditions such as extremely high temperatures, several catalysts, and vacuum atmosphere were required to generate higher molecular weight polyester from BG and succinic acid (Figure 49).

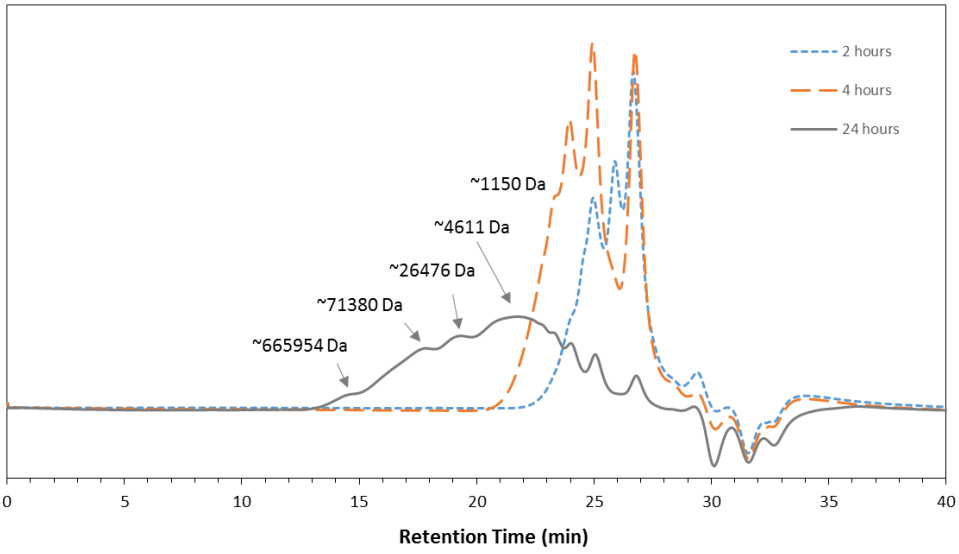

Figure 49. Overlaid GPC traces showing the growth of BG-succinic acid polyester.

A common example of aromatic polyester is polyethylene terephthalate (PET). PET is produced via the condensation of terephthalic acid and ethylene glycol. It is key to note that in the synthesis of PET the reactive hydroxyl groups are basic, lending themselves good nucleophilicity. Conversely, the aromatic hydroxyl groups in BG (and other

bisphenols) are more acidic and therefore poorer nucleophiles. The condensation reaction to form polyester requires a nucleophilic hydroxyl oxygen. For this reason, harsh conditions were required to form anything greater than dimers and trimers of BG-succinic acid polyester.

In an effort to work around this inherent molecular flaw, the acid chloride of succinic acid was employed. By enhancing the electrophilicity of the succinic carbonyl, the inherent acidity of the bisphenolic hydroxyl groups can be overcome and the reaction can progress. BPA was employed first to probe the efficacy of this alternate synthetic route, and results were encouraging. A tan-colored powder was obtained after purification, which was slowly soluble in chloroform and THF, and completely insoluble in water; signs that a thermoplastic, non-crosslinked polymer was formed. GPC analysis of the product (Figure 50) indicated high molecular weight polymer ^{1}H-NMR of the product confirmed the identity of the polyarylate product. DSC analysis (Figure 51) indicated the produced polyarylate possessed a T_g of 94.1 °C.

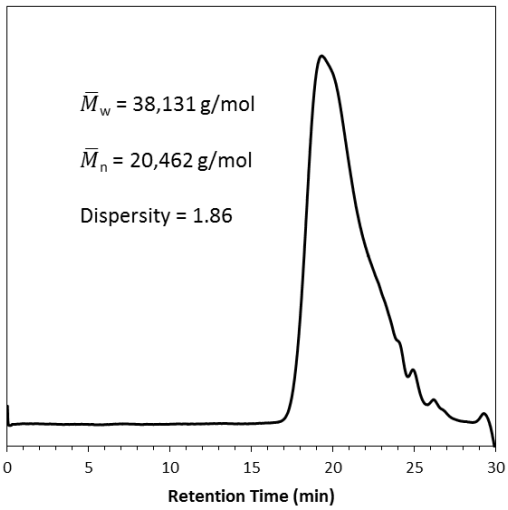

Figure 50. GPC trace of BPA-succinyl chloride polyarylate product.

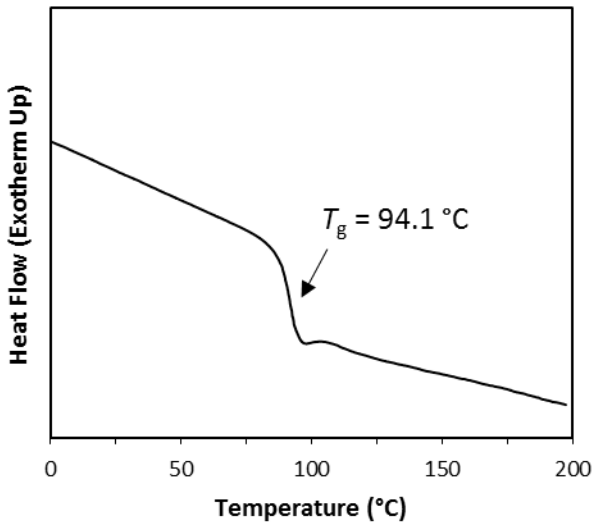

Figure 51. DSC trace of BPA-succinyl chloride polyarylate product.

After the encouraging results of the BPA-based polyarylate synthesis, BG was employed in a similar reaction procedure. The only variation between the two syntheses was that in the BPA-polyarylate synthesis, the acid chloride monomer solution was added slowly dropwise over 20 minutes. In the BG-polyarylate synthesis, the acid chloride monomer solution was added rapidly via cannula. This change, and the less-than-linear isomeric nature of BG, likely contributed to the decreased properties (molecular weight distribution and T_g) exhibited by the produced BG-polyarylate (Figures 52 and 53).

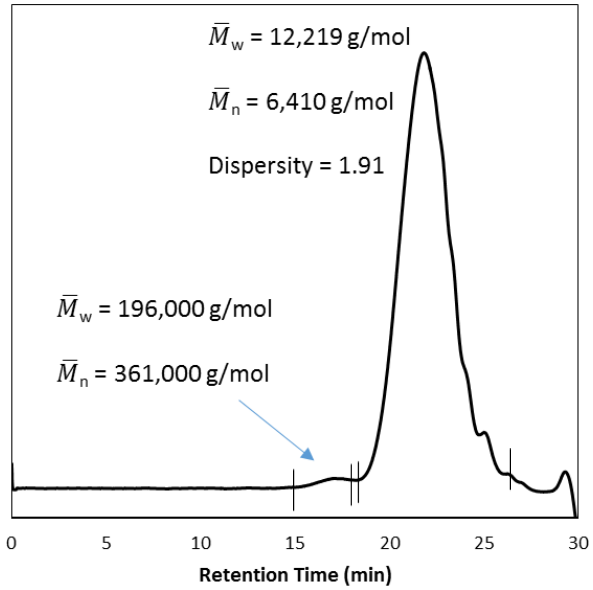

Figure 52. GPC trace of BG-succinyl chloride polyarylate product.

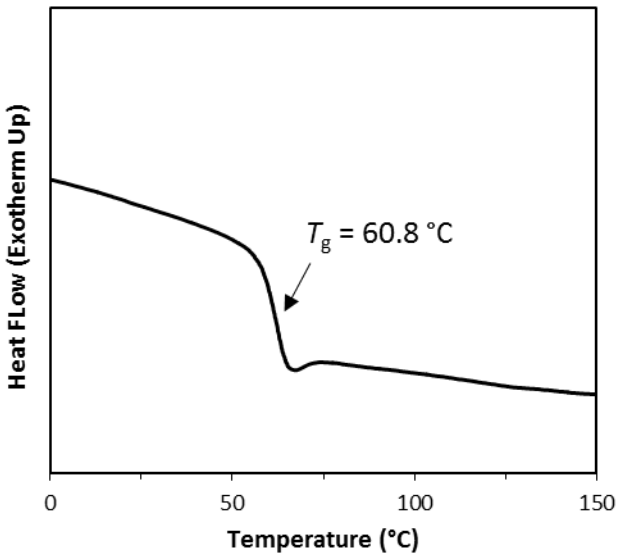

Figure 53. DSC trace of BG-succinyl chloride polyarylate product.

Because polyarylates are used industrially for high strength films and coatings, attempts to cast films out of the BPA-polyarylate were done. Approximately 10 wt% polymer was dissolved in chloroform and the solution was applied to a glass slide and dried

at 70 °C for 1 hour. The resultant films were highly transparent and resistant to scratching from glass rods. The films could be removed from the slide by soaking for a few minutes in water. However, after drying again, the very thin films were brittle to the touch. Films and coatings such as these made out of a bio-based, high performance polyarylate could be industrially and commercially important.

4.5 Trisguaiacol

The synthesis of trisguaiacol (**24**) was proposed in order to produce species capable of higher crosslinking than BG while possessing similar structure. It was hypothesized that this higher degree of crosslinking (when utilized in an epoxy-amine system) would increase T_g and thermal properties. Even if extent of cure issues involving the structural locking of the third reactive site after two sites have reacted, TrisG could be employed as an additive in lesser proportions. The method used to synthesize trisguaiacol was analogous to that of the synthesis of BG. The current method involves the use of excess BG (2.5 equivalents relative to vanillyl alcohol) which at first glance seems to be an inefficient use of BG; currently a time- and money-intensive chemical to produce. However, it was determined that the excess BG could be recovered during the chromatography product purification step (similarly to the recovery of excess guaiacol in the synthesis of BG). A difficulty surrounding the purification of trisguaiacol was discovered while drying the product under vacuum. After rotary evaporation, the clear oil product was placed in a vacuum oven at room temperature to remove the final traces of solvents. However, the product quickly began to foam, making the removal of solvents more difficult and time-intensive. After several day under vacuum, it was possible to begin to crush the product into a crystalline form under atmospheric pressure, and then replace it under vacuum. This process was the

most effective method used to remove all solvent from the trisguaiacol as quickly as possible, however several days under vacuum were still required, and complete removal of solvent was not possible, with trace ethyl acetate visible by NMR.

Another concern with the current state of TrisG is the isomeric impurity of the product. Because BG itself is a mixture of isomers and because the condensation of vanillyl alcohol onto the BG structure can occur at multiple sites, the resulting product can contain a handful of different isomers. This will make structure-property relationship studies using TrisG difficult at the current time.

4.6 Bissyringol

The synthesis of bissyringol (**33**) proceeded in an analogous manner to the synthesis of BG. Two syntheses were attempted, one using chloroform and one using DCM as the minimal reaction solvent. The chloroform reaction was able to be heated to approximately 80 °C to reflux for 48 hours, while the DCM reaction was only able to be heated to about 60 °C. The reagents were significantly more soluble in chloroform than in DCM. This presumably helped the reaction proceed more quickly. Indeed, upon filtration of the catalyst after the reaction had proceeded for two days, the reaction in DCM yielded a substantial amount of solid filter cake besides the catalyst beads. The reaction that was performed in chloroform did not exhibit this cake formation. This cake is most likely comprised of unreacted reagents, as BS is fully soluble in the quantities of DCM and chloroform employed during workup. The purification of BS proved to be the limiting factor in the development of this monomer, as the residual syringyl alcohol and product BS were inseparable by chromatography.

4.7 Novel Hetero-Difunctional Monomers and Styrene Replacement

Efforts to epoxidize 4-VG into a potentially high-value chemical building block were fraught with difficulties. Namely, the addition of strong sodium hydroxide solution at the end of the epoxidation reaction presumably serves to anionically polymerize the system through the vinyl groups. Attempts to epoxidize 4-VG in a manner similar to commercial epoxidation of glycidyl methacrylate were equally unsuccessful. Any contact of the vinyl moiety with strong base initiated anionic polymerization, indicating that the vinyl function group is much more sensitive to basic conditions than the similar methacrylate unsaturation. Reactions produced primarily an insoluble white or off-white substance which was presumed to be polymer formation. An unacceptably small amount (several milligrams) of epoxidized 4-VG (Ep4VG) was isolated over the course of several attempts at this synthesis. This was enough to obtain an NMR of the product (Figure 54), but enough yield was never achieved from any single reaction to warrant continued pursuit of this product via common and available epoxidation methods.

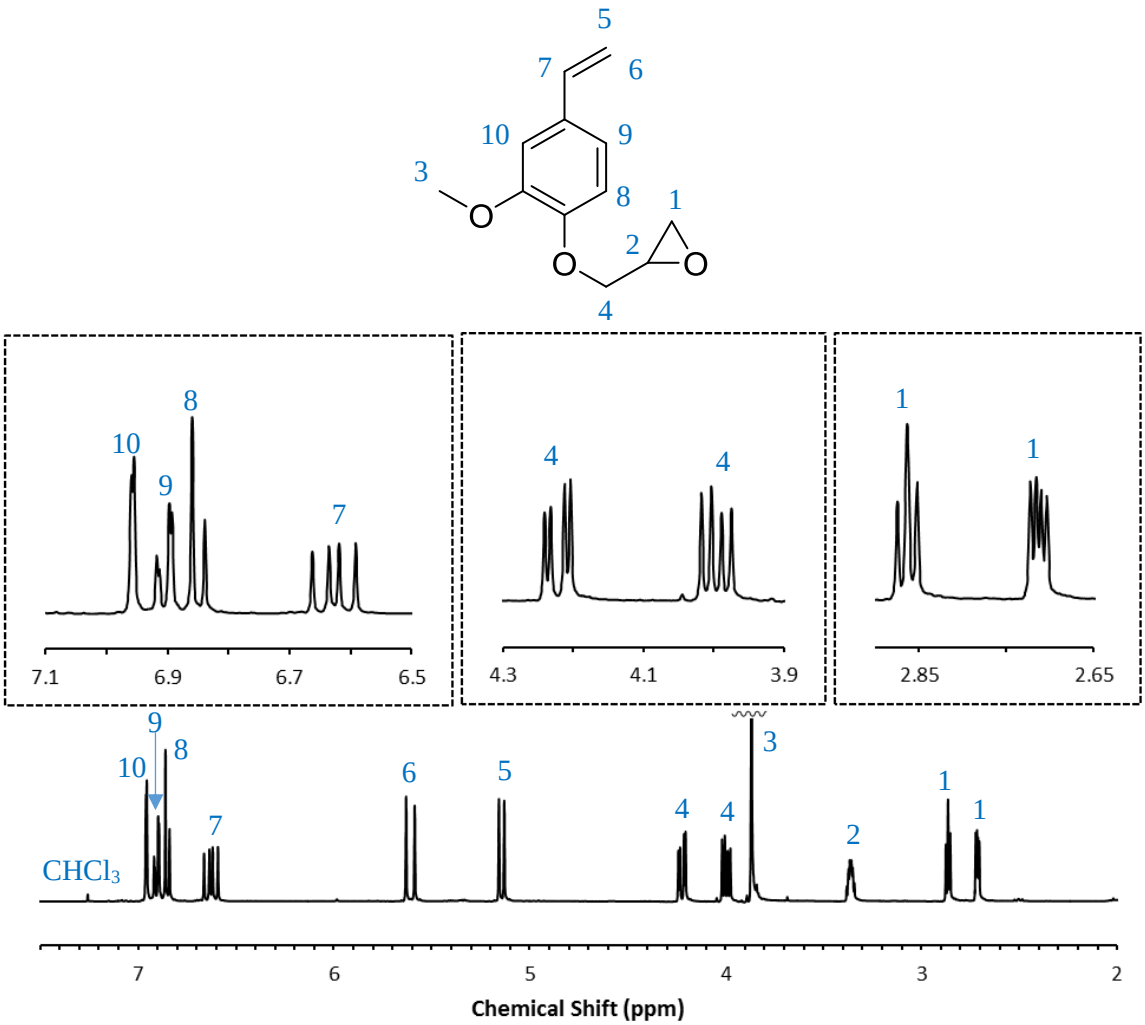

Figure 54. ^{1}H NMR of epoxidized 4-vinyl guaiacol (Ep4VG) with proton assignments.

However, 4-VG is readily functionalized by both allyl bromide and acetic anhydride to respectively prepare Al4VG and Ac4VG for use as di- and monofunctional styrene replacements. Polymerization of Al4VG and Ac4VG initiated by 1.5 wt% cumyl hydroperoxide (Trigonox) performed at 120 °C for 6 hours yielded a tacky solid, translucent polyAl4VG polymer but a hard, crystal clear, glassy polyAc4VG polymer. N-FTIR spectrum of the resultant polyAl4VG polymer is shown in Figure 55.

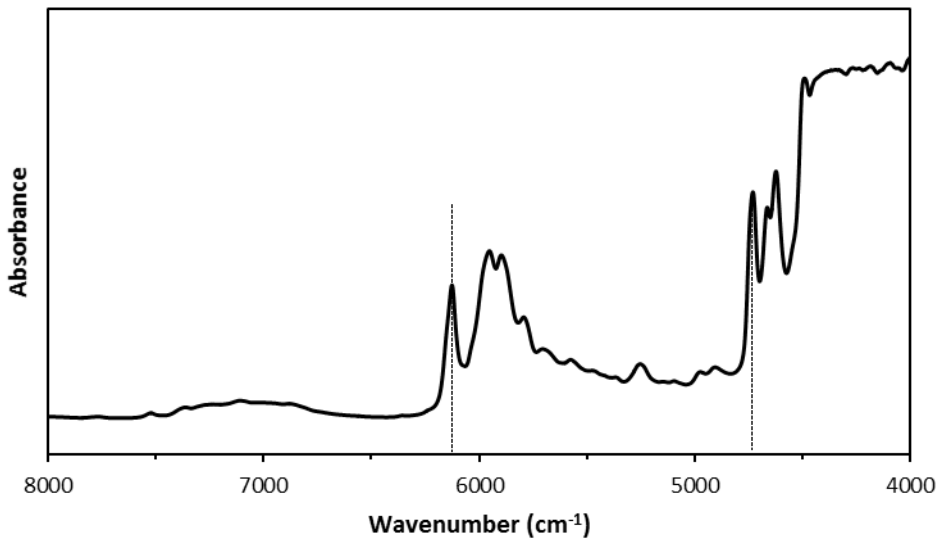

Figure 55. n-FTIR spectrum of polyAl4VG.

The presence of carbon-carbon double bond functionality, be it from the allyl ethers or vinyl groups, can be seen with dotted lines as the peaks around 6150 and 4700 cm^{-1}, indicating the polymer was not fully cured.

PolyAc4VG displayed no vinyl groups by n-IR indicating complete curing (Figure 56), exhibited a T_g of 99 °C by DSC (Figure 57), and demonstrated good thermal stability by TGA with and *IDT* of 254 °C and $T_{50\%}$ of 401 °C (Figure 58). DSC analysis of polyAc4VG offered an initial screening of the properties this sort of monomer could impart to polymers as a potential styrene replacement. Previous work on other polymers indicates that the presence of a methoxy group on an aromatic ring in the polymer backbone serves to lower T_g, however polyAc4VG has a T_g nearly identical to that of polystyrene (T_g = 100 °C). This indicates that some other chemical structure effect is occurring which is facilitating strong intermolecular interaction between polymer chains; presumably some sort of stacking through the acetyl groups. Methylation or some other functionalization of the hydroxyl in 4VG, and subsequent polymerization of the monomer would prove this extra effect. GPC

analysis of polyAc4VG (Figure 59) indicate the formation of high molecular weight polymer. Results of TGA indicate complete degradation of the polymer, with zero char yield, and rapid degradation rate after initial degradation (as high as 2.05 wt% loss $°C^{-1}$). This rapid degradation is indicative of the depolymerization of thermoplastics that can occur above the sample's ceiling temperature (T_c). The reversion of the polymer into its monomer units at high temperature would allow the volatilization of these shorter units and therefore complete mass loss at such high temperatures.

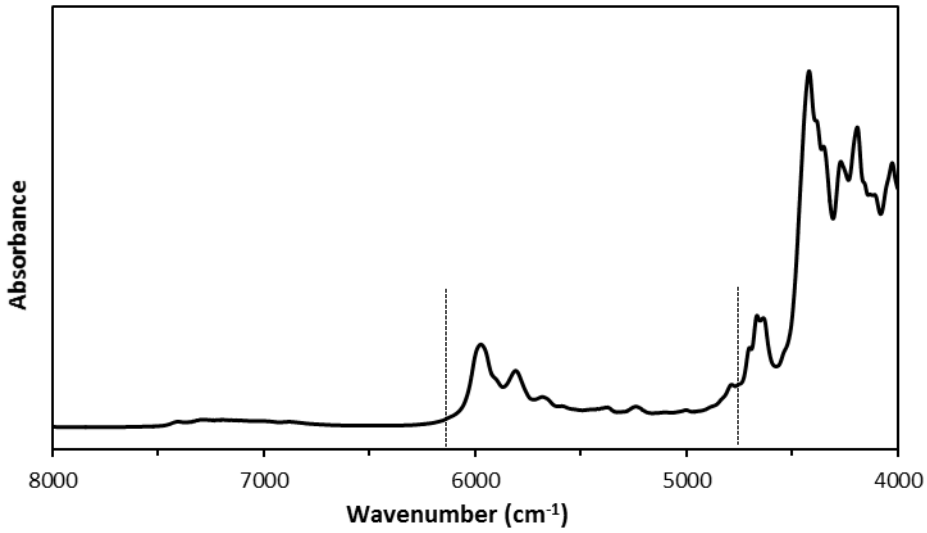

Figure 56. n-FTIR spectrum of polyAc4VG.

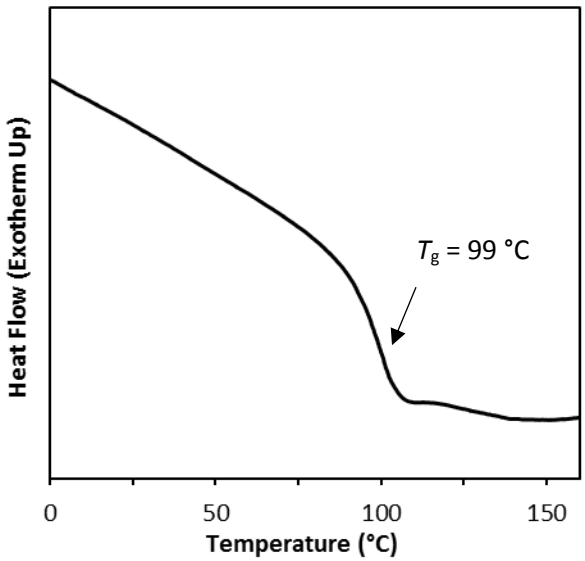

Figure 57. DSC trace of polyAc4VG showing T_g.

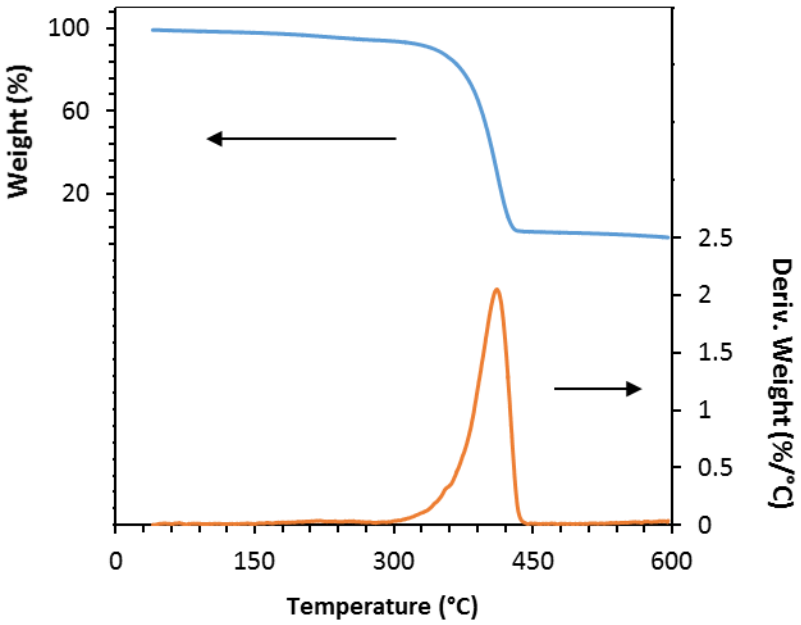

Figure 58. TGA trace of polyAc4VG.

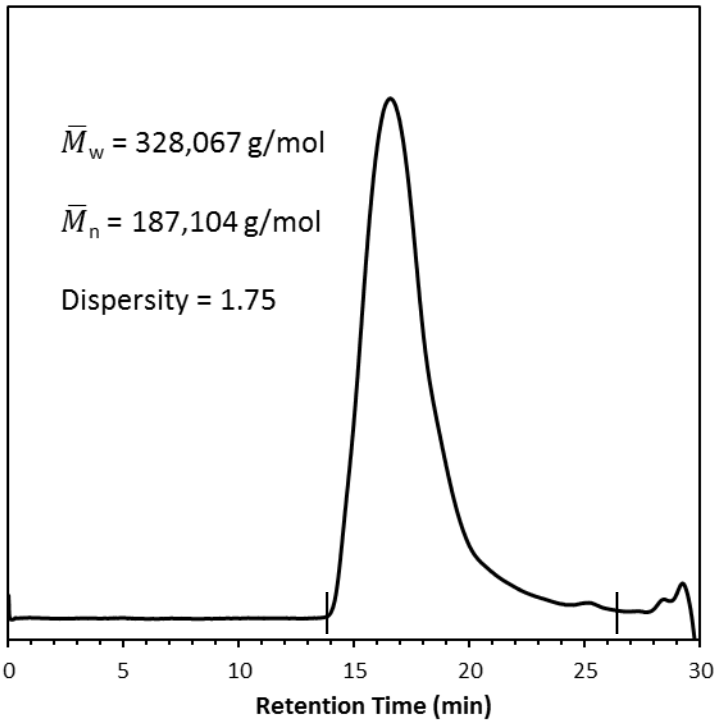

Figure 59. GPC trace of polyAc4VG with weight distributions (14.0 min to 25.5 min peak range).

While Al4VG did not produce a glassy polymer after the limited testing performed for this work, allyl ethers are readily polymerized by thiols and this combination of functional groups makes Al4VG, and molecules like it, interesting due to their potential for use in self-healing and other applications. Presumably, the allyl groups in Al4VG actually served to absorb radicals during the polymerization resulting in chain termination and substantially decreasing the molecular weight of the final polymer. The rubbery polyAl4VG produced in this work qualitatively swelled to several times its original size in THF, and rebounded very well when a load was applied. A route to cure every vinyl moiety in Al4VG while leaving the allyl ether groups intact would allow the controllable utilization of those groups in click chemistry such as crosslinking or thiolene-type chemistry.[22, 90]

Chapter 5

Conclusions and Recommendations for Future Work

5.1 Conclusions

The development and use of lignocellulosic biomass-derived chemicals in polymer applications was examined in this work. Epoxy-amine thermoset resins with very high bio-derived carbon contents were synthesized and their thermomechanical and thermal degradation properties were investigated. Lignin-derived diepoxies including a bisphenolic diepoxy and a cellulose-derived furanyl diamine were shown to produce thermoset resins with good T_gs over 90 °C and excellent thermal resistances. The same lignin-derived bisphenol was shown to produce high-molecular weight polycarbonate, relative to the critical entanglement molecular weight, with both a good T_g of 100 °C and good thermal resistance displaying *IDT* of 375 °C and T_{max} of 450 °C.

Poyarylates synthesized using bio-mass derived diacid chlorides and bisphenols exhibited good properties, even after only preliminary efforts to produce such species. The novel monomers produced in this work proved that they have the potential to be used in high performance polymer applications, such as polystyrene replacements or in reactive polymer click chemistry. All of these biomass-derived polymers were compared to similar systems produced using conventional petrochemical building blocks and exhibited different properties at both greater and lesser levels than the conventional systems.

5.2 Recommendations for Future Work

One of the main drawbacks of certain biomass-derived monomeric chemicals is their physical state at and around room temperature. With as much potential as BG offers toward

high performance polymer applications, it is a crystalline solid with a melting point of 105 °C. This introduces difficulties into any process in which it is involved. It would be preferred to have a liquid resin for easy of processing and blending with other chemicals. Based on data such as EEW and MW, it is known that the BG epoxy used in this work is a pure monomer with an n-value of exactly zero (Figure 60).

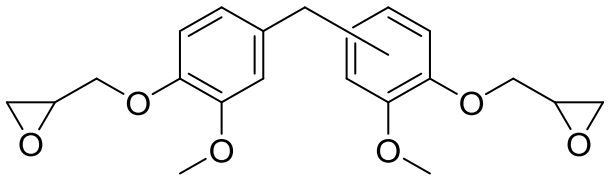

Figure 60. Pure DGEBG monomer with an n-value of 0.

It is hypothesized that via an oligomerization reaction this n-value could be increased and the product resin would become a liquid; similarly to how BPA is a solid but EPON828 resin (n-value = 0.14) is a viscous liquid and EPON825 (n-value = 0) is a solid. A promising method employed was adapted from Fache et al. and involves the chain extension of diepoxies via the fusion process.[91] These researchers were able, albeit through a methodical small-scale DSC characterization study, to successfully oligomerize diglycidyl ether of methoxyhydroquinone (DGEMHQ) into brown glassy to viscous solids. However, it is not clear in the results from that study which combinations of reagents yielded the least viscous products. An initial attempt to adapt the aforementioned study toward BG oligomerization produced a brown glassy solid mass that did not explicitly melt at any reasonable temperature. While a method needs to be developed which can broadly

oligomerize biomass-derived monomers for ease of processing, this problem is beyond the scope of this work and would most likely involve enough work for nearly another entire thesis.

Another practical problem that needs to be addressed is the significant byproduct that is produced by the epoxidation reactions currently employed by this research group. Around 30% of the product of any given epoxidation reaction is monoglycidyl ether. Up until recently this product was discarded. However over the course of this work, an isolated and pure product containing one epoxy group and one reactive hydroxyl group was collected as an interesting potential hub chemical toward other hetero-difunctional monomers or macromonomers. Interesting chemicals to pursue are shown below in Figures 61 through 63.

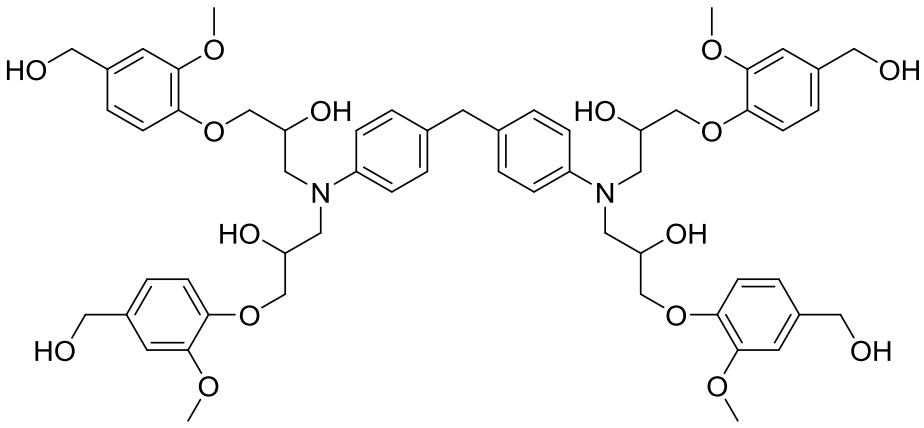

Figure 61. Proposed macromonomer produced from 4,4'-methylenedianiline (MDA) and four equivalents of monoglycidyl ether of vanillyl alcohol (MGEVA).

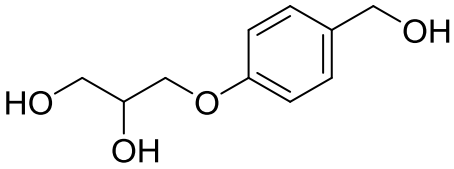

Figure 62. Proposed trifunctional monomer produced from the hydrolysis of monoglycidyl ether of gastrodigenin (MGEGd).

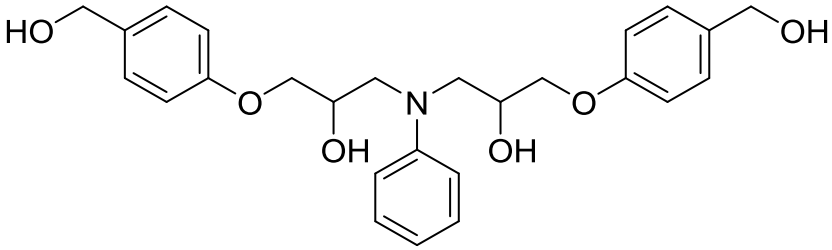

Figure 63. Proposed macromonomer synthesized from aniline and two equivalents of monoglycidyl ether of gastrodigenin (MGEGd).

The structures proposed in Figures 61 and 63 could be used as additives in other polymer applications to increase rigidity due to their aromatic content, or as a crosslinker via their many functionalizable hydroxyl groups. The structure proposed in Figure 62 could be used to produce interesting crosslinked thermoset polymers due to its trifunctionality, and could yield a polymer with good T_g (from its aromatic content) and good flexibility (from its short carbon chain). Presumably, various combinations of monoglycidyl ethers and anilines or amines could be used to produce macromonomeric species with many desirable properties and balance of rigidity and flexibility.

The synthesis and purification of bissyringol and polymers made from it are just in their infancy, as the investigation of those species was begun toward the end of the work for this thesis. While epoxy resins produced from bissyringol would likely suffer a decrease in T_g

due to the increased number of methoxy substituents, other polymers such as polycarbonates and acrylate-based polymers might benefit from the increased linearity imparted by a highly *p,p'*-monomer. In fact, the methacrylate of syringol was shown to possess a higher T_g than that of similar species with fewer substitutions such as guaiacol methacrylate or catechol methacrylate.[92] For these reasons bissyringol should be further pursued and applied to various polymer systems. Perhaps a synthetic method employing a formaldehyde coupling reaction would solve the downstream purification problem.

As Ac4VG was shown to be capable of producing polymers with good T_g and clarity, other analogues of anhydrides reacted with 4-VG could be synthesized to examine the effect of longer pendant carbon chains on polymer properties. Good candidates for such a study include the products of the reaction of 4-VG with propionic anhydride, butyric anhydride, and heptanoic anhydride (Figure 64) due to the presumed ease of synthesis and single variable alteration.

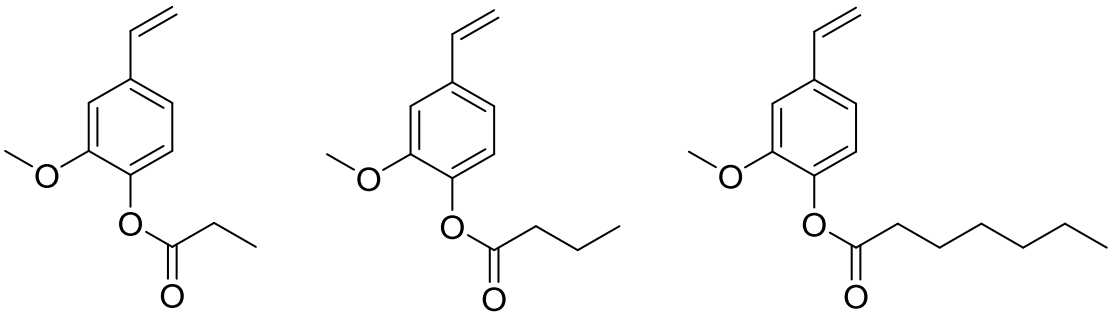

Figure 64. Analogs to Ac4VG to be synthesized to determine effect of pendant carbon chain length on properties of polystyrene-like polymers.

Another interesting study would involve the synthesis of polyarylate analogues similar to those produced in this work, but with varying alkyl carbon chain lengths. Adipoyl chloride, glutaryl chloride, and terephthaloyl chloride (Figure 65) could be used to synthesize a series of similar polyarylates that would allow a structure-property relationship study to investigate the effect of substituting differing lengths of alkyl chain for the terephthalic moiety. It could be expected, based on literature, that extending the length of the carbon chain unit in the polymer backbone would serve to decrease T_g, but could lead to an increase in other properties such as flexibility and toughness. By studying the structure-property relationships of these polymers, more educated hypotheses could be made about the properties that other more interesting bio-derived diacids and diacid chlorides might impart to polyesters.

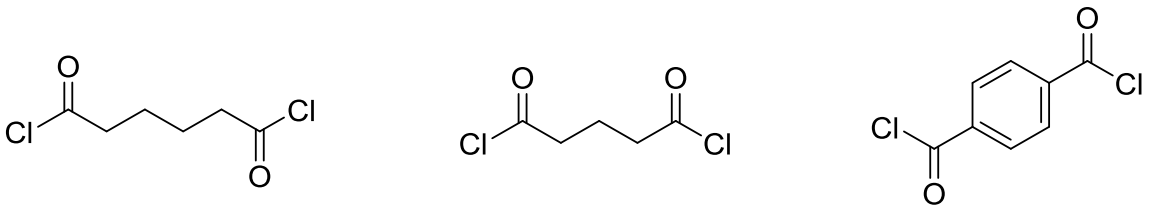

Figure 65. Adipoyl (left), glutaryl (middle), and terephthaloyl (right) chlorides.

Further study into these and other bio-derived polyarylates should be conducted to determine the full extent of their properties and applications to which they could be applied.

References

[1] A. J. Cavallo. (2005) Hubbert's model: uses, meanings, and limits-1. *Oil&Gas Journal*.

[2] R. E. Aguilera, R.; Lagos G.; Tilton, J., "Depletion and the Future Availability of Petroleum Resources," *The Energy Journal*, vol. 30, pp. 141-174, 2009.

[3] D. J. Murphy and C. A. Hall, "Energy return on investment, peak oil, and the end of economic growth," *Ann N Y Acad Sci*, vol. 1219, pp. 52-72, Feb 2011.

[4] I. Joseph F. Stanzione, "Lignin-Based Monomers: Utilization in High-Performance Polymers and the Effects of Their Structures on Polymer Properties," Doctor of Philosophy Dissertation, Chemical Engineering, University of Delaware, Ann Arbor, MI, 2013.

[5] K. Liu, "Novel plant oil-based thermosets and polymer composites," Master of Science Thesis, Department of Materials Science and Engineering, Iowa State University, 2014.

[6] D. Lockwood. (2016) Cheap Catalyst Converts Tough Plant Lignin into Valuable Chemicals. *C&EN*.

[7] P. G. Nihul, S. T. Mhaske, and V. V. Shertukde, "Epoxidized Rice Bran Oil (ERBO) as a Plasticizer for poly(vinyl chloride) (PVC)," *Iran Polymer Journal*, vol. 23, pp. 599-608, 2014.

[8] M. J. Rak, T. Friscic, and A. Moores, "Mechanochemical synthesis of Au, Pd, Ru and Re nanoparticles with lignin as a bio-based reducing agent and stabilizing matrix," *Faraday Discuss*, vol. 170, pp. 155-67, 2014.

[9] W. Thielemans, E. Can, S. S. Morye, and R. P. Wool, "Novel applications of lignin in composite materials," *Journal of Applied Polymer Science*, vol. 83, pp. 323-331, 2002.

[10] M. C. Monte, E. Fuente, A. Blanco, and C. Negro, "Waste management from pulp and paper production in the European Union," *Waste Manag*, vol. 29, pp. 293-308, Jan 2009.

[11] R. J. A. Gosselink, E. de Jong, B. Guran, and A. Abächerli, "Co-ordination network for lignin—standardisation, production and applications adapted to market requirements (EUROLIGNIN)," *Industrial Crops and Products*, vol. 20, pp. 121-129, 2004.

[12] M. Fache, B. Boutevin, and S. Caillol, "Vanillin Production from Lignin and Its Use as a Renewable Chemical," *ACS Sustainable Chemistry & Engineering*, vol. 4, pp. 35-46, 2016.

[13] J. N. Murwanashyaka, H. Pakdel, and C. Roy, "Separation of syringol from birch wood-derived vacuum pyrolysis oil," *Separation and Purification Technology*, vol. 24, pp. 155-165, 2001.

[14] W. J. J. Hujigen, R. Van der Linden, J. H. Reith, and H. den Uil, "Development of a Lignocellulose Biorefinery for Production of Second Generation of Biofuels and Chemicals," in *Netherlands Process Technology Symposium*, Arnhem, The Netherlands, 2011.

[15] J. Qin, H. Liu, P. Zhang, M. Wolcott, and J. Zhang, "Use of eugenol and rosin as feedstocks for biobased epoxy resins and study of curing and performance properties," *Polymer International*, vol. 63, pp. 760-765, 2014.

[16] J. W. Holladay, J.; Bozell, J.; Johnson, D., "Top Value-Added Chemicals from Biomass: Volume II - Results of Screening for Potential Candidates from Biorefinery Lignin," U. S. D. o. Energy, Ed., ed: Pacific Northwest national Laboratory, 2007.

[17] J. Wan, B. Gan, C. Li, J. Molina-Aldareguia, E. N. Kalali, X. Wang, *et al.*, "A sustainable, eugenol-derived epoxy resin with high biobased content, modulus, hardness and low flammability: Synthesis, curing kinetics and structure–property relationship," *Chemical Engineering Journal*, vol. 284, pp. 1080-1093, 2016.

[18] E. Darroman, N. Durand, B. Boutevin, and S. Caillol, "Improved cardanol derived epoxy coatings," *Progress in Organic Coatings*, vol. 91, pp. 9-16, 2016.

[19] A. Llevot, E. Grau, S. Carlotti, S. Grelier, and H. Cramail, "From Lignin-derived Aromatic Compounds to Novel Biobased Polymers," *Macromol Rapid Commun*, Oct 26 2015.

[20] H. Priefert, J. Rabenhorst, and A. Steinbüchel, "Biotechnological production of vanillin," *Applied Microbiology and Biotechnology*, vol. 56, pp. 296-314, 2001.

[21] J. B. Zakzeski, P; Jongerius, A.; Weckhuysen, B., "The catalytic valorization of lignin for the production of renewable chemicals," *Chemical Review*, vol. 110, 2010.

[22] M. Fache, E. Darroman, V. Besse, R. Auvergne, S. Caillol, and B. Boutevin, "Vanillin, a promising biobased building-block for monomer synthesis," *Green Chemistry*, vol. 16, p. 1987, 2014.

[23] M. Fache, B. Boutevin, and S. Caillol, "Vanillin, a key-intermediate of biobased polymers," *European Polymer Journal*, vol. 68, pp. 488-502, 2015.

[24] N. K. Sini, J. Bijwe, and I. K. Varma, "Renewable benzoxazine monomer from Vanillin: Synthesis, characterization, and studies on curing behavior," *Journal of Polymer Science Part A: Polymer Chemistry*, vol. 52, pp. 7-11, 2014.

[25] M. M. Bomgardner. (2016) The Problem With Vanilla. *C&EN*.

[26] M. B. Hocking, "Vanillin: Synthetic Flavoring from Spent Sulfite Liquor," *Journal of Chemical Education*, vol. 74, pp. 1055-1059, 1997.

[27] D. J. Tenenbaum, "Food vs. Fuel," *Environmental Health Perspectives*, vol. 116, pp. 254-257, 2008.

[28] R. N. Shreve, *The Chemical Process Industries*, 2 ed. Tokyo: Kogakusha Company, Ltd., 1956.

[29] R. J. van Putten, J. C. van der Waal, E. de Jong, C. B. Rasrendra, H. J. Heeres, and J. G. de Vries, "Hydroxymethylfurfural, a versatile platform chemical made from renewable resources," *Chem Rev*, vol. 113, pp. 1499-597, Mar 13 2013.

[30] N. Shibuya and A. Misaki, "Structure of Hemicellulose Isolated from Rice Endosperm Cell Wall : Mode of Linkages and Sequences in Xyloglucan, β-Glucan and Arabinoxylan," *Agricultural and Biological Chemistry*, vol. 42, pp. 2267-2274, 2014.

[31] L. Zhao, L. Zhang, and Z. Wang, "Synthesis and degradable properties of cycloaliphatic epoxy resin from renewable biomass-based furfural," *RSC Adv.*, vol. 5, pp. 95126-95132, 2015.

[32] C. Li, Z. Zhang, and Z. K. Zhao, "Direct conversion of glucose and cellulose to 5-hydroxymethylfurfural in ionic liquid under microwave irradiation," *Tetrahedron Letters*, vol. 50, pp. 5403-5405, 2009.

[33] M. S. Holfinger, A. H. Conner, D. R. Holm, and C. G. Hill, "Synthesis of Difurfuryl Diamines by the Acidic Condensation of Furfurylamine with Aldehydes and Their Mechanism of Formation.," *Journal of Organic Chemistry*, vol. 60, pp. 1595-1598, 1995.

[34] F. Hu, J. J. La Scala, J. M. Sadler, and G. R. Palmese, "Synthesis and Characterization of Thermosetting Furan-Based Epoxy Systems," *Macromolecules*, vol. 47, pp. 3332-3342, 2014.

[35] F. Hu, S. K. Yadav, J. J. La Scala, J. M. Sadler, and G. R. Palmese, "Preparation and Characterization of Fully Furan-Based Renewable Thermosetting Epoxy-Amine Systems," *Macromolecular Chemistry and Physics*, vol. 216, pp. 1441-1446, 2015.

[36] V. T. Lipik and M. J. Abadie, "Process Optimization of Poly(E-caprolactone) Synthesis by Ring Opening Polymerization," *Iranian Polymer Journal*, vol. 19, pp. 885-893, 2010.

[37] J. R. Fried, *Polymer Science and Technology*, 3 ed. Upper Saddle River, NJ: Pearson Education, Inc., 2014.

[38] M. Chalid, H. J. Heeres, and A. A. Broekhuis, "Green Polymer Precursors from Biomass-Based Levulinic Acid," *Procedia Chemistry*, vol. 4, pp. 260-267, 2012.

[39] I. Bechthold, K. Bretz, S. Kabasci, R. Kopitzky, and A. Springer, "Succinic Acid: A New Platform Chemical for Biobased Polymers from Renewable Resources," *Chemical Engineering & Technology*, vol. 31, pp. 647-654, 2008.

[40] H. Hong, B. G. Harvey, G. R. Palmese, J. F. Stanzione, H. W. Ng, S. Sakkiah, *et al.*, "Experimental Data Extraction and in Silico Prediction of the Estrogenic Activity of Renewable Replacements for Bisphenol A," *Int J Environ Res Public Health*, vol. 13, 2016.

[41] C. Asada, S. Basnet, M. Otsuka, C. Sasaki, and Y. Nakamura, "Epoxy resin synthesis using low molecular weight lignin separated from various lignocellulosic materials," *Int J Biol Macromol*, vol. 74, pp. 413-9, Mar 2015.

[42] K. Rogers, "Bisphenol A (BPA)," in *Encyclopaedia Britannica*, ed, 2014.

[43] S. K. Ritter. (2011) Debating BPA's Toxicity. *Chemical and Engineering News*. 14-19.

[44] C. A. Staples, P. B. Dorn, G. M. Klecka, S. T. O'Block, and L. R. Harris, "A review of the environmental fate, effects, and exposure of bisphenol A," *Chemosphere*, vol. 36, pp. 2149-2173, 1998.

[45] "Bisphenol A," N. T. P. a. N. I. o. E. H. Sciences, Ed., ed: National Institute of Health, 2010.

[46] "Bisphenol A (BPA)," N. I. o. E. H. Science, Ed., ed: National Institutes of Health, 2016.

[47] K. H. Reno, J. F. I. Stanzione, R. P. Wool, J. M. Sadler, J. J. La Scala, and E. D. Hernandez, "Bisphenol Alternatives Derived from Renewable substituted phenolics and their industrial application," 2015.

[48] K. A. Ehlert, "Migration of bisphenol A into water from polycarbonate baby bottles during microwave heating," *Food Additives and Contaminants: Part A*, vol. 25, pp. 904-910, 2008.

[49] C. Erler and J. Novak, "Bisphenol a exposure: human risk and health policy," *J Pediatr Nurs*, vol. 25, pp. 400-7, Oct 2010.

[50] L. N. Vandenberg, R. Hauser, M. Marcus, N. Olea, and W. V. Welshons, "Human exposure to bisphenol A (BPA)," *Reprod Toxicol*, vol. 24, pp. 139-77, Aug-Sep 2007.

[51] S. K. Ritter. (2011) BPA Is Indispensible For Making Plastics. *Chemical & Engineering News*.

[52] S. Eladak, T. Grisin, D. Moison, M. J. Guerquin, T. N'Tumba-Byn, S. Pozzi-Gaudin, *et al.*, "A new chapter in the bisphenol A story: bisphenol S and bisphenol F are not safe alternatives to this compound," *Fertil Steril*, vol. 103, pp. 11-21, Jan 2015.

[53] A. K. Rosenmai, M. Dybdahl, M. Pedersen, B. M. A. van Vugt-Lussenburg, E. B. Wedebye, C. Taxvig, *et al.*, "Are Structural Analogues to bisphenol A safe alternatives?," *Toxicological Sciences*, vol. 139, pp. 35-47, 2014.

[54] E. D. Hernandez, A. W. Bassett, J. M. Sadler, J. J. La Scala, and J. F. Stanzione, "Synthesis and Characterization of Bio-based Epoxy Resins Derived from Vanillyl Alcohol," *ACS Sustainable Chemistry & Engineering*, 2016.

[55] J. McMurry, *Organic Chemistry*, 8 ed.: Brooks/Cole, Cengage Learning, 2012.

[56] Q. Tang and H. Wu, "Synthesis technology of bisphenol F," China Patent, 1996.

[57] R. Auvergne, S. Caillol, G. David, B. Boutevin, and J. P. Pascault, "Biobased thermosetting epoxy: present and future," *Chem Rev*, vol. 114, pp. 1082-115, Jan 22 2014.

[58] F. Ferdosian, Z. Yuan, M. Anderson, and C. Xu, "Sustainable lignin-based epoxy resins cured with aromatic and aliphatic amine curing agents: Curing kinetics and thermal properties," *Thermochimica Acta*, vol. 618, pp. 48-55, 2015.

[59] E. A. Baroncini, S. K. Yadav, G. R. Palmese, and I. Joseph F. Stanzione, "Recent advances in bio-based epoxy resins and bio-based epoxy curing agents," *Journal of Applied Polymer Science*, vol. 133, 2016.

[60] J. Xin, P. Zhang, K. Huang, and J. Zhang, "Study of green epoxy resins derived from renewable cinnamic acid and dipentene: synthesis, curing and properties," *RSC Advances*, vol. 4, p. 8525, 2014.

[61] L. Krahling, J. Krey, G. Jakobson, J. Grolig, and L. Miksche, "Allyl Compounds," in *Ullmann's Encyclopedia of Industrial Chemistry*, ed: Wiley & Sons 2000.

[62] E. Santacesaria, R. Tesser, M. Di Serio, L. Casale, and D. Verde, "New Process for Producing Epichlorohydrin via Glycerol Chlorination," *Industrial & Engineering Chemistry Research,* vol. 49, pp. 964-970, 2010.

[63] C. H. Childers, S. J. Tucker, and J. S. Wiggins, "Molecular Dynamics Study of the Effect of Molecular Weight Between Crosslinks on Thermomechanical Properties of Aerospace Epoxies," *Polymer Preprints,* vol. 51, pp. 815-816, 2010.

[64] S. Fukuoka, M. Kawamura, K. Komiya, M. Tojo, H. Hachiya, K. Hasegawa, *et al.*, "A novel non-phosgene polycarbonate production process using by-product CO2 as starting material," *Green Chemistry,* vol. 5, p. 497, 2003.

[65] J. D. Borak, Werner, "Phosgene Exposure: Mechanisms of Injury and Treatment Strategies," *Journal of Occupational and Environmental Medicine,* vol. 43, pp. 110-119, 2001.

[66] E. B. Martin, William, "A Convenient Laboratory Preparation of Aromatic Polycarbonate," *Polymer Bulletin,* vol. 47, pp. 517-520, 2002.

[67] O. I. Haba, Isao; Ueda, Mitsuru; Kuze, Shigeki, "Synthesis of Polycarbonate from Dimethyl Carbonate and Bisphenol-A Through a Non-Phosgene Process," *Journal of Polymer Science,* vol. 37, pp. 2087-2093, 1999.

[68] B. A. Sweileh, Y. M. A-Hiari, and K. M. Aiedeh, "A new, nonphosgene route to poly(bisphenol a carbonate) by melt-phase interchange reactions of alkylene diphenyl dicarbonates with bisphenol A," *Journal of Applied Polymer Science,* vol. 110, pp. 2278-2292, 2008.

[69] Y. Xin and H. Uyama, "Synthesis of new bio-based polycarbonates derived from terpene," *Journal of Polymer Research,* vol. 19, 2012.

[70] G.-H. Choi, D. Y. Hwang, and D. H. Suh, "High Thermal Stability of Bio-Based Polycarbonates Containing Cyclic Ketal Moieties," *Macromolecules,* vol. 48, pp. 6839-6845, 2015.

[71] (2015, Nov. 20, 2016). *Polyarylates (Aromatic Polyesters).* Available: http://polymerdatabase.com/polymer%20classes/Polyarylate%20type.html

[72] J. M. Sadler, F. R. Toulan, G. R. Palmese, and J. J. La Scala, "Unsaturated polyester resins for thermoset applications using renewable isosorbide as a component for property improvement," *Journal of Applied Polymer Science,* vol. 132, pp. n/a-n/a, 2015.

[73] C. Berti, V. Bonora, and F. Pilati, "Synthesis of Aromatic Polyesters based on bisphenol A and phthalic acids," *Macromolecules*, vol. 24, pp. 5269-5272, 1991.

[74] W. J. Yoon, S. Y. Hwang, J. M. Koo, Y. J. Lee, S. U. Lee, and S. S. Im, "Synthesis and Characteristics of a Biobased High-TgTerpolyester of Isosorbide, Ethylene Glycol, and 1,4-Cyclohexane Dimethanol: Effect of Ethylene Glycol as a Chain Linker on Polymerization," *Macromolecules*, vol. 46, pp. 7219-7231, 2013.

[75] J. Dai, S. Ma, X. Liu, L. Han, Y. Wu, X. Dai, *et al.*, "Synthesis of bio-based unsaturated polyester resins and their application in waterborne UV-curable coatings," *Progress in Organic Coatings*, vol. 78, pp. 49-54, 2015.

[76] P. Liu, T. Wu, M. Shi, G. Ye, and J. Xu, "Synthesis and characterization of readily soluble polyarylates derived from either 1,1-bis(4-hydroxyphenyl)-1-phenylethane or tetramethylbisphenol A and aromatic diacid chlorides," *Journal of Applied Polymer Science*, vol. 119, pp. 1923-1930, 2011.

[77] (2008). *Products*. Available: https://www.bio-amber.com/bioamber/en/products#lca

[78] M. Lomelí-Rodríguez, M. Martín-Molina, M. Jiménez-Pardo, Z. Nasim-Afzal, S. I. Cauët, T. E. Davies, *et al.*, "Synthesis and kinetic modeling of biomass-derived renewable polyesters," *Journal of Polymer Science Part A: Polymer Chemistry*, vol. 54, pp. 2876-2887, 2016.

[79] R. Busch, H.-J. Kneuper, T. Weber, W. Muller, A. Stamm, and J. Henkelmann, "Method for producing acid chlorides," 2004.

[80] "Public Health Statement - Styrene," Agency For Toxic Substances and Disease Registry2012.

[81] S. Coghe, K. Benoot, F. Delvaux, B. Vanderhaegen, and F. Delvaux, "Ferulic Acid Release and 4-Vinyl Guaiacol Formation During Brewing and Fermentation: Indications for Feruloyl Esterase Activity in Saccharomyces cerevisiae," *Journal of Agricultural and Food Chemistry*, vol. 52, pp. 602-608, 2004.

[82] E. D. Becker, "A Brief History of Nuclear Magnetic Resonance," *Analytical Chemistry*, vol. 65, pp. 295-302, March 15 1993.

[83] D. L. Pavia, G. M. Lampman, G. S. Kriz, and J. R. Vyvyan, *Introduction to Spectroscopy*, 4 ed.: Brooks/Cole, Cengage Learning, 2009.

[84] P. C. Painter and M. M. Coleman, *Fundamentals of Polymers Science: An Introductory Text*. Lancaster, PA: Technomic Publishing Company, Inc., 1997.

[85] M. Rubinstein and R. H. Colby, *Polymer Physics*. New York: Oxford University Press Inc., 2003.

[86] J. Bicerano, *Prediction of Polymer Properties*, 3 ed. New York, NY: Marcel Dekker Inc., 2002.

[87] A. S. o. T. a. Methods, "Standard Test Method for Epoxy Content of Epoxy Resins," vol. D1652-11, ed. West Conshohocken, PA, United States: ASTM International, 2012.

[88] C. S. Lecher, "Sodium Borohydride Reduction of Vanillin: A Low Solvent Synthesis of Vanillyl Alcohol," 2007.

[89] I. M. McAninch, G. R. Palmese, J. L. Lenhart, and J. J. La Scala, "DMA testing of epoxy resins: The importance of dimensions," *Polymer Engineering & Science*, vol. 55, pp. 2761-2774, 2015.

[90] Y. Xin, J. Sakamoto, A. J. van der Vlies, U. Hasegawa, and H. Uyama, "Phase separation approach to a reactive polycarbonate monolith for “click” modifications," *Polymer*, vol. 66, pp. 52-57, 2015.

[91] M. Fache, A. Viola, R. Auvergne, B. Boutevin, and S. Caillol, "Biobased epoxy thermosets from vanillin-derived oligomers," *European Polymer Journal*, vol. 68, pp. 526-535, 2015.

[92] A. L. Holmberg, K. H. Reno, N. A. Nguyen, R. P. Wool, and T. H. Epps, 3rd, "Syringyl Methacrylate, a Hardwood Lignin-Based Monomer for High-Tg Polymeric Materials," *ACS Macro Lett*, vol. 5, pp. 574-578, May 17 2016.

Appendix A

^{1}H and ^{13}C NMR Spectra

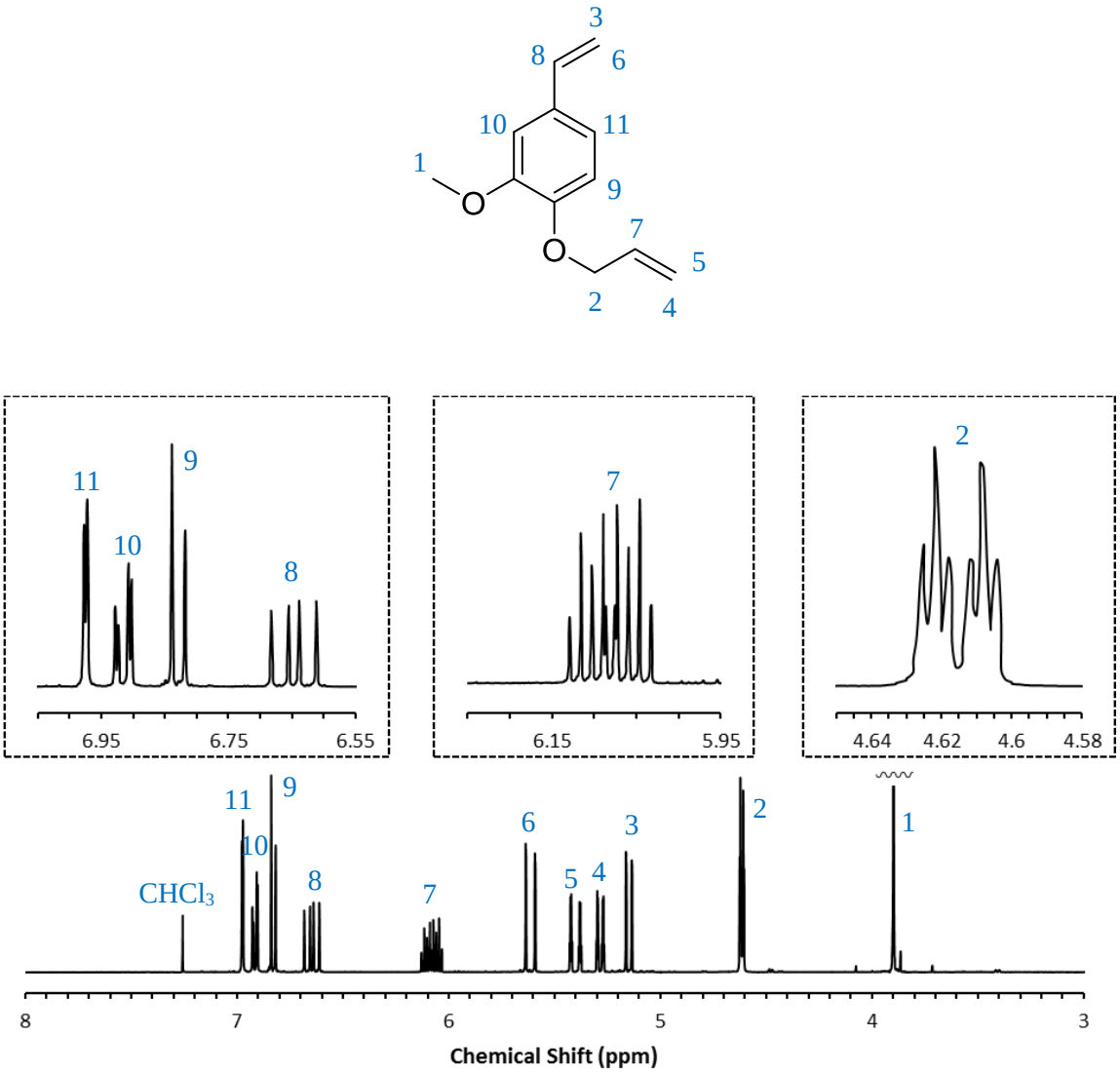

Figure A1. ^{1}H NMR spectrum of allylated 4-vinyl guaiacol (Al4VG) with proton assignments.

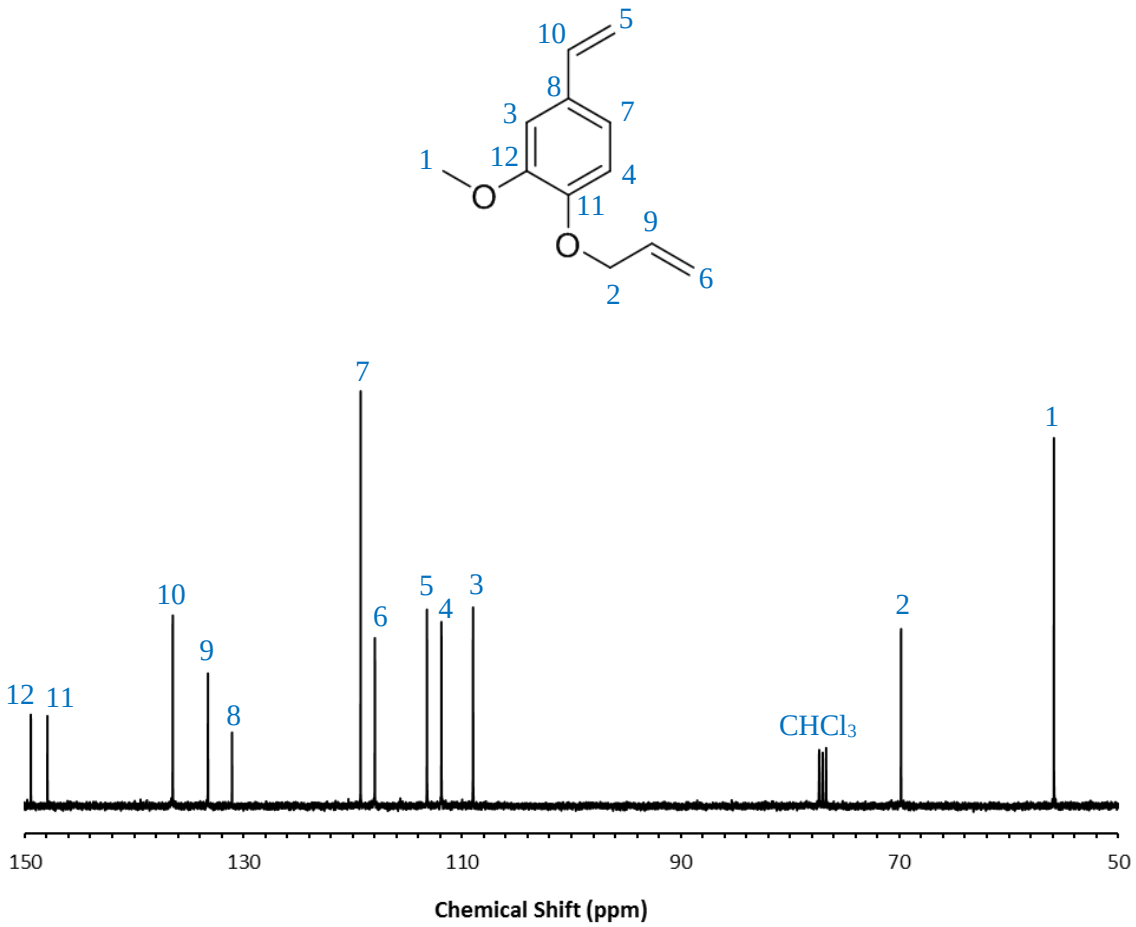

Figure A2. ^{13}C NMR spectrum of allylated 4-vinyl guaiacol (Al4VG) with proton assignments.

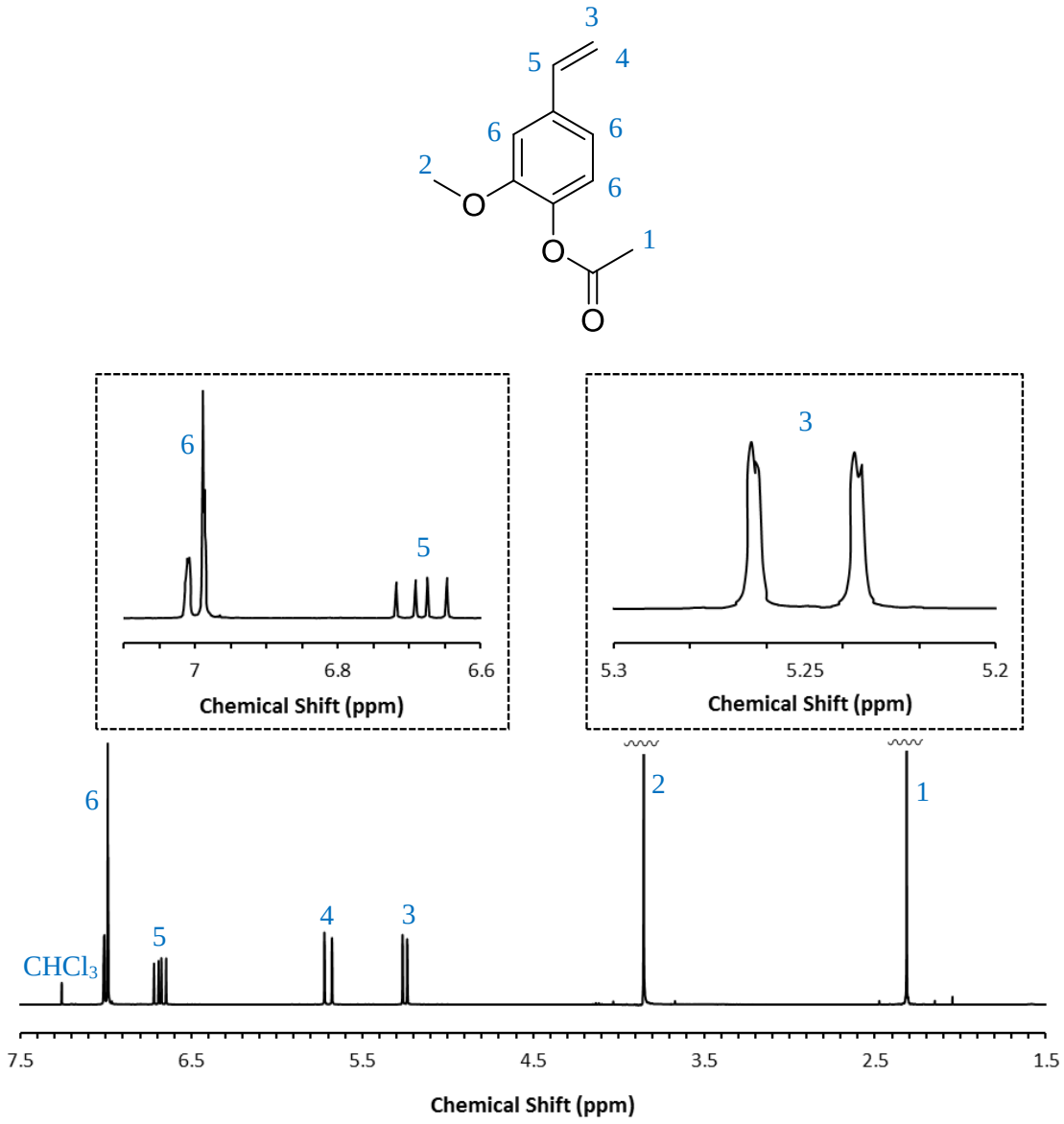

Figure A3. ^{1}H NMR spectrum of acetylated 4-vinyl guaiacol (Ac4VG) with proton assignments.

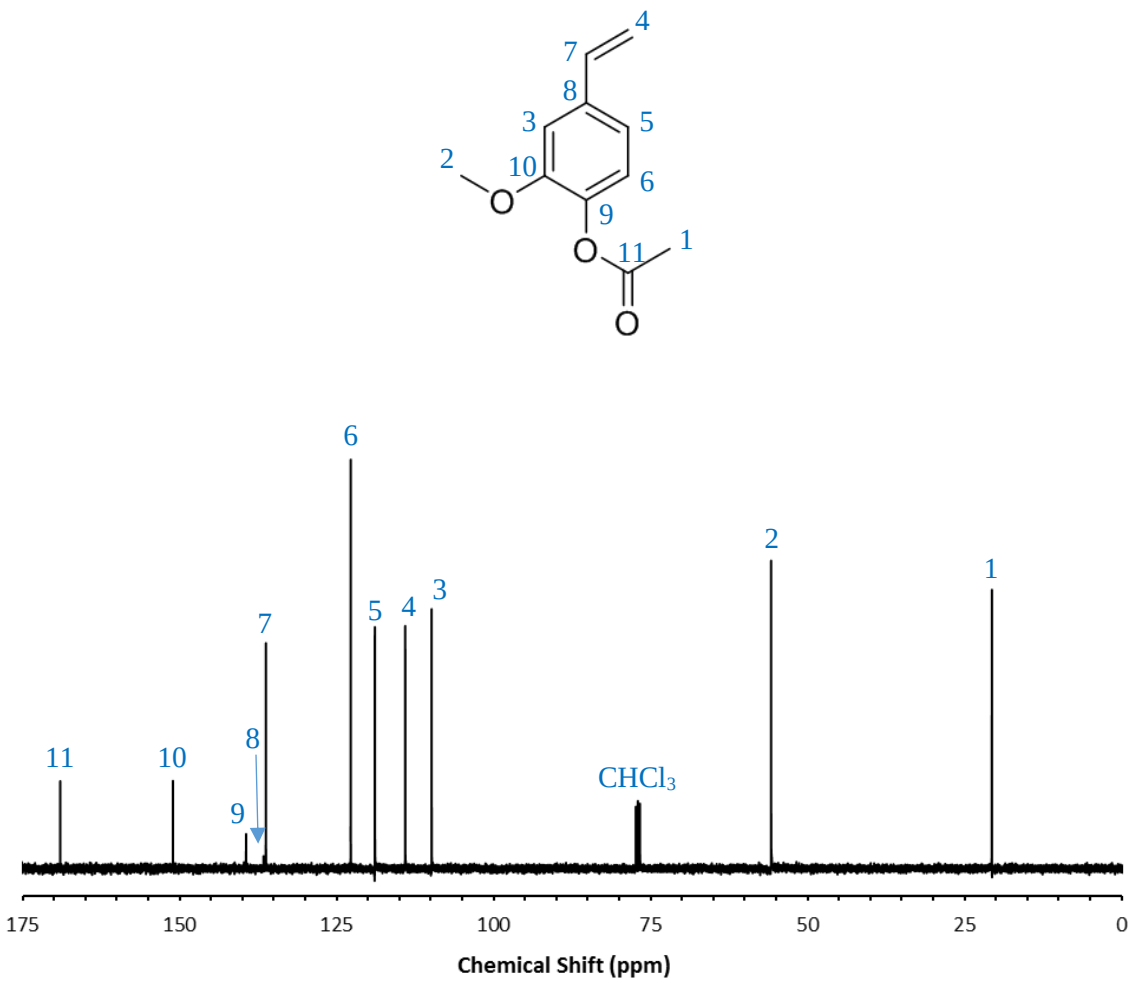

Figure A4. ^{13}C NMR spectrum of acetylated 4-vinyl guaiacol (Ac4VG) with proton assignments.

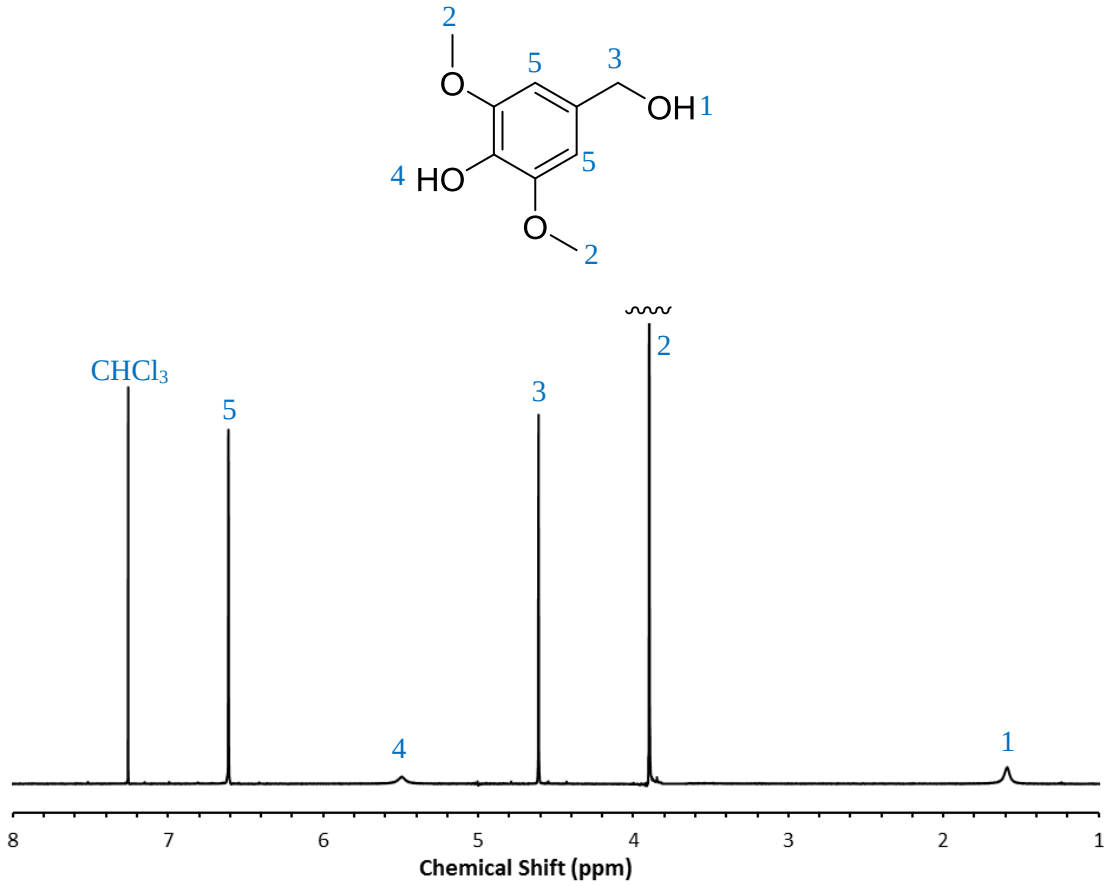

Figure A5. ^{1}H NMR spectrum of syringyl alcohol with proton assignments.

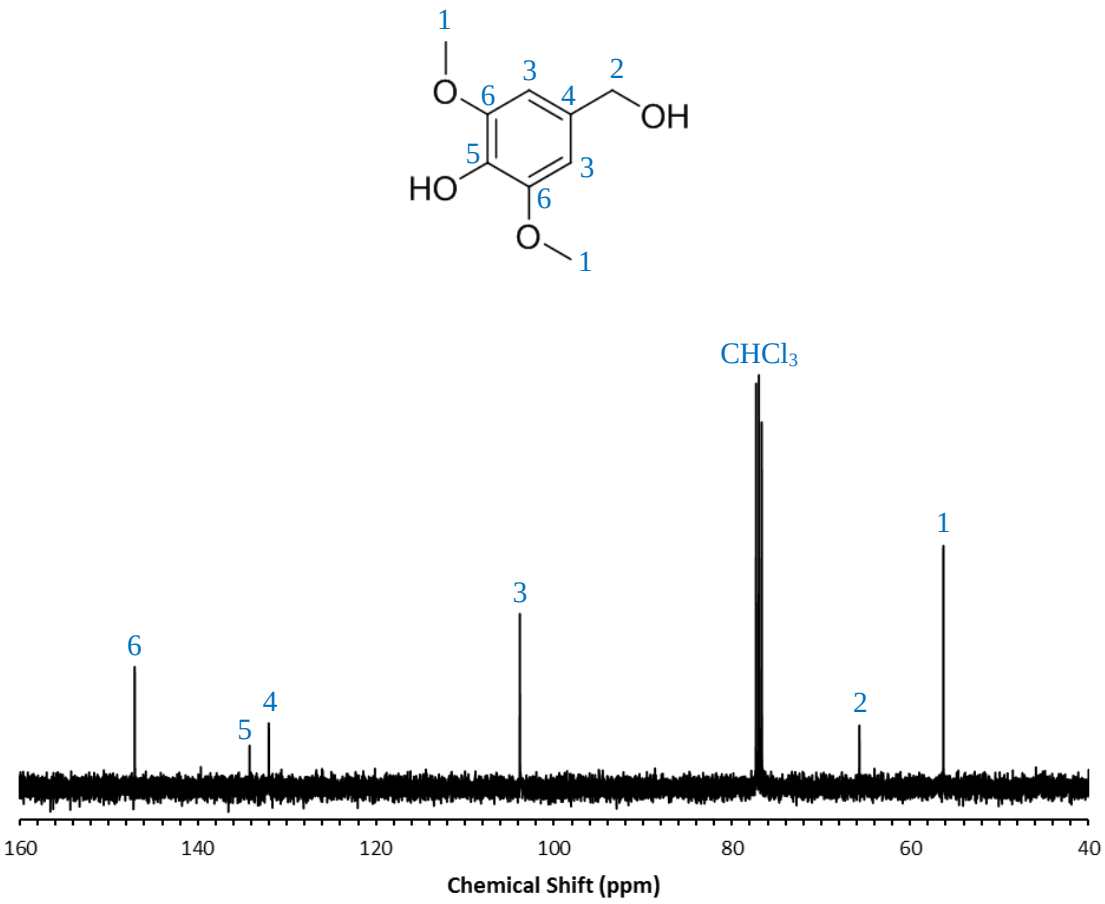

Figure A6. ^{13}C NMR spectrum of syringyl alcohol with proton assignments.

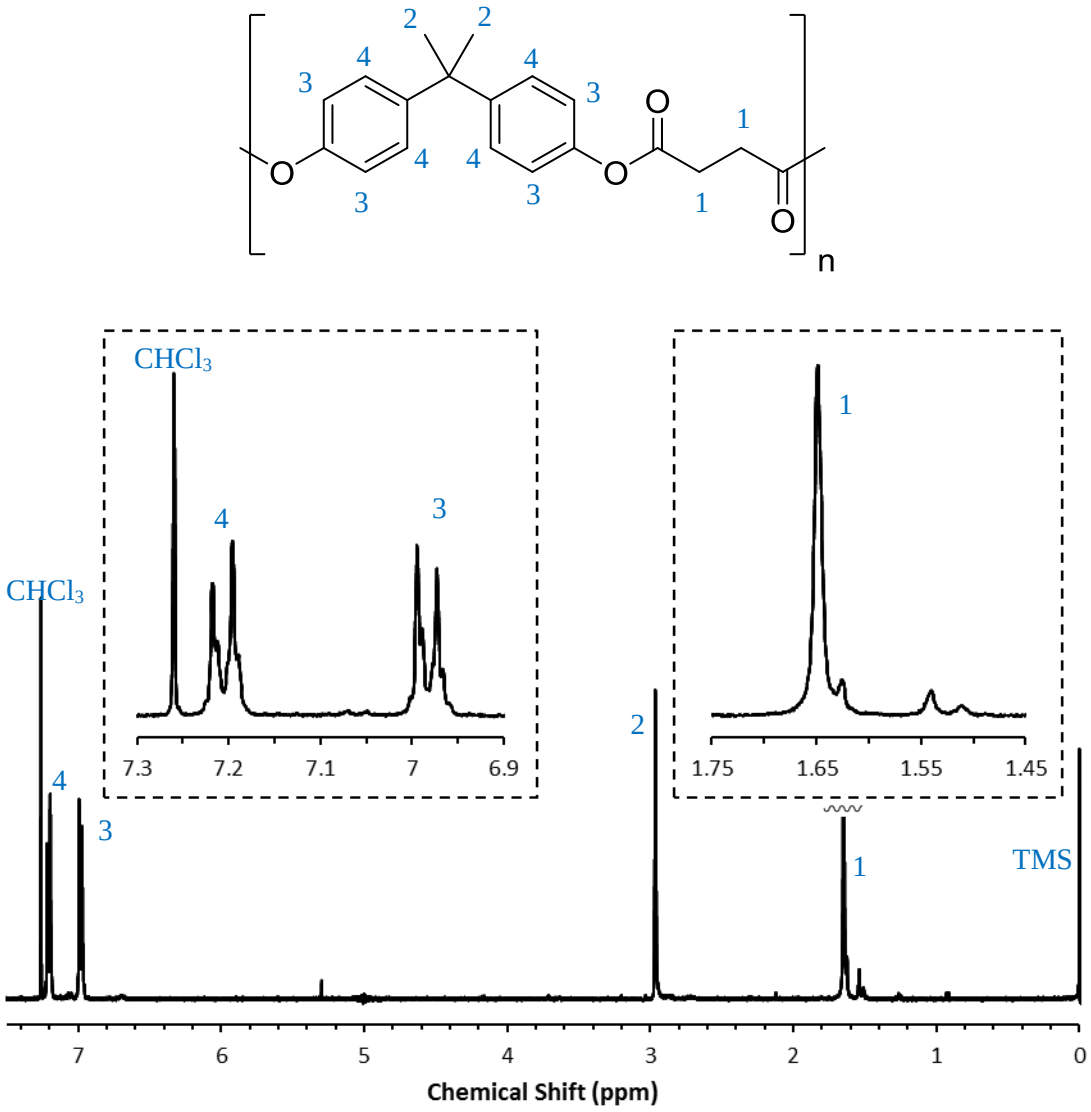

Figure A7. [1]H NMR spectrum of polyarylate of BPA and succinyl chloride with proton assignments.

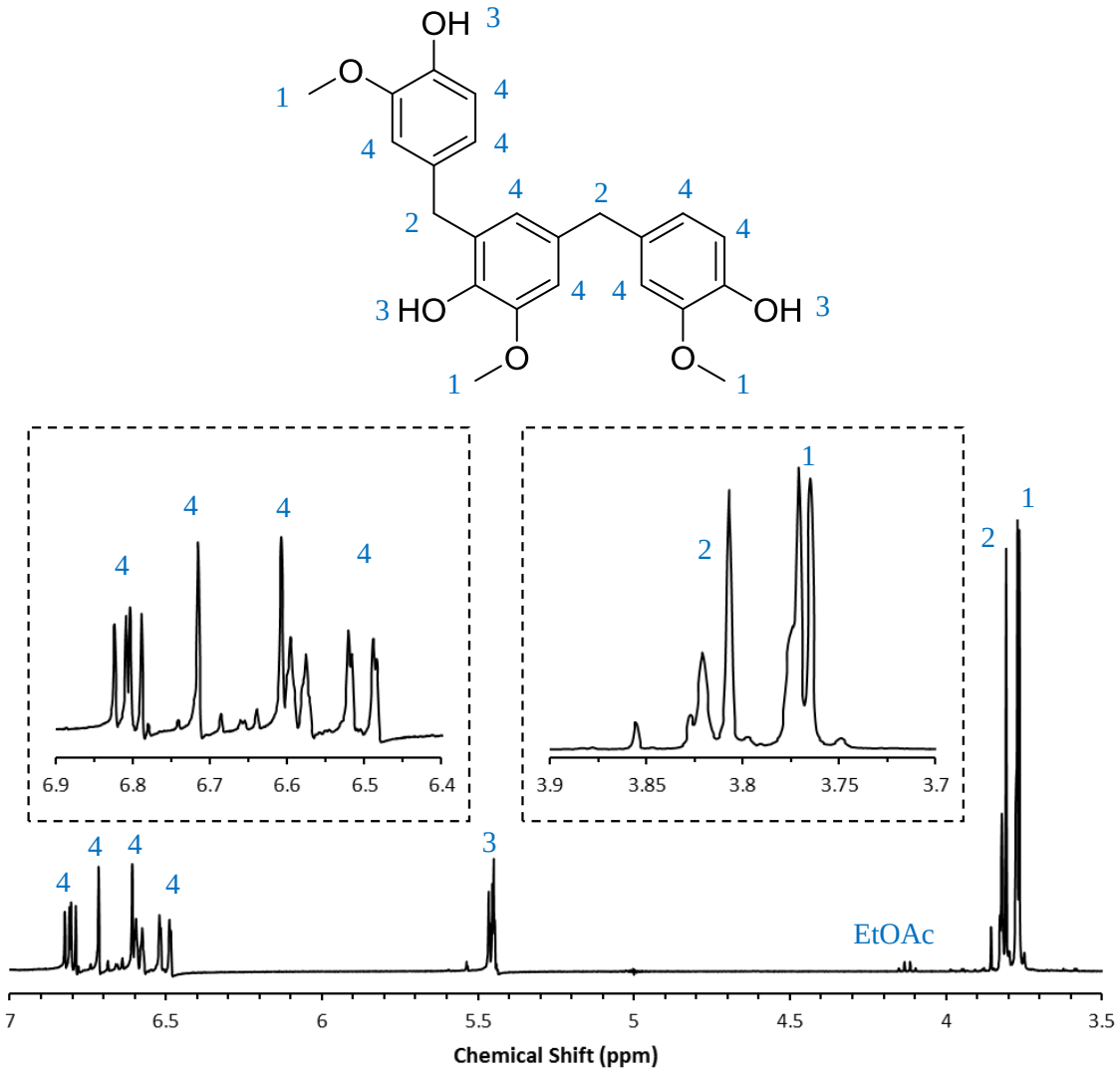

Figure A8. [1]H NMR spectrum of trisguaiacol (trisG) with proton assignments.

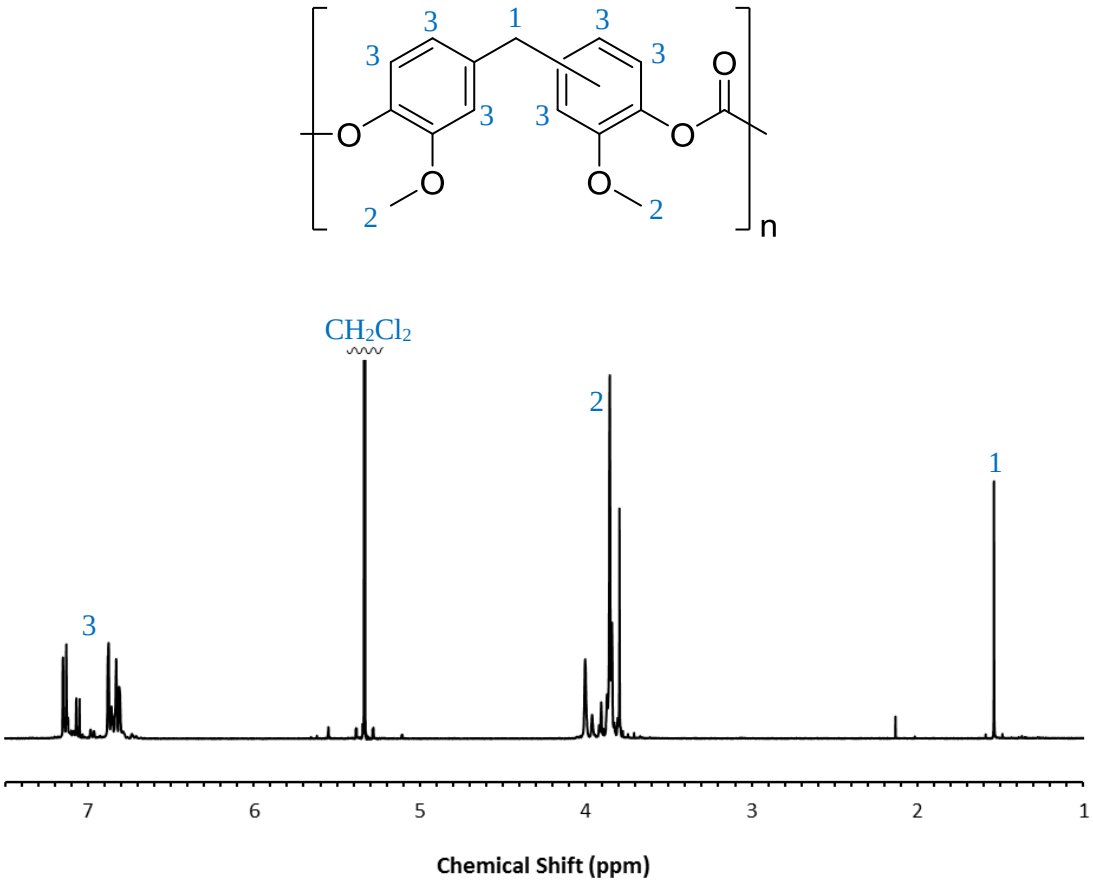

Figure A9. ^{1}H NMR spectrum of polycarbonate of bisguaiacol (BG-PC) with proton assignments.

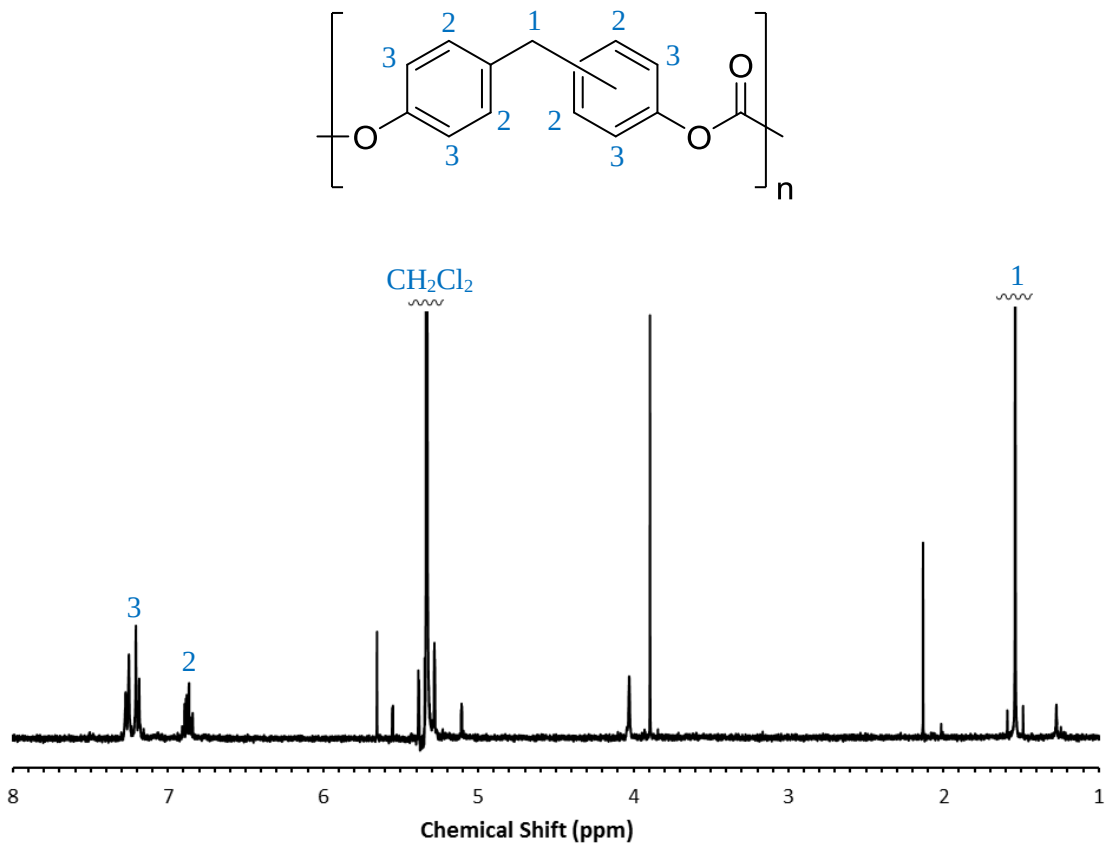

Figure A10. ^{1}H NMR spectrum of polycarbonate of bisphenol F (BPF-PC) with proton assignments.

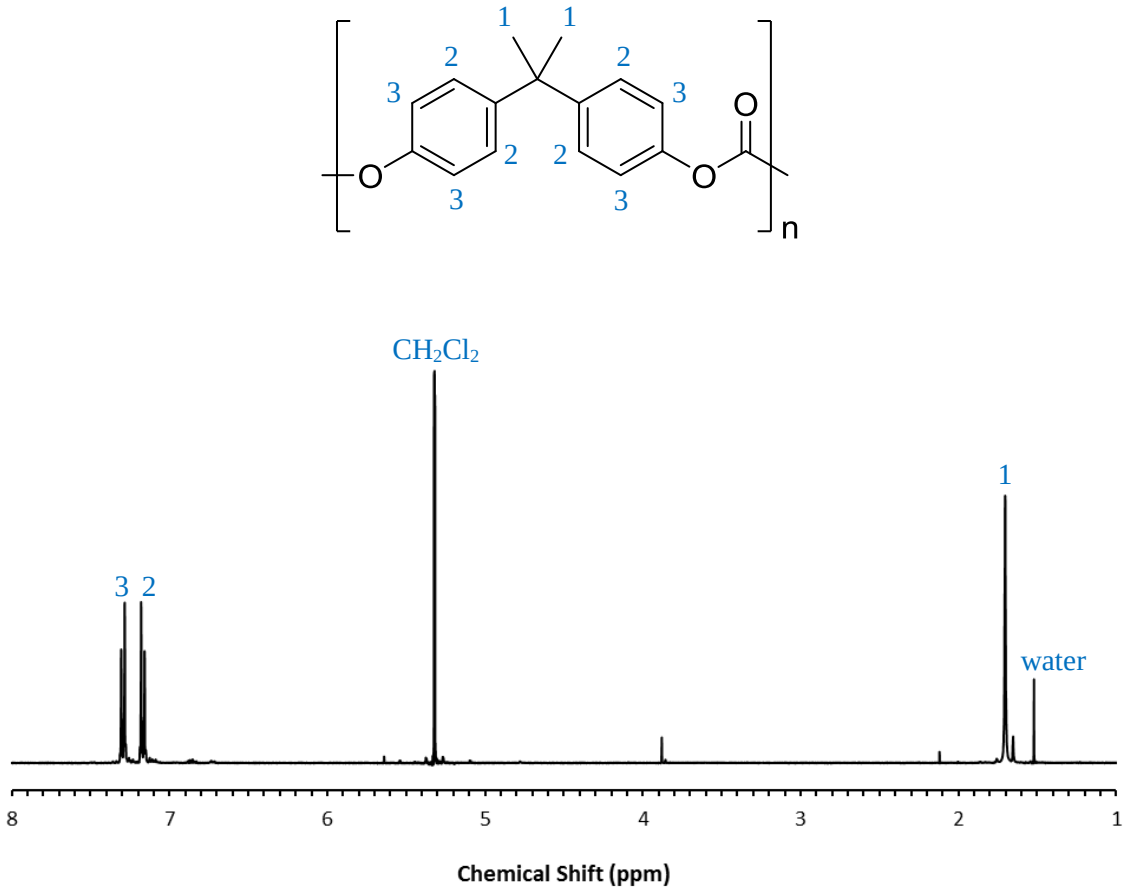

Figure A11. ^{1}H NMR spectrum of polycarbonate of bisphenol A (BPA-PC) with proton assignments.

Appendix B

FTIR Spectra

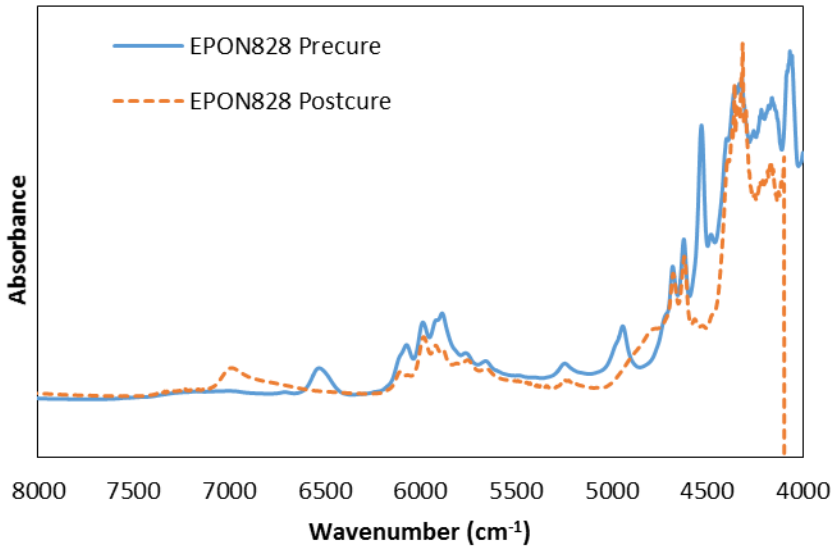

Figure B1. Near-FTIR spectrum of EPON828 mixed with DFDA precure and postcure overlaid.

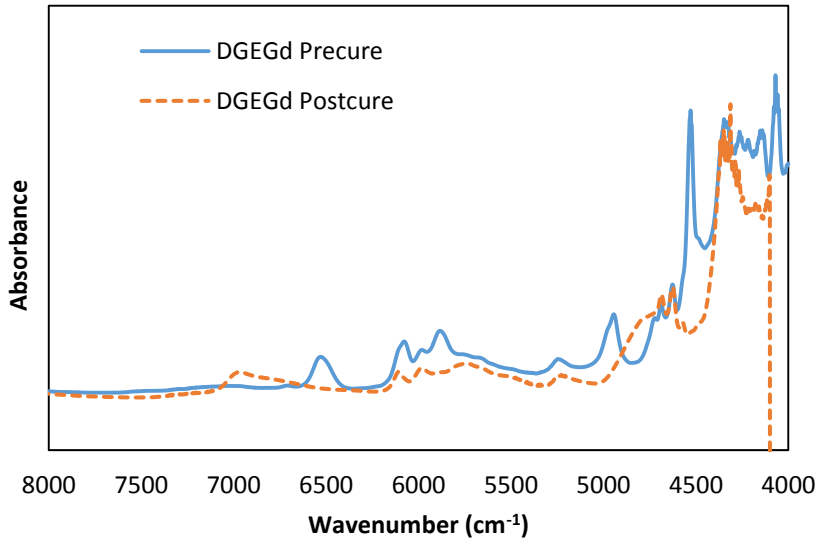

Figure B2. Near-FTIR spectrum of DGEGd mixed with DFDA precure and postcure overlaid.

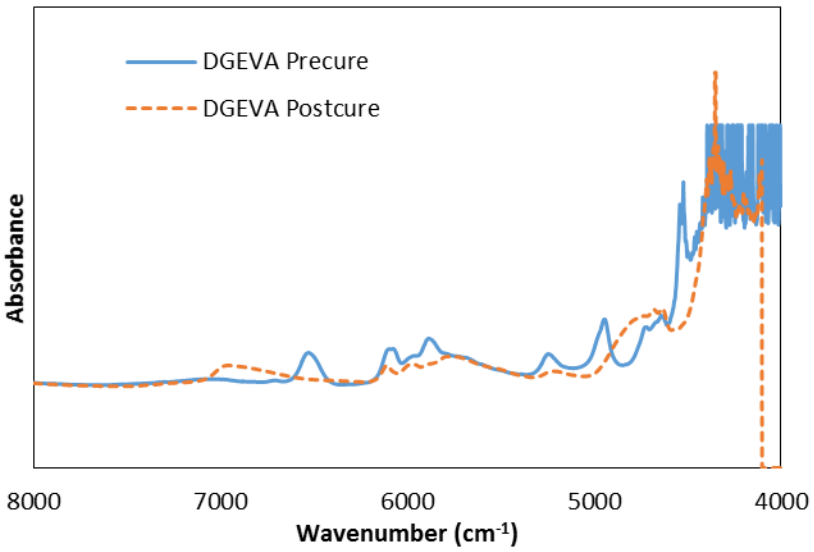

Figure B3. Near-FTIR spectrum of DGEVA mixed with DFDA precure and postcure overlaid.

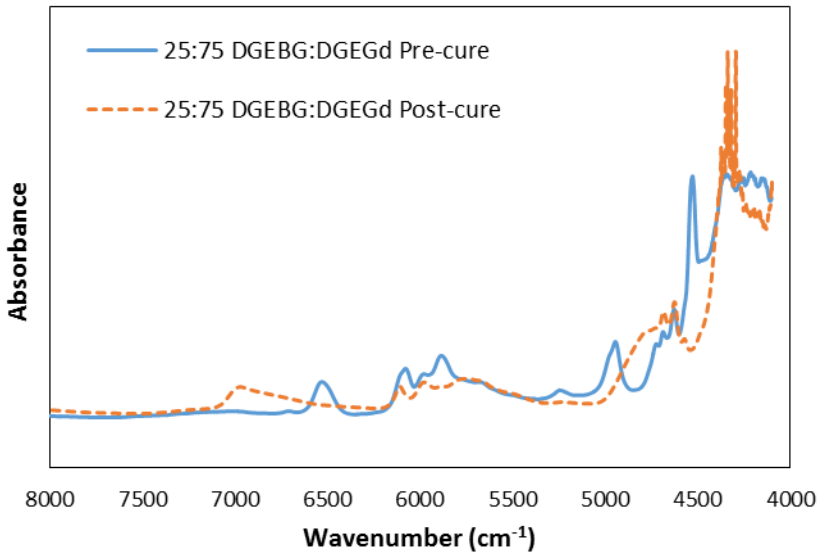

Figure B4. Near-FTIR spectrum of 25:75 mixture of DGEBG in DGEGd mixed with DFDA precure and postcure overlaid.

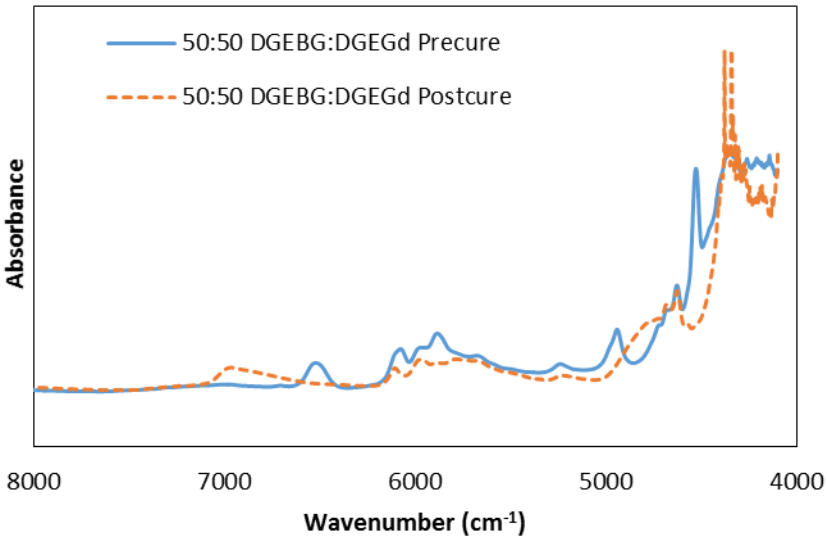

Figure B5. Near-FTIR spectrum of 50:50 mixture of DGEBG in DGEGd mixed with DFDA precure and postcure overlaid.

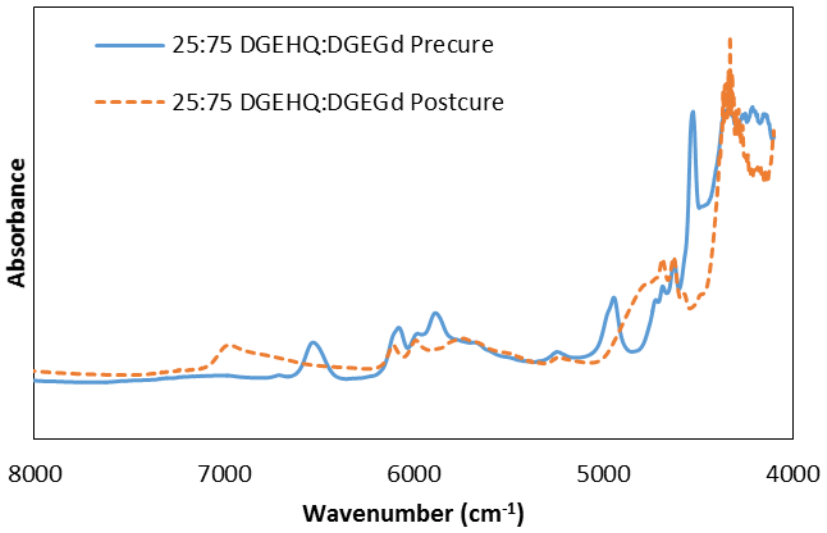

Figure B6. Near-FTIR spectrum of 25:75 mixture of DGEHQ in DGEGd mixed with DFDA precure and postcure overlaid.

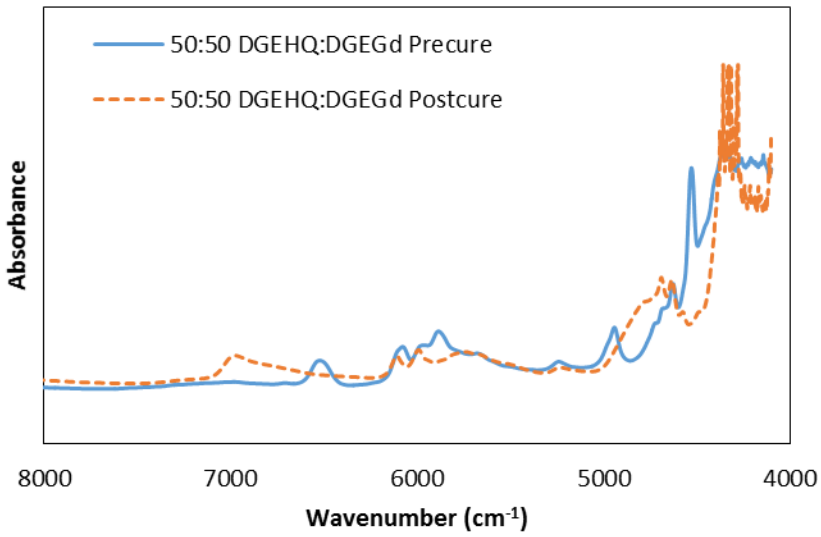

Figure B7. Near-FTIR spectrum of 50:50 mixture of DGEHQ in DGEGd mixed with DFDA precure and postcure overlaid.